Organic carbon accumulation in Hardangerfjorden

A micropaleontological and geochemical study of benthic environmental impact from fish farming

Lars Birkeland Sjetne

Master Thesis
Environmental geology – environmental stratigraphy
60 credits

Institute of Geosciences
The Faculty of Mathematical and Natural Sciences

UNIVERSITY OF OSLO

06/2017

Organic carbon accumulation in Hardangerfjorden

A micropaleontological and geochemical study of benthic environmental impact from fish farming

Lars Birkeland Sjetne

Master Thesis
Environmental geology – environmental stratigraphy
60 credits

Institute of Geosciences
The Faculty of Mathematical and Natural Sciences

UNIVERSITY OF OSLO

06/2017

2017

Organic carbon accumulation in Hardangerfjorden

Lars Birkeland Sjetne

http://www.duo.uio.no/

Trykk: Reprosentralen, Universitetet i Oslo

Abstract

The present study investigated the impact of organic loading from fish farm waste on the benthic environment surrounding a fish farm, and the organic carbon accumulation in fjord sediments in a Western Norwegian fjord. One sediment core collected 100 m from the fish farm was compared with a control core collected 500 m from the farm. Both cores were radiometrically dated to 1927. Interpretation of depositional environment was done based on grain size distribution analysis. Benthic foraminifera (protists) were utilized to assess the ecological quality status (EcoQS) of the benthic environment in each sample, based on foraminiferal species diversity, foraminiferal assemblage composition and benthic foraminiferal accumulation rates (BFAR). Total organic carbon- and total nitrogen content in the sediments, together with stable C- and N-isotope ratios and C- and O-isotope ratios in the tests of selected foraminiferal species, were used to interpret the source of organic matter in the sediments. Heavy metal concentrations were measured and the sediments classified according to official guidelines for sediment pollution. Stable isotope signals and carbon- and nitrogen content was stable throughout the period since 1927 until present-day in both cores, and showed no evidence for increased organic loading related to fish production. Both cores had C/N-ratios characteristic of marine organic matter in sediments deposited after 1927. Foraminiferal species assemblage compositions reflected naturally different benthic environments in the two cores, and showed no clear response to fish production. EcoQS was ‘good’ in both cores. BFAR in the control core increased since the onset of fish production.

Acknowledgements

I would like to thank my supervisor Elisabeth Alve who facilitated this project and for always being available for insightful comments and guidance. An equal thanks to my co-supervisor Silvia Hess for invaluable lab assistance and for pushing me in the right direction, and Paul Renaud for helpful comments. Excellent service was provided by lab engineers Mufak Said Naoroz and Siri Simonsen at the Department of Geosciences, UiO. M/S Solvik skipper Leon Pedersen deserves praise for his ingenuity and for making the Hardangerfjord cruise very enjoyable, as does the rest of the crew members. Thanks to Kristian Råsberg at Alsaker Fjordbruk AS for providing fish farm data, Lars Asplin at IMR for hydrographic data and Anouk Tosca Klootwijk, Astrid Harendza and the other participants of the Jellyfarm project for their help. Thanks to fellow students, friends and family for keeping up the morale.

Table of Contents

List of figures and tables:

1 Introduction

The Norwegian coastline is perforated by deep and long fjords. The picturesque landscapes are tourist magnets as well as the home and livelihood of many people. The unique physiographic features of the underwater valleys of fjords are the foundation of special natural processes which has yet to be fully understood.

Fjords are deep, steep-sided estuaries formed by glaciers that stretch from deep within continents into the ocean (Syvitski et al., 1987). Fjords typically have a moraine sill at the fjord mouth which results in partially isolated basins that are disconnected from the open ocean in various degree (Sætre, 2007). The water masses in fjord basins comprise of both oceanic water entering the basins above the sills and fresh water from rivers along the coast. The density difference in the water mass result in a stratified water column with heavy, saline waters in the basins below sill depth, an intermediate layer and a lighter, brackish upper layer. The layered water mass drive an estuarine circulation (Sætre, 2007), which is an important factor in the distribution of nutrients, dissolved oxygen and sediment within fjord basins (Syvitski et al., 1987).

The steep mountainous terrain which typically surrounds fjords, combined with severe runoff (fjords are naturally confined to high latitudes with strong seasonal contrasts) often result in high rates of sediment accumulation in fjord basins (Syvitski et al., 1987). Estuaries may act as sediment traps, and fjords are exceptionally effective as such. There are great variations regarding sediment accumulation however, some fjords may only receive 100g m^{-2} yr^{-1} per year (Skei, 1983) while others accumulate more than 8000g m^{-2} during the same period (Gilbert et al., 2002). Sediments deposited in fjords are land sourced siliciclastic material and particulate organic matter (POM), both terrestrial and marine. Because of the high sediment accumulation rates much of the organic matter will not be remineralised before it gets buried in the sediments (Hilton et al., 2011). For this reason, it has recently been shown that fjords account for a large part of the total amount of carbon buried within sediments globally – much larger than previously assumed (Keil, 2015; Smith et al., 2015).

In addition to terrestrially and marine sourced POM, a large part of organic carbon found in fjord sediments originates from anthropogenic activity (Strohmeier et al., 2014). Norwegian fjords are hotspots for fish farming, as the fjords provide shelter from the open ocean and the sites are logistically convenient close to land. Since the onset of the fish farming industry in

the 1970s, fish production in Norway has bloomed and reached an all-time high in 2015 with 1 380 841 tons of produced food fish (Statistics Norway, 2016). With such intense fish farming, dispersal of waste and byproducts from fish production to waters surrounding the fish farm net pens is inevitable (Ackefors and Enell, 1994; Hansen et al., 1990; Kutti, Ervik, et al., 2007). Based on the total amount of fish food used in Norwegian coastal waters in 2015 it is estimated that 292 000 tons of POM was released from fish farms during 2015 (Svåsand et al., 2016). A number of authors have done research on carbon waste from fish farms, e.g. by quantifying discharge of POM (Kutti, Ervik, et al., 2007; Valdemarsen et al., 2012), modelling dispersal of fish farm waste (Skogen et al., 2009) and monitoring fish farm impacts on benthic environments under different current conditions (Sweetman et al., 2014; Valdemarsen et al., 2015). Apart from spreading of salmon lice and farm fish escaping the net pens, perhaps the biggest environmental concern related to fish farming is organic loading on the sea floor. POM (in the form of fish feces and uneaten feed pellets) sink to the sea floor where the organic loading may lead to increased oxygen consumption which can be detrimental to benthic ecosystems (Valdemarsen et al., 2015). Studies on fish farm impacts such as those mentioned show evidence of environmental impacts from fish farming in various degrees. These variations are to be expected, considering the highly different conditions within and between fjords (Sætre, 2007), the most notable differences being current velocities and water depth (Findlay et al., 1995; Kutti, Ervik, et al., 2007; Valdemarsen et al., 2012). Therefore, there is need for further investigation of different study sites, as expressed by the authorities (Strohmeier et al., 2014). Although fish farming companies are obliged to perform regular surveys to monitor the environmental conditions at the farm sites (Akvakulturloven, 2005), little is known about the natural conditions from before any possible anthropogenic effects on sea floor sediments.

In light of the carbon storage capacity of fjords and the plea from the authorities this work seeks to contribute to the pool of fjord sediment data. By analysing two sediment cores – one collected close to a fish farm and a second at an ambient, assumed unimpacted locality – this work attempts to trace the source and geochemical composition of sea floor sediments in the immediate vicinity of a fish farm and comparing these sediments with those from a control station. The stratigraphy of sea floor sediments provides a historical record of several environmental parameters. Analysing sediment cores allows for interpretation of the depositional environment in the study area back in time. This method puts the present-day sediment surface in a historical context and allows to reconstruct the development of the

sediment record from natural conditions before anthropogenic activity started to recent conditions (Dolven et al., 2013). By establishing a "baseline" the aim is to study temporal (up-core) changes and how present-day conditions may differ from conditions of previous times. Comparison with a control station allows to study spatial changes of benthic environmental condition in the vicinity of an active fish farm.

Both cores have been dated using radiometric methods. Particle size distributions in both cores were analysed for the purpose of understanding depositional environment. By measuring total organic carbon (TOC) and total nitrogen (TN) content, coupled with stable isotope ratios of ^{13}C and ^{15}N in the sediments, an attempt is made to trace the origin of organic material in both cores (Lamb et al., 2006). Based on measured heavy metal concentrations the sediments have been classified according guidelines set by The Norwegian Environmental Agency (Miljødirektoratet, 2016). Microfossil assemblages (foraminifera) at different sediment depths in both cores were analysed.

Benthic foraminifera are small (generally < 1mm) protists living on and within sea floor sediments. Foraminifera are characterized by tests composed either of calcium carbonate or agglutinated sediment which can fossilize and accumulate in the sediment. The microfaunal organism have shown to be a precise indicator of changes in benthic environment e. g. from pollution sources, due to their narrow niches of living conditions and rapid response to environmental changes (see Bouchet et al. 2012 and references therein). Foraminifera are present in almost all marine environments and leave an abundant fossil record reflecting the benthic environmental conditions in which they lived – information which can be used to assess ecological quality status (EcoQS, as defined by the EU Water Framework Directive (WFD, 2000/60/EC)) in the analysed samples. In addition to fauna analysis, $\delta^{18}O$ and $\delta^{13}C$ from the tests of selected species were measured as the isotope composition may give additional insight in environmental conditions (Rohling and Cooke, 1999).

By combining the mentioned parameters an attempt is made to interpret the past and present depositional environment, bottom water conditions and general climate signal in the ambient bottom water at both localities from which the sediment cores were collected. Based on this, it is possible to look for changes and similarities both through time and between the localities. Are the two localities comparable, in terms of depositional environment? If so, is there evidence for a different sediment accumulation rate between the two localities and can this be attributed to organic matter sourced from the fish farm? Do the foraminiferal species

assemblages at the two localities indicate differences in environmental conditions and if so, how do the differences change over time? By answering these questions this work will contribute to the pool of fjord data and increase the knowledge of fish farm impacts under various fjord conditions. In addition, the work may shed light on the carbon storage potential of fjords in a setting with an increased supply of organic matter.

2 Study area

2.1 Hardangerfjorden

Hardangerfjorden is the second largest fjord in Norway, and third largest in the world. The fjord stretches from its outermost sill (at 190 m depth) by the island Huglo and around 180 km inland in a north-eastern direction (Figure 2.1). The main fjord is 2-6 km wide and in total the fjord area covers approximately 700 km^2 (Aure, 2015). There are several basins within the fjord with various depth, the deepest at approximately 850 m below sea level (Svåsand et al., 2016), the mean basin depth however is 260 m below sea level (Aure, 2015).

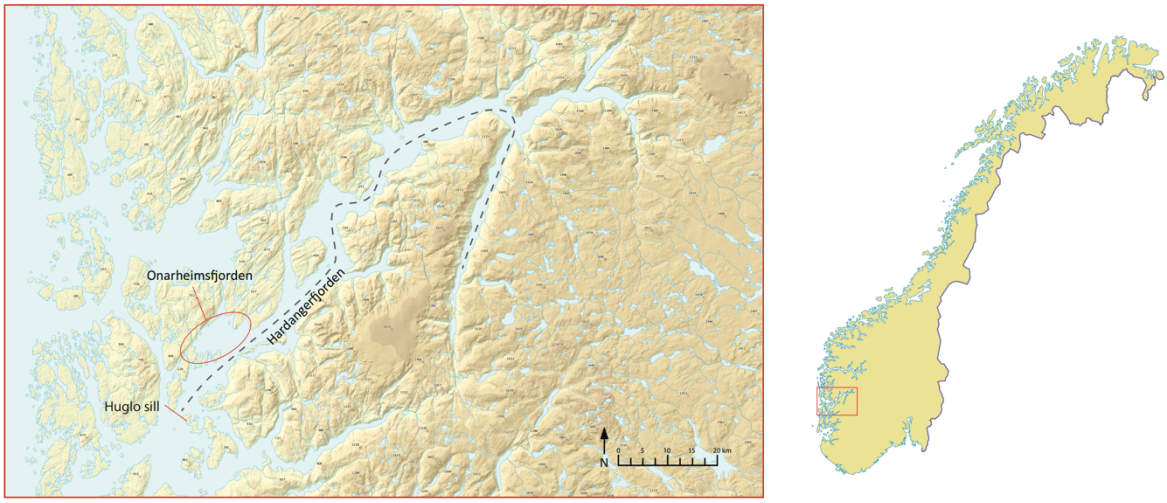

Figure 2.1: Dashed line indicate the extent of Hardangerfjorden, from the sill at Huglo into the innermost Sørfjorden. Red circle marks the extent of Onarheimsfjorden and the red line marks the sill at Huglo (map modified from www.kartverket.no).

2.2 Hydrography

Differences in water salinity and –temperature and their relationship forms what is described as a water mass (Sætre, 2007). The waters of Hardangerfjorden consist of coastal water entering the fjord mouth and fresh water from precipitation and runoff (Ervik et al., 2008). The coastal water is a mix of Atlantic Water and water from the Norwegian Coastal Current. The Atlantic Water originates from a branch of the North Atlantic Current which enters the Norwegian Sea between Shetland and the Faroe Islands. From there, the Atlantic Water flows in a northerly direction along the Norwegian coastal zone (Sætre, 2007). The Atlantic Water holds a mean temperature of 9°C and by definition a salinity > 35 (Aure and Østensen, 1993).

When reaching the coastal zone of Norway, the Atlantic water mixes with more brackish water in the Norwegian Coastal Current (NCC). This current originates from the Baltic and Skagerrak Sea, from where it flows north along the Norwegian coast. Fresh water input reduces the coastal current salinity to < 35 (Sætre, 2007). The salinity- and density difference between the coastal water and the Atlantic Water, makes the NCC flow on top of the Atlantic Water in a wedge-shape. The wedge runs deep and is laterally constricted during winter, when temperatures are low. A converse situation happens during summer, when the wedge is laterally extended and is shallower because of higher temperatures and decreased density (Sætre, 2007). Mean annual precipitation at the last 10 years was 2088 mm (Figure 2.2) and numerous rivers and streams along the coast (Petterson, 2008). It has an estimated annual mean fresh water input of 400 m^3/s (Ervik et al., 2008). The fresh water mixes with the coastal water in Hardangerfjorden to establish a surface layer with a salinity < 25 which floats on top of the denser coastal water mass. The thickness of the surface layer depends on the fresh water discharge which has substantial inter annual variations. During seasons with little fresh water discharge it might be absent, while summer seasons may see a surface layer 10 m deep (Lars Asplin pers. comm. Apr. 2017).

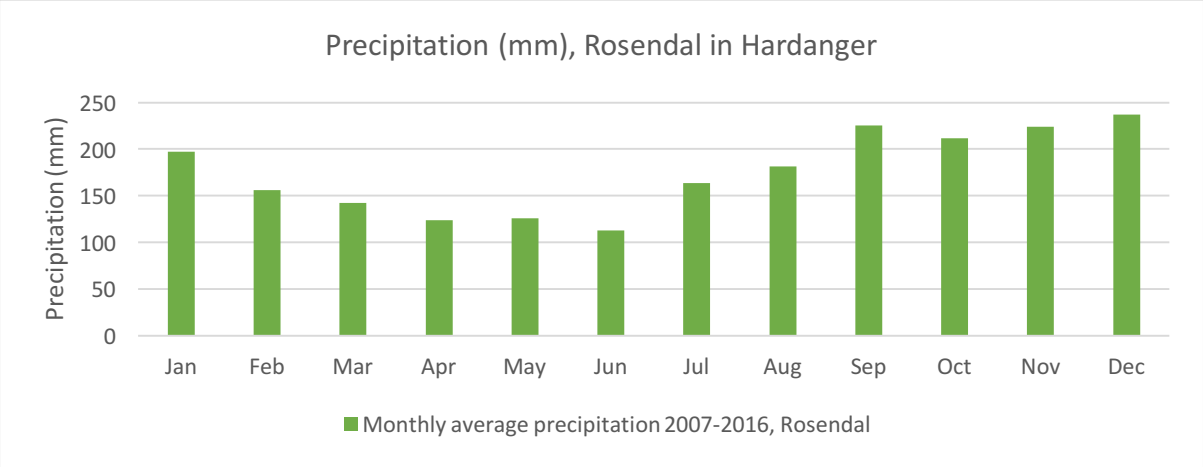

Figure 2.2: Monthly average precipitation for the period 2007-2016 measured at a weather station in Rosendal, East of Onarheimsfjorden. Average annual precipitation in this period was 2088mm (data from Meteorologisk Institutt, www.eklima.met.no).

The main forces driving water mass distribution are estuarine circulation, intermediate circulation (in- and outflow of coastal water driven by wind) and density driven deep water inflow (Ervik et al., 2008). The estuarine circulation is limited to the upper brackish layer which flows on top of denser water towards the sea by gravitational pull (Syvitski et al., 1987). Because of the Coriolis effect the brackish outflowing current is stronger along the

west coast of Hardangerfjorden which results in an inward flow on the opposite side by the water that is entrained by the upper layer (Ervik et al., 2008). Intermediate circulation takes place during periods of consistent coastal north- or southerly winds (Ervik et al., 2008). Northerly winds force down-welling of coastal water which drains the fjord basin of the intermediate layer, while southerly winds have an opposite effect, causing inflow of coastal water in the intermediate layer to around 50 m water depth (Sundfjord, 2010). Below sill depth (about 190 m), the deep basin water is for the most part unaffected by the types of circulation described above. This leads to a stagnant basin water mass where deep water renewal only happens occasionally (Sætre, 2007). Such occasions are when the density of the outer lying coastal water is greater than that of the basin water and gets flushed in over the sill by tidal forcing (Ervik et al., 2008; Sætre, 2007). This typically takes place during summer when the relatively warm brackish water runs shallow and allows for dense, saline water to reach sill level (Aure, 2015). Based on observations, the bottom water in Hardangerfjorden has a residence time of about 6 months (Aure, 2015). Renewal of basin water is important for the level of oxygen availability, as oxygen concentrations will diminish after prolonged periods with no replenishment of basin water (Aure and Stigebrandt, 1989; Sætre, 2007). Given the size and geometry of Hardangerfjorden, it may be considered a fjord system with several branches, rather than one fjord (Asplin et al., 2014). The complex structure of the water masses in Hardangerfjorden and various local differences in topography both on land and within the fjord yield complicated current conditions, which vary in space and time. The circulation described above gives an overall sketch of the current conditions in Hardangerfjorden, however, local differences make it unjustified to generalise the current patterns of the fjord.

2.3 Influence of fish farming in Hardangerfjorden

The amount of organic waste released into the water surrounding a fish farm is proportional to its fish production (Svåsand et al., 2016). Based on production data from 2012 an estimated (maximal) 5000 tons of carbon (as feces and uneaten food pellets) were released into Hardangerfjorden in this year (Aure, 2015). The amount equals to a 6% increase of the natural carbon input to Hardangerfjorden (Aure, 2015). Such an increase may potentially affect the water quality in terms of eutrophication and oxygen depletion. However, few data series describing the water quality or biological conditions in Hardangerfjorden in general are

available, apart from the innermost part of Hardangerfjorden, which has been closely monitored due to its history of severe industrial pollution (Skei et al., 1972). Model experiments have been performed, however, to study the effects on primary production in Hardangerfjorden caused by nutrient discharge from fish farms (Skogen et al., 2009). The results from the simulation indicated that primary production in Hardangerfjorden was only slightly increased by the estimated nutrient supply from fish farming. Even when simulated for a 10-fold increase of fish farm outlets the increase in primary production was no more than 5%. The low effect is attributed to the water circulation and flushing of water masses. Estimates made in Aure's study (2015) suggest that the calculated amount of organic waste from fish production in Hardangerfjorden will reduce minimum oxygen level in the basin water by around 1.3%. The calculations are based on only two oxygen level measurements (April and November 2010) as no time series exist. If the simulations are to be trusted, the estimates show that Hardangerfjorden is capable of sustaining healthy biological conditions even with large increase of organic matter supply. The small reduction in oxygen consumption is again a result of the large (below sill depth-) basin volume and the naturally high supply and consumption of POM in deep basins such as that in Hardangerfjorden.

Studies on the regional effects of fish farming in Hardangerfjorden are in agreement with the results from the mentioned model experiments, in that the sea floor sediments exhibit a good assimilative capacity (Husa et al., 2014). Directly beneath fish farm facilities, however, studies have found significant impacts on the benthic community due to increased fluxes of nutrients. At one study site the POM sedimentation rate on the sea floor (at 250 m depth) was 2-4 times as high within 250 m distance from the fish farm compared to sediment traps 550 m away (Kutti, Ervik, et al., 2007). The increased fluxes of organic matter lead to elevated infauna abundance and biomass (Kutti, Hansen, et al., 2007) which were dominated by pollution tolerant species. Similar findings are reported by Sweetman et al. (2014) and Valdemarsen et al. (2015), who compared deep water fish farm localities under different current conditions. Interestingly, the two publications found different effects of the current speeds in their respective studies. While higher current velocity had only a smaller effect on the benthic community in the 2014 study, Valdemarsen et al. (2012) found that comparable current conditions in their study sites had a negative effect on the ecological state of the sea floor sediments.

2.4 Onarheimsfjorden

The material used in this work was collected in Onarheimsfjorden, an area on the western rim of Hardangerfjorden, some 10km inside the Huglo sill in Tysnes municipality (Figure 2.1). Onarheimsfjorden has an area of approximately 35 km^2. Relative to the main fjord it is a shallow basin: in general, the area has a flat surface at around 100 m water depth with the deepest point at 136 m depth. A sound in the NW corner of the basin connects Hardangerfjorden with Børnafjorden. In the sound, the tidal currents which change direction every two hours may reach velocities up to 1,5-3 m/s (Kartverket Sjødivisjonen, 2016). Several streams run into Onarheimsfjorden. The largest, Onarheimselva, has a mean discharge of 2.181 m^3/s (Hellen et al., 2013). Settlement of people is sparse along the coast of Onarheimsfjorden presumably because of the topography in the area. A hatchery is located at the river mouth of Onarheimselva. Two other fish farms are found in Onarheimsfjorden, the one used for this study (Figure 2.3) and another fish farm is located in the NE corner of area, directly above the rim of the Onarheimsfjorden shelf. The fish farm used for this study has 10 25x25 m net cages plus three 35x35 m net cages. The facility is moored in one end, which enables the cages to rotate freely around the anchoring point with the prevailing wind and current direction (Figure 2.5). The length of the facility including the mooring cable is 284 m, which means potential waste is distributed over a much larger area (0.25 km^2) than if it was stationary.

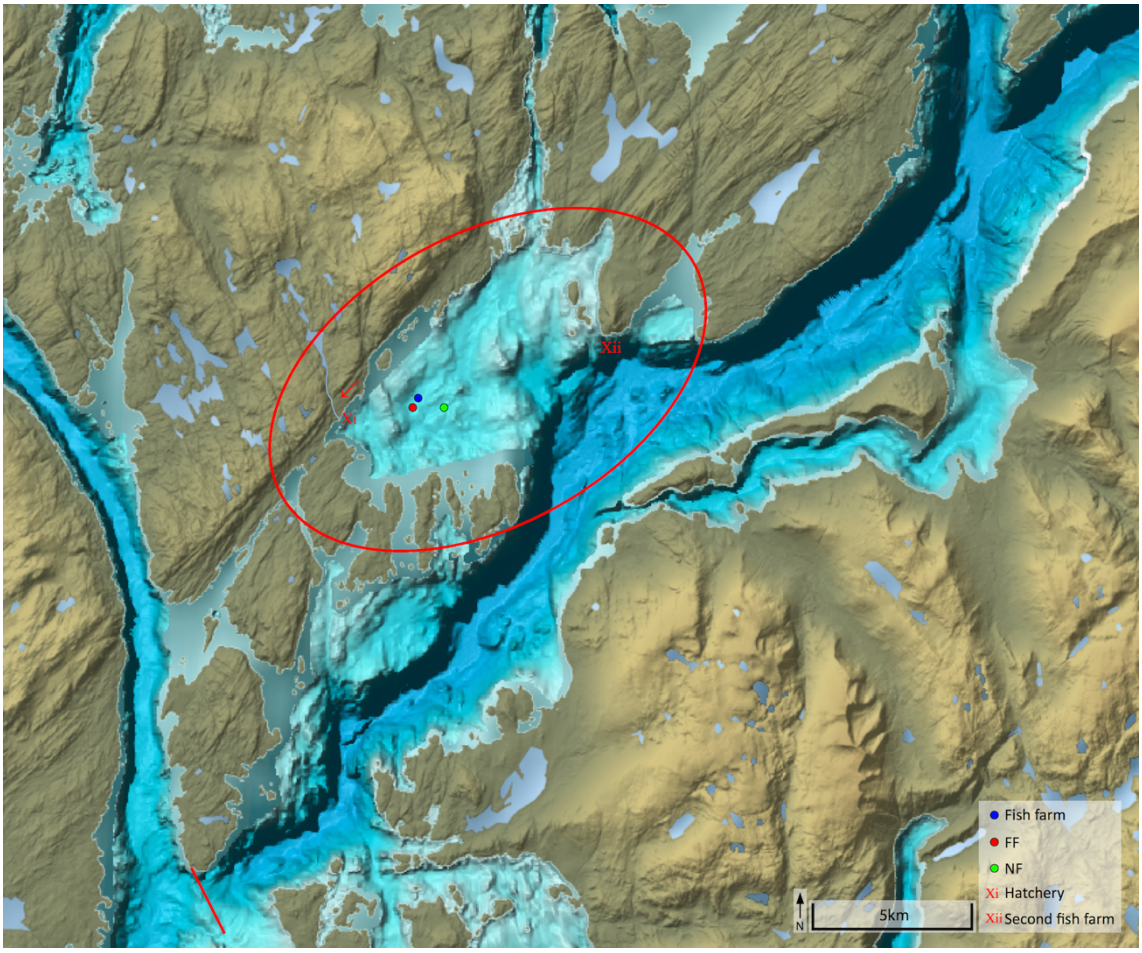

Figure 2.3: Bathymetric map of Onarheimsfjorden (encircled) in Hardangerfjorden. FF = fish farm, 100 m from the fish farm. NF = non-fish farm, 500 m away from the fish farm. Red line in bottom left corner marks the outer sill by Huglo (Figure 2.1), red arrow marks position of Onarheimselva (modified from www.kartverket.no).

Current measurements were conducted below the fish farm over a 4-week period in 2012 and showed a mean current velocity of 4.9 and 4.6 cm/s at 5 and 15 m water depth, respectively (Anon, 2012), which indicates moderately good conditions with respect to particle dispersal (Y. K. Johansen, 2016). Current directions were evenly distributed along each sector in the shallow part of the water column, which means the orientation of the fish farm varies a lot. The current which is considered the most important for particle dispersion at 15m depth showed a more dominant (57%) SW direction (Anon, 2012). There are no available data on bottom currents in the basin.

To monitor the influence of farming operations on the fjord ecosystems, fish farmers in Norway are obliged to conduct environmental surveys (Modelling-Ongrowing fish-farm Monitoring, abbreviated MOM) directly beneath and in the recipient area of the fish farm (in accordance with NS 9410:2016). The environmental conditions are classified according to standards set by The Norwegian Environmental Agency (Bakke et al., 2007; Molvær, 1997).

Extensive surveys (MOM-C) are required before establishing new farm sites and less thorough surveys are routinely conducted every year, or more frequently depending on previous results. No hydrographic measurements were performed in the study area during the cruise in 2016, so CTD-measurements from a MOM-C survey in March 2014 (Ingebrigtsen et al., 2014) are used as basis for the water quality evaluation in the area around the fish farm.

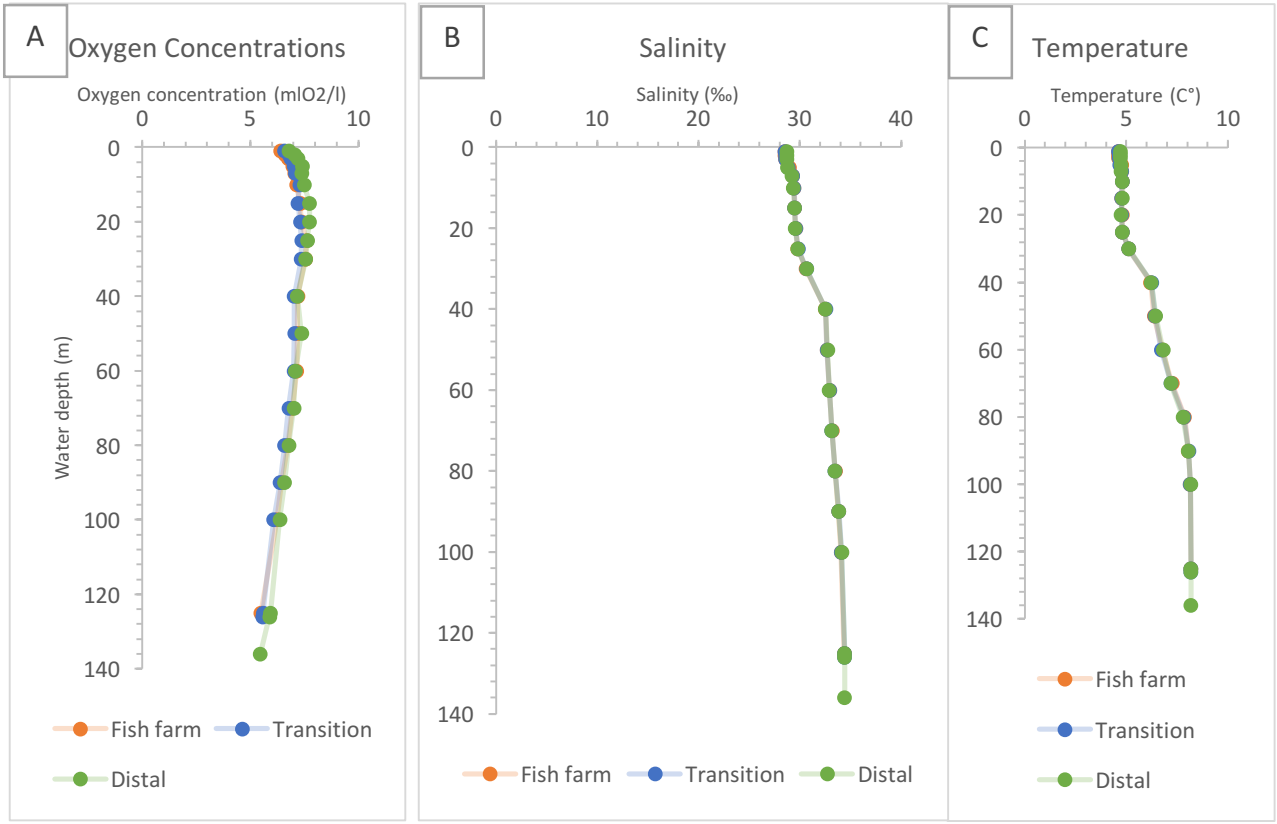

Figure 2.4 A-C: CTD-data from MOM-C survey conducted in March 2014. 'Fish farm' is located directly below the fish farm, 'Transition' and 'Distal at 300 m and 1000 m away from the fish farm, respectively. A: Oxygen concentrations. B: Water salinity. C: Water temperature (Ingebrigtsen et al., 2014).

All three stations show similar results throughout the water column (Figure 2.4 A-C). A salinity increase (29 – 32%) in the depth interval 25 – 40 m indicate the transition from the upper brackish layer to coastal water. The highest recorded salinity value is 34.4‰, which indicates that Atlantic water is not present. As mentioned above, deep water renewal would be expected to happen later than March. However, CTD data from two stations located in the main fjord north and south of Onarheimsfjorden recorded salinities > 35 at 100 m depth on only one occasion in the period between 2004 – 2016. Regardless, the measured oxygen concentrations are within class 1 (very good), throughout the water column (Molvær, 1997). Water temperature increases in the same depth interval as the salinity, suggesting the pycnocline is reached at 40 m.

The fish farm has been in production since 1994. Mean annual fish feed consumption in the period 2011-2013 was 2500 tons, which would result in 437 tons of organic waste dispersed in the Onarheimsfjorden basin, following the estimates of Brooks and Mahnken (2003). Previous environmental surveys (Børsheim, 2007; Haveland, 2005, 2009, 2011; Ingebrigtsen et al., 2014; P. O. Johansen and Botnen, 2008; Y. K. Johansen, 2016) have shown evidence for a benthic impact due to organic loading, but the environmental condition at the site was within acceptable limits (ranging between 1, "very good" to 2, "good") at the time of all investigations.

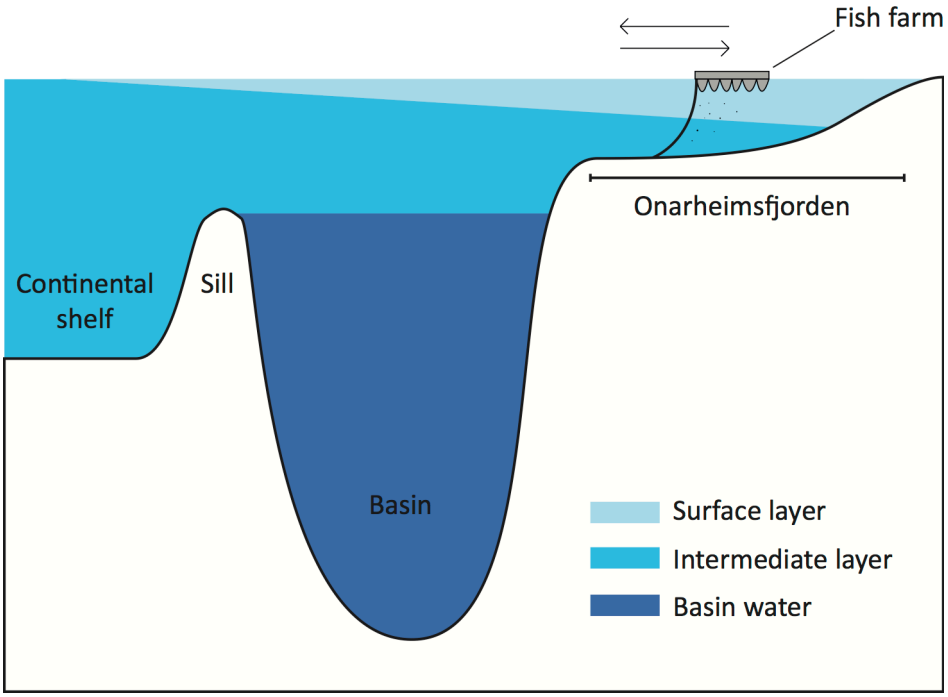

Figure 2.5: Conceptual illustration of Hardangerfjorden (basin) and Onarheimsfjorden with the fish farm anchored at the sea floor. Arrows indicate the fish farm's movement. Colors indicate the theoretical stratification of the water column. Note that proportions are not correct.

3 Methods

3.1 Sample collection and preparations

Sediment samples were collected during a cruise with the vessel M/S Solvik, conducted as a part of the NFR funded "Jellyfarm" project on 29 August 2016. Sediments from two stations were collected, one fish farm (FF) station and one control station, non-fish farm (NF). The FF station, 100 m south of the fish farm, represented the sea floor in the area under most influence of the fish production. The original plan was to sample within 50 m from the fish farm, but the crew was not allowed closer than 100 m due to safety reasons. The NF station, situated 500 m east of the fish farm, served as an example of conditions unaffected by potential organic waste from the fish farm. Using a random stratified sampling design in excel, random coordinates at correct distance from the fish farm were selected for both stations. Bathymetric measurements were done before sampling to make sure the sea floor was adequately flat.

The device used for sampling was a Gemini Gravity Corer (Winterhalter, 2001). This device has a set of twin cylinders (8 cm diameter) and is lowered into the sediments from a winch on deck. Once the device descends into soft sediment, a lock is released so that two beams trap the sediment inside the cylinders. This way it is possible to penetrate soft sea floor with minimal physical disturbance on the sediments. Two deployments were performed at each station, yielding four replicates from each station. Station details are listed in Table 3-1.

Table 3-1: Station details.

Station	Fish farm	Fish farm	Control	Control
Replicate name	AKS199	AKS201	AKS202	AKS203
Depth	127m	127m	113m	113m
Position	59 57.000N 005 40.043E	59 57.000N 005 40.043E	59 57.132N 005 41.058E	59 57.132N 005 41.058E
Used for	Logging	Analysis (FF)	Analysis (NF)	Logging

After visual inspection on board, the sediment cores were extruded by a piston and sliced as following: one core from each site was sliced in 1 cm thick intervals down to 20 cm, from

where every 2 cm was sliced. The longest fish farm core (AKS201, referred to as FF-core from here on) was sliced down to 29cm while the control core (AKS202, referred to as NF-core from here on) was sliced down to 30 cm. Each core yielded 25 samples. Samples were immediately stored in a freezer (- 20° C). The remaining twin core from each station was sliced every cm down to 10 cm depth. The remaining sediment in the second core was then pushed out on deck where it was split vertically, allowing for logging the sediment characteristics.

After the cruise, the samples were transported frozen to the University of Oslo (UiO). In the lab, the samples were weighed in their frozen (wet) state before they were freeze dried using a Christ Alpha 1-4LD pluss and a Christ Alpha 1-4 freeze dryer. At the right temperature and pressure, the frozen water sublimates and goes directly to gas phase, effectively removing water with minimal disturbance to the material. After freeze drying the samples were weighed again. The water content was calculated as % of wet weight by subtracting the dry weight from the wet weight.

3.2 Sediment dating

Approximately 7 g of dry sediment from each layer was weighed, labelled and shipped to Environmental Radioactivity Laboratory at Liverpool University for geochronological dating. Each sample was analysed for ^{210}Pb, ^{226}Ra, and ^{137}Cs by direct gamma assay, using Ortec HPGe GWL series well-type coaxial low background intrinsic germanium detectors (Appleby et al., 1986). The ^{210}Pb radioactive isotope has a half-life time of 22.3 years which makes it useful for dating recent (0 – 150 years) sediments. ^{210}Pb is produced in the ^{238}U decay series. ^{210}Pb will therefore be produced naturally within sediments, termed supported ^{210}Pb. In addition, fallout of ^{210}Pb from the atmosphere creates a flux of unsupported ^{210}Pb, which is assumed to be constant. The decay of the unsupported lead isotopes can be calculated once buried within the sediments by subtracting the supported ^{210}Pb from the total activity, and the values corresponds to sediment age (Appleby, 2001). ^{137}Cs is an artificial radionuclide which were dispersed in relation to atmospheric testing of nuclear weapons (from which ^{137}Cs fallout peaked in the early to mid 1960s) and more recently, to the nuclear disaster in Chernobyl, 1986 (Appleby, 2001). The ^{137}Cs peaks are used for calibrating the ^{210}Pb dating. At a point in each core the unsupported ^{210}Pb signal gets too weak, from where the dating is unreliable. Samples below this point may be dated by extrapolating the mean age-difference between the two deepest dated samples in each core.

3.3 Organic carbon (TOC) content, total nitrogen (TN) content and δ15N and δ13C of the sediments

Approximately 1.5 g of dry, pulverized sediment was shipped to Iso Analytical, a UK lab specialised in stable isotope analysis. Each sample was analysed for total organic carbon (TOC), total nitrogen (TN) as well as stable N- and C isotopes. For the carbon analysis 500 mg of each sample was prepared by adding 1M hydrochloric acid which was left overnight. The treatment removed inorganic carbon in the sediments. The samples were then neutralised by repeated washing and oven dried at 60 °C. The analysing procedure was identical for both measurements: samples and reference material was placed in a Europa Scientific elemental analyser where they were loaded into a combustion furnace. In short, the gases produced during combustion goes through a series of filtering processes before the gas of interest (CO_2 for carbon analysis and N_2 for nitrogen) are led into a Europa Scientific 20-20 Isotope Ratio Mass Spectrometer where it is ionised and accelerated. Isotopomers with the correct mass/charge ratio for the analysis in question (N_2 at m/z 28, 29, and 30, CO_2 at m/z 44, 45, and 46) is separated in a magnetic field and measured in a Faraday cup collector array (see Appendix B for more details). The TOC values were normalised to sand content (TOC63) according to Rygg (1995).

3.4 Heavy metal concentrations

Analysis of samples for heavy metals was performed according to Norwegian Standard (NS4770/1994). Approximately 1 g of dried sediment was ground in an agate mortar and put in teflon containers. 20 ml 7,22M HNO^3 nitric acid was added to each container before they were put in an autoclave. The autoclave enables samples to reach higher temperatures without boiling. Samples were heated under 200 kPa (corresponding to 120 °C) for 30 minutes. The acidification and heat treatment adsorbed any metals attached to sediment so that the metals were dissolved when the process was finished. The samples were then centrifuged before 5 ml of the upper, clear solution was extracted and put in separate containers. From the 5 ml undiluted samples 0.02 ml was put in new containers, which was then diluted 50 times by 1 M HNO_3. The diluted samples were then set up for analysis using a Multicollector-ICPMS. The device was programmed to measure values of chromium (Cr), copper (Cu), zink (Zn), cadmium (Cd), lead (Pb). These are common pollutants frequently being analysed for in similar studies and in MOM-surveys, which then are comparable.

3.5 Particle size distribution analysis

A Beckman Coulter LS13320 laser instrument was used for particle size analysis. Each sample was gently dry sieved through a 2mm sieve. Grains larger than 2mm were weighed and put aside in separate containers, as they were too big for the instrument. Sediments < 2 mm was then homogenised and placed on a scale. A small amount of material (ranging between 0.8 g – 1.2 g) was extracted and mixed with the deflocculating agent calgon $(NaPO_3)_6$ before the containers were put in a sonic bath. This procedure dissolves any fecal pellets and other aggregates in the sediment. Samples were then poured into the Beckman Coulter keeping the obscuration below 12%. In short, the instrument measures the scattering pattern formed by particles as they flow past a laser beam. Each pattern corresponds to particle size, and different pattern detections are counted and grouped according to their corresponding size. The cumulative percentages of each group for each sample was then calculated. The analysis was run twice for each sample and the mean value for each parallel analysis was calculated.

3.6 Micropaleontological analysis

From each sample, 5 g of dry sediment was wet sieved through both a 500 μm sieve and a 63 μm sieve. The larger mesh was used to filter out macrofauna and clastic material while the 63 μm mesh is an adequate size for most foraminiferal studies (Murray, 2006). Samples were dried to constant mass at 40-50° C. To avoid clusters of grains, the fine fraction was carefully dry sieved (500 μm) before both fractions from each sample were weighed and put in separate containers. The sediment of 63 - 500 μm was divided into four equal parts by an Otto Microsplitter. ¾ of each sample was used for picking foraminiferal tests for stable isotope analysis, while the remaining ¼ was used for fauna analysis. The sediments from the NF-core did not have enough sediment/microfossils for fauna analysis after the wet sieving of 5 g. An additional 10 g of sediment was therefore extracted from the control samples and the process was repeated.

One sample from every 5 cm interval from each core was used for foraminiferal assemblage analysis. Additional samples were analysed in intervals of particular interest. The fraction 63-500 μm of the selected samples was evenly distributed in a tiled picking tray placed under a binocular microscope. Where possible, at least 200-300 individuals were picked (Murray, 2006). Individuals were sorted by species, counted and catalogued in a spreadsheet. The

absolute abundance of individuals was normalised to the dry weight of the sediments. Benthic foraminiferal accumulation rates (BFAR) were calculated following Herguera and Berger (1991), based on calculated sediment accumulation rates from sediment dating. By the use of PRIMER (Plymouth Routines In Multivariate Ecological Research) version 6.1.13. (Clarke and Gorley, 2006) the diversity indices H'_{log2} (Shannon and Weaver, 1949) and ES_{100} (Hurlbert, 1971) were calculated. The mentioned formulas produce a number based on the foraminiferal composition, which were used to assess Ecological Quality Status (EcoQS) (Veileder 02:2013). In Alve et al. (2016) different species of benthic foraminifera were assigned to ecological groups based on their tolerance to organic matter supply, following the criteria for AZTI Marine Biotic Index (AMBI) (Borja et al., 2000). The relative abundance of foraminifera from each group were used to calculate a Foram-AMBI in each sample. The resemblance among pairs of samples was based on the Bray-Curtis similarity coefficient (Bray and Curtis, 1957). √-transformation was performed, but omitted as the transformation did not yield substantially different values. PRIMER was also used to analyse faunal similarities through cluster analyses a non-metric multidimensional scaling (MDS) ordinations (Clark et al., 2001).

3.7 Stable isotope analyses of foraminiferal tests

Well preserved foraminiferal tests of 3 calcareous species (*Cassidulina laevigata, Hyalinea balthica* and *Uvigerina peregrina*) were picked to be used for ^{18}O isotope and ^{13}C isotope analysis. To avoid ontogenetic effects from smaller individuals and because a certain mass of foram tests are needed, each sample was carefully dry sieved through a 150 μm mesh. The selected species have proven to be useful in such analyses (Brückner and Mackensen, 2008; Kjennbakken et al., 2011; Schmiedl et al., 2004). Every test (ranging between 2 – 20) of the species was identified under a microscope and picked from every horizon in both cores and shipped to The Leibniz Laboratory for Radiometric Dating and Stable Isotope Research in Kiel, Germany. Stable isotope composition was measured using a Kiel IV preparation device connected to a MAT253 mass spectrometer and calibrated to the international carbonate standard NBS-19 and lab internal standards. The precision of the measurements was ± 0.03‰ for ^{13}C and ± 0.08‰ for ^{18}O. For samples with sufficient tests, duplicate analyses were performed to confirm the precision. Results are expressed relative to Vienna Pee Dee Belemnite (VPDB).

4 Results

The results for each core are described individually below. Raw data can be found in the appendices (C-G). Table 4-1. gives an overview of the ecological classes genrally used to classify the sediments and their limitation values.

Table 4-1: Classification intervals for soft marine sediment. Diversity indices based on H' and ES(100) (Veileder 02:2013), heavy metal concentrations (Veileder M-608:2016).

EcoQS	Background	Good	Moderate	Poor	Bad
H'	>3.8	3.0-3.8	1.9-3.0	0.9-1.9	<0.9
ES(100)	>25	17-25	10-17	5-10	<5
mg Cd/kg	<0.2	0.2-2.5	2.5-16	16-157	>157
mg Cr/kg	<60	60-660	660-6000	6000-15500	>15500
mg Cu/kg	<20	20-84	-	84-147	>147
mg Pb/mg	<25	25-150	150-1480	1480-2000	>2000
mg Zn/kg	<90	90-139	139-750	750-6690	>6690

4.1 Fish farm station, FF-core

The lower 14 cm of the FF-core were homogenous, dense and predominantly dark blue clay. Streaks of lighter, brown sediments were observed at 15 cm depth, from where a transition was observed to 4 cm core depth. In this interval, the dark blue sediments became increasingly lighter and brown. Between 7 - 4 cm core depth the sediments became less dense with increasing water content. The topmost 4 cm sediments were gray with a greenish tint. These layers were soft with 50 - 60% water content (Figure 4.1B). Traces of bioturbation were observed down to 6 cm core depth. A sea urchin was found at 3 cm core depth. A small depression in the otherwise smooth surface are possibly a result of burrowing from the sea

urchin. One bivalve shell (< 10 mm) was observed on the sediment surface. The core was sliced down to 29 cm depth.

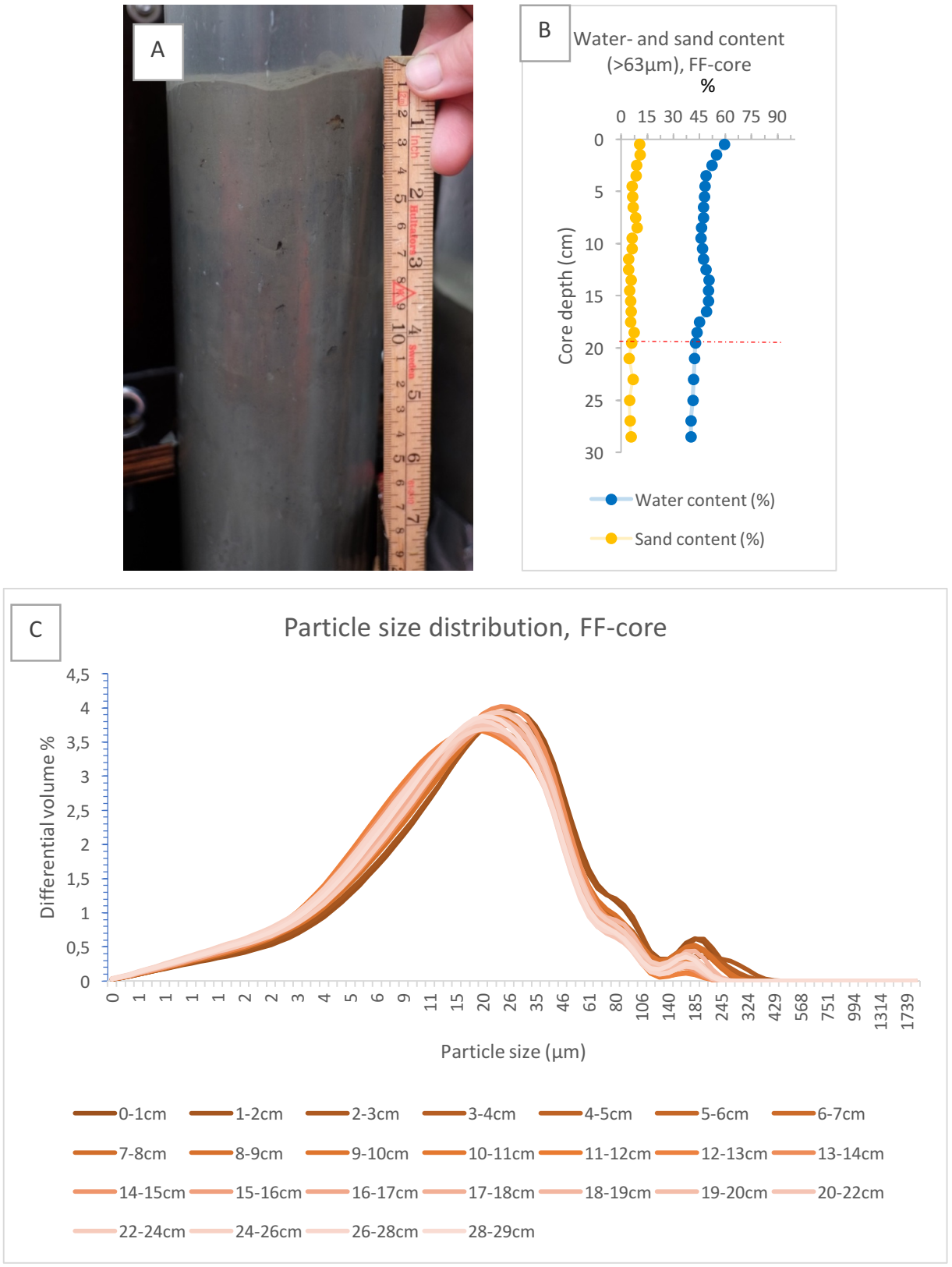

Figure 4.1A-C: A: FF-core under inspection. B: Water- and sand content. Red line marks the dating horizon. C: Differential volume of the complete grain size range.

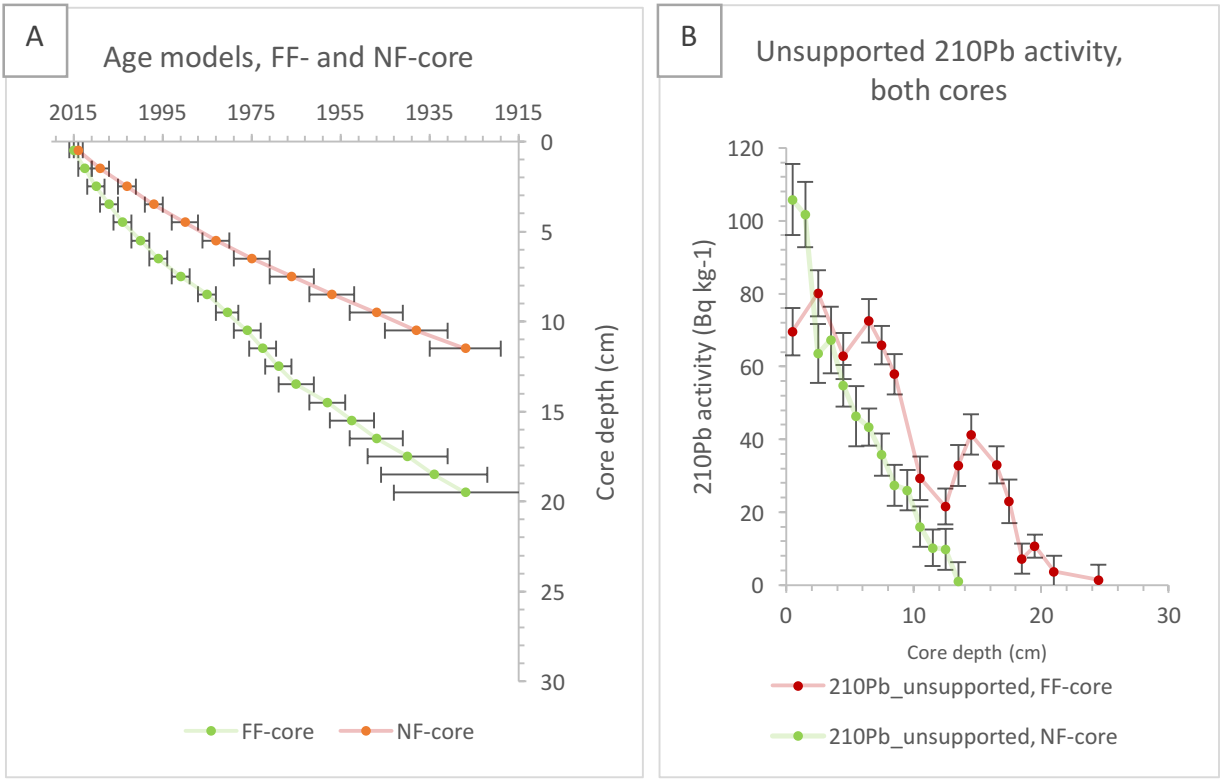

Figure 4.2A-B: A: Age models for FF- and NF-core. Note how error margins are increasing down core. B: Unsupported (i. e. radionuclides from atmospheric fallout) 210Pb-activity in both cores.

The $^{210}Pb/^{226}Ra$ equilibrium was reached at 20 cm core depth, below which point dating was not possible (B). This dating horizon is indicated with a dashed red line in the included figures. The lowermost measured sample at (19.5 cm) is dated to 1927 (89 (± 16) years old). Two ^{137}Cs peaks were identified. The lower peak was in good agreement with the ^{210}Pb dating at 1963 and is thus considered to mark the end of nuclear testing period (Appleby, 2001). The upper ^{137}Cs peak at 6 – 7 cm corresponds to the mid-1990s and cannot be considered a reliable calibration by the Chernobyl accident. Calculated sediment accumulation is stable from 1927 – 1965 (0.13 (± 0.02) g $cm^{-2}y^{-1}$). Between 1969 and 1991 the average sediment accumulation increased to 0.17 g $cm^{-2}y^{-1}$ and from 1996 to present it is calculated to 0.23 (± 0.02) g cm^{-2} y^{-1} (Figure 4.9)

The lower 11 cm of the core had just over 40% water content (B). From this point water content had an increasing trend (40 – 50%) up to 4 cm from where water content increased to 60% in the surface sediment. Average sand content (> 63 µm) in the FF-core was 6.5%. Sand content was stable at 4 – 6% in sediments below 10 cm before it increased to 10% in the surface sediment (Figure 4.1B).

Figure 4.1C displays differential volume of the complete grain size range for each sample. It shows a well sorted, uniform grain size distribution centered around 20µm (silt size).

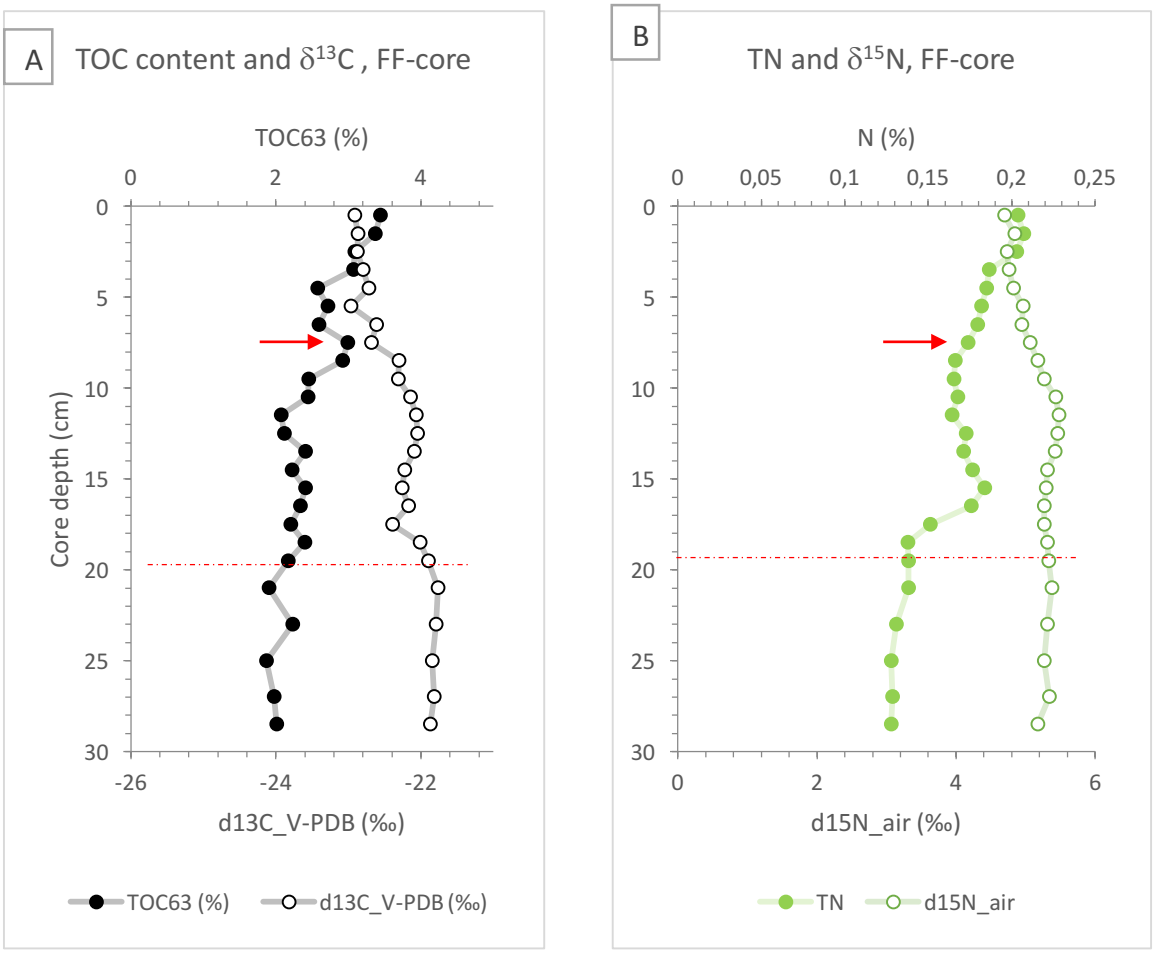

Figure 4.3A-B: A: TOC content and stable carbon isotope ratio, FF-core. B: Total nitrogen content and stable nitrogen isotope ratio, NF-core. Dashed red line indicates dating horizon. Red arrow marks the onset of fish farming.

Total organic carbon (TOC63) content ranged between 1.8 – 2% in the lower 18 cm of the core (Figure 4.3A). From 10 cm core depth, TOC content increased gradually to its highest recorded value in the surface sample at 3.4%. A similar trend was observed with total nitrogen (TN) (Figure 4.3B). The lower 10 core centimeter TN concentrations ranged around 0.13% before they increased to 0.18% at 16 cm core depth. From here on the signal was stable before they increased in the upper 3 cm (to 0.2% in average). The C/N signal was stable throughout the core with a mean value of 7.9 (± 0.35). The stable C-isotope signal was stable at around -21.8‰ in the lowermost 10 cm of the core. It became gradually lighter towards the surface sediment which had the lowest recorded value (-22.91‰ relative to Vienna Pee Dee Belemnite). The stable N-isotope composition followed a similar discrete trend with an increasingly lighter signal up-core.

Heavy metal concentrations (Figure 4.4) followed an increasing trend up-core, with the exception of Cr which had its highest concentrations in 20 – 29 cm core depth. However, concentration peaks of Cr, Pb and Zn are identified throughout the core, and the highest values are reached at 16 cm core depth (dated to 1947). All heavy metal concentrations indicate 'good' classification, apart from Zn which is classified as 'moderate' in the surface layer and at 13 and 16 cm depth.

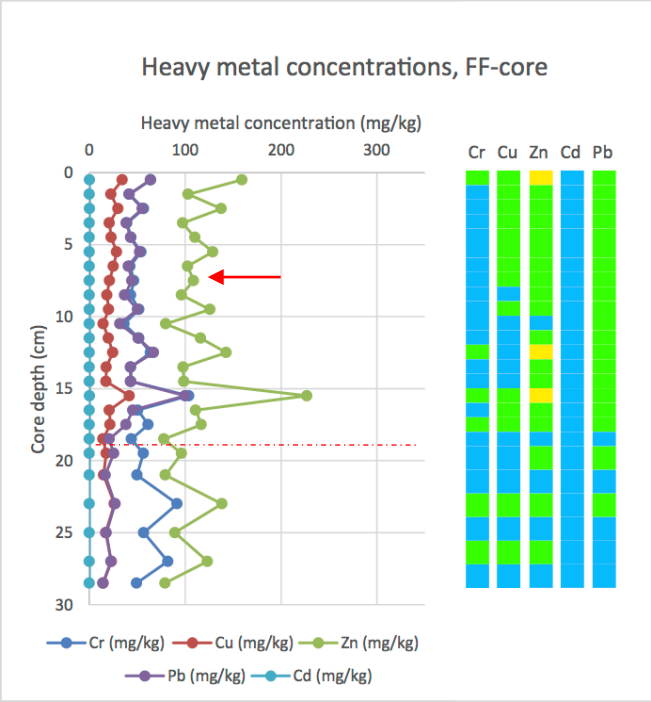

Figure 4.4: Heavy metal concentrations and their corresponding environmental classification (Table 4-1). Dashed red line marks the dating horizon, red arrow marks the onset of fish production.

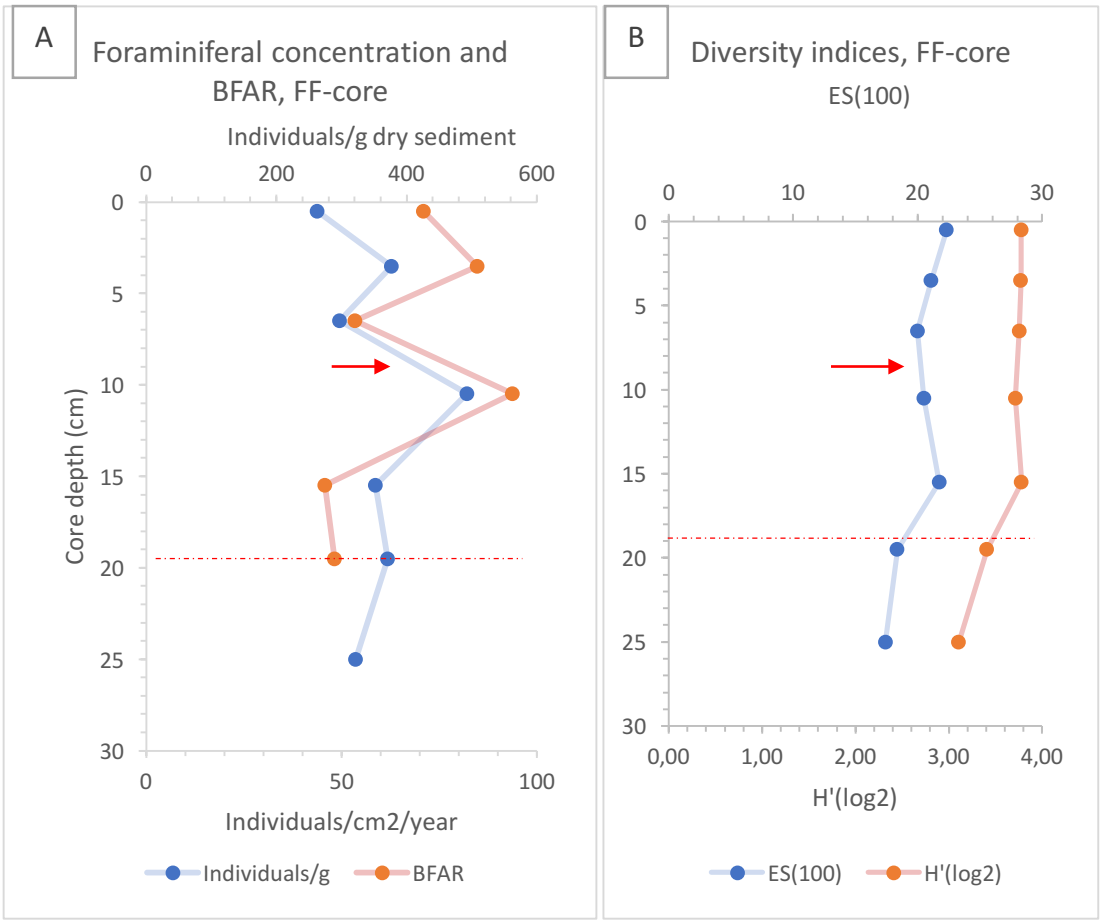

Figure 4.5 A-B: A: Foraminiferal concentration and BFAR, FF-core. Diversity indices (ES(100) and H'(log2)), FF-core. Dashed red line marks dating horizon, red arrow marks start of fish production.

Benthic foraminifera were abundant throughout the core. The average foraminifera concentration (individuals/g dry sediment) was 350 in the analysed samples, the highest concentration occurred at 10 – 11 cm core depth (493 individuals/g dry sediment) and the lowest in the surface sediments (263 individuals/g dry sediment) (Figure 4.5A). The BFAR however, generally increased up-core, from 48 individuals cm^{-2} y^{-1} at 19 – 20 cm core depth to 70 individuals cm^{-2} y^{-1} in the surface sediment. In regards to the foraminiferal fauna assemblages the environment in all analysed samples were within 'good' EcoQS (average diversity indices: ES(100) = 20.2; H'(log2) = 3.6) (Figure 4.5B). The most dominant species was *Bulimina marginata* with an average relative abundance of 27%. *Brizalina skagerrakensis* occurred at 4% and 2% in 19 – 20 and 24 – 26 cm core depth, respectively, before it rapidly increased to an average of 14% in the upper 16 core cm. The other recorded species were evenly distributed in the sediments. Figure 4.16A-F and Figure 4.17A-E illustrate a relatively even distribution of the dominant species. The exception is *Textularia earlandi,* which is more abundant in samples deposited from 1996 until present, and *Nonionella iridea*, which has a decreasing relative abundance in recent samples. In the MDS-

diagrams (Figure 4.16A-F, Figure 4.17A-C) post-1927 samples clustered within one group with 65 similarity. The 1927 and pre-1927 sample clustered in a separate group. The relative abundance of agglutinated foraminifera increased up-core from 6% in the lowermost sample to 27% in the surface layer.

The stable carbon isotope composition in the tests of *C. laevigata*, *H. balthica* and *U. peregrina* (>150 µm) showed similar trends between the species (Figure 4.6A), although the variations were significantly greater in the signal from the tests of *H. balthica.* The heaviest signal was found in the interval between 29 – 17 cm core depth (-0.9 – -1.1‰ relative to VPDB for *H. balthica*). A rapid shift to a lighter signal occurred between 18 – 20 cm core depth, from where the signal was relatively stable up-core to the surface (-2 - -3‰ in *H. balthica*). The ^{18}O signal was relatively stable for all three species in the lower 10 cm of the core. At the dating horizon, the values decreased and stabilised again. From here, the signal was stable to the surface sediment for *U. peregrina* while a small decrease in $\delta^{18}O$ is observed in *H. balthica* and *C. laevigata* (Figure 4.6B).

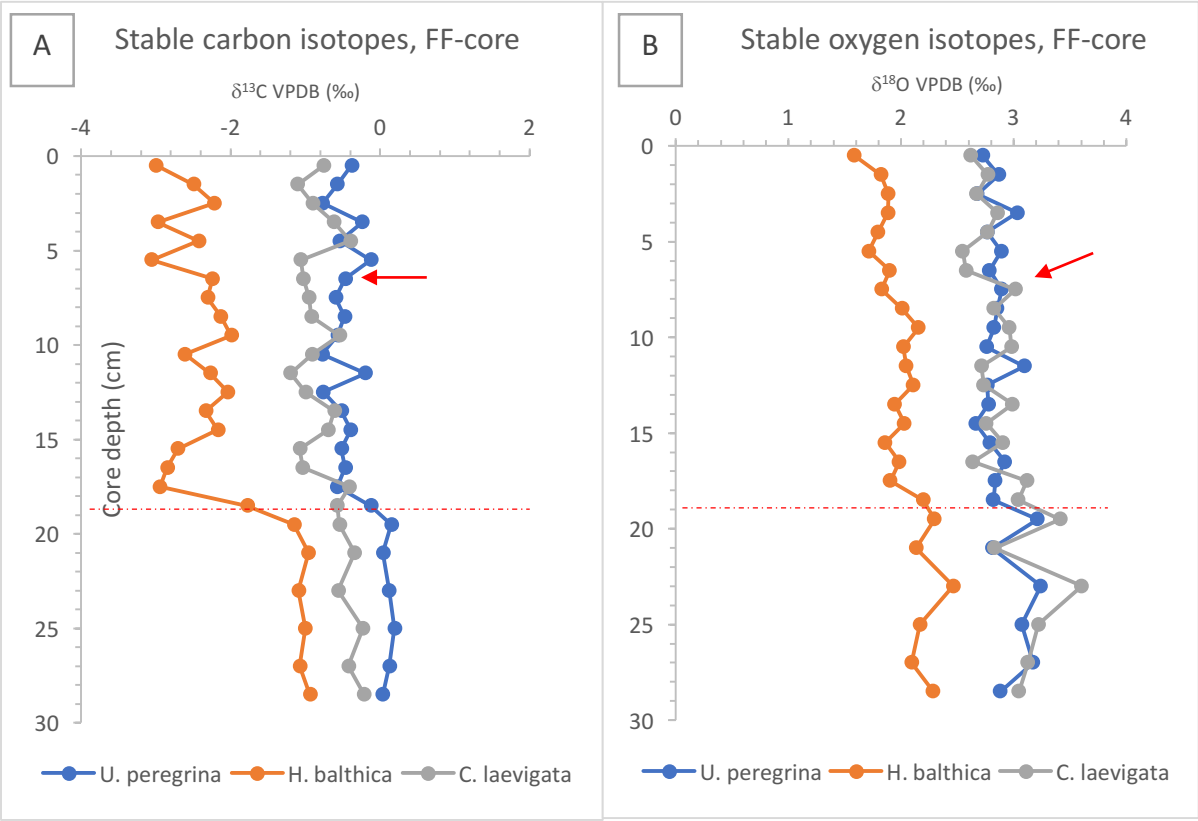

Figure 4.6 A-B: A: Stable carbon isotope composition in tests of *Uvigerina peregrina*, *Hyalinea balthica* and *Cassidulina laevigata*. B: Stable oxygen composition of the aforementioned species. Dashed red line mark the dating horizon, red arrow marks the start of fish production.

4.2 Non-fish farm station, NF-core

The lower 15 cm of the core consisted of homogenous sediments with a dense, sticky texture and dark blue colour only interrupted by a few streaks of brown at 22 – 24 cm (Figure 4.7A). Between 15 – 3 cm core depth the sediments gradually became brown/gray, with streaks of dark blue sediments. At 3 cm core depth, the sediments were loose with a water content of ~50 – 60% (Figure 4.8). The upper 3 cm were gray with a slight green hue. Signs of bioturbation were observed down to 10 cm. Bivalve shell fragments were visible in the upper 5 cm. Worm tubes were observed on the surface (roughly 1/cm^2). The surface was even and undisturbed. One replicate core was split vertically and illustrate the same sediment characteristics (Figure 4.7B).

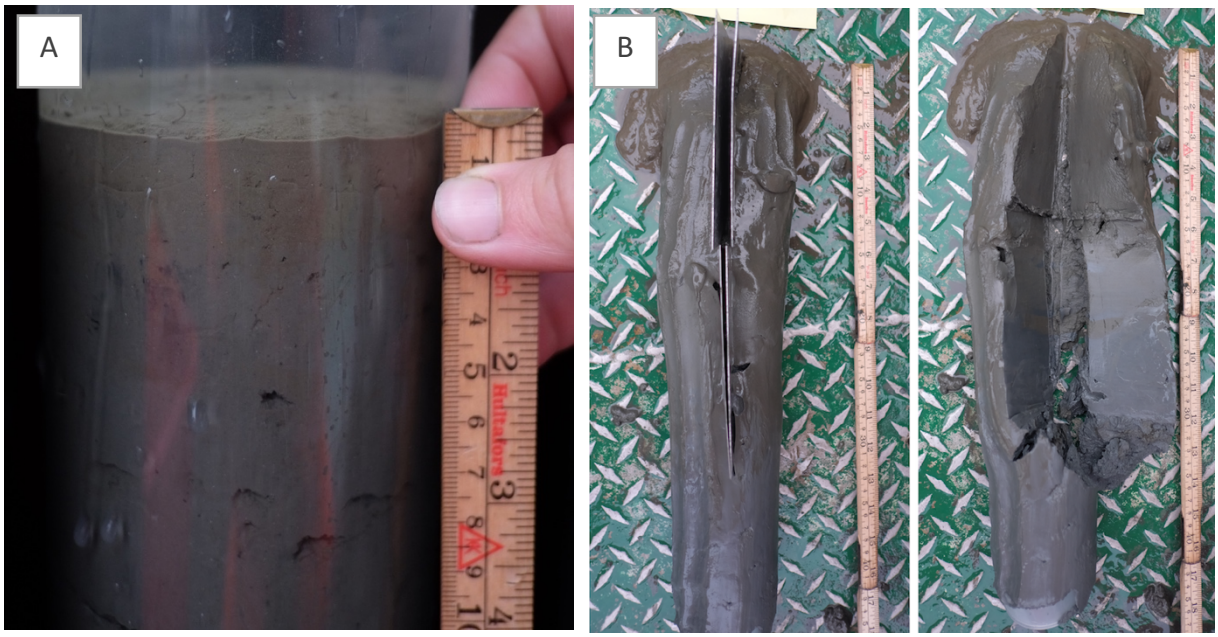

Figure 4.7 A-B: A: NF-core during inspection. B: Replicate core (AKS203) from control station split vertically.

The dating horizon where ^{210}Pb/^{226}Ra equilibrium was reached occurred at 11.5 cm core depth, dated to 1927 (). This horizon is indicated by a dashed red line in figures. The ^{210}Pb activity had an almost exponential decline to the point of ^{210}Pb/^{226}Ra equilibrium which suggests a stable rate of sedimentation. One ^{137}Cs peak was identified at 1 – 2 cm, which does not correspond to the 1987 Chernobyl fallout. Another ^{137}Cs peak was identified at 6 – 7 cm. According to ^{210}Pb activity however, the depth of the second ^{137}Cs is not in perfect agreement with nuclear weapon testing at 1963 and should be interpreted with caution. Sedimentation rate from 1927 was stable at 0.9 (± 0.01) g cm^{-2} y^{-1}, before increasing to its maximum (0.12 (± 0.01) g cm^{-2} y^{-1}) from 1975 to present-day (Figure 4.9).

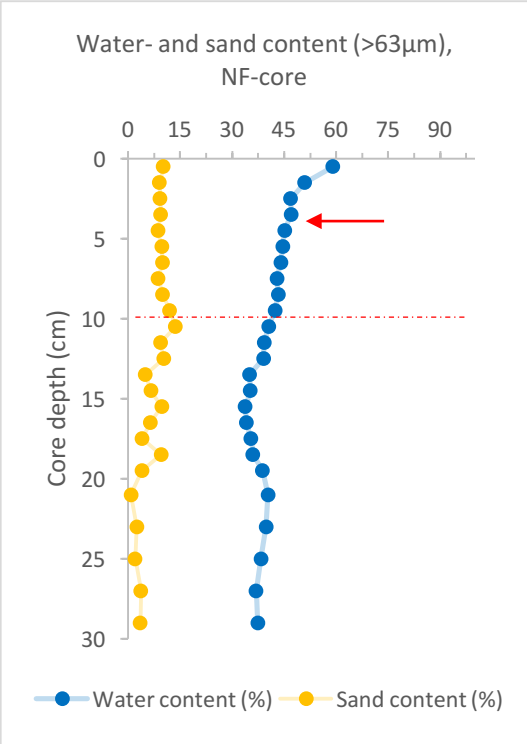

Figure 4.8: Water- and sand content NF-core. Dashed red line marks the dating horizon, red arrow marks the start of fish production.

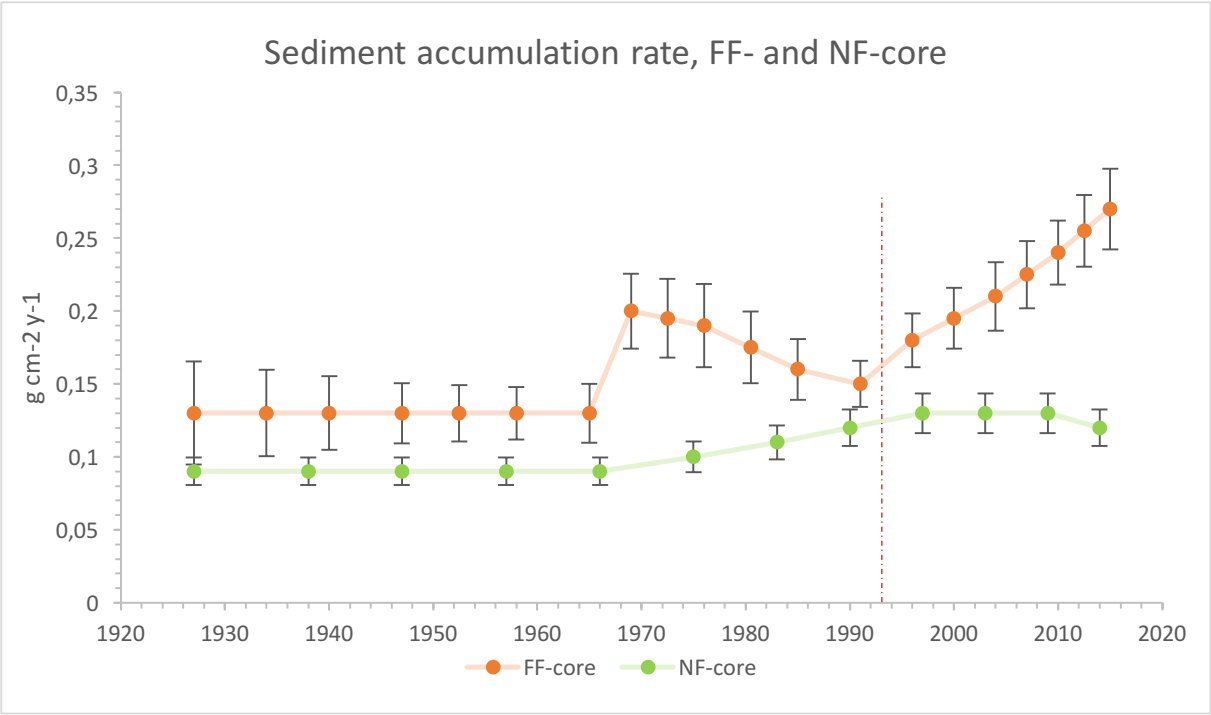

Figure 4.9: Sediment accumulation rates in FF- and NF-core. Dashed red line marks the start of fish production.

The lower 10 cm of the core had a stable water content of 40%, from where it decreased to 33% at 15 cm core depth (Figure 4.8). From 15 cm on, the water content increased steadily up to 60% in the surface layer. Sand (> 63 µm) content in the lowermost 10 cm of the core was 2% on average. There was a general increase in sand content in the interval between 20 – 10 cm core depth with small peaks due to pebbles (2 – 10 mm in size) found in some samples. The curve is stable from 10 cm core depth on to the surface with around 10% sand content. The complete size range plot for each sample is given in (Figure 4.10). The curves of the upper 11 cm samples formed an accentuated dome shape skewed to the right, the peak centered around 30 µm particle size. In the interval between 15 – 11 cm core depth, there was a transition to finer grain distribution from where the curves centered around 9 µm.

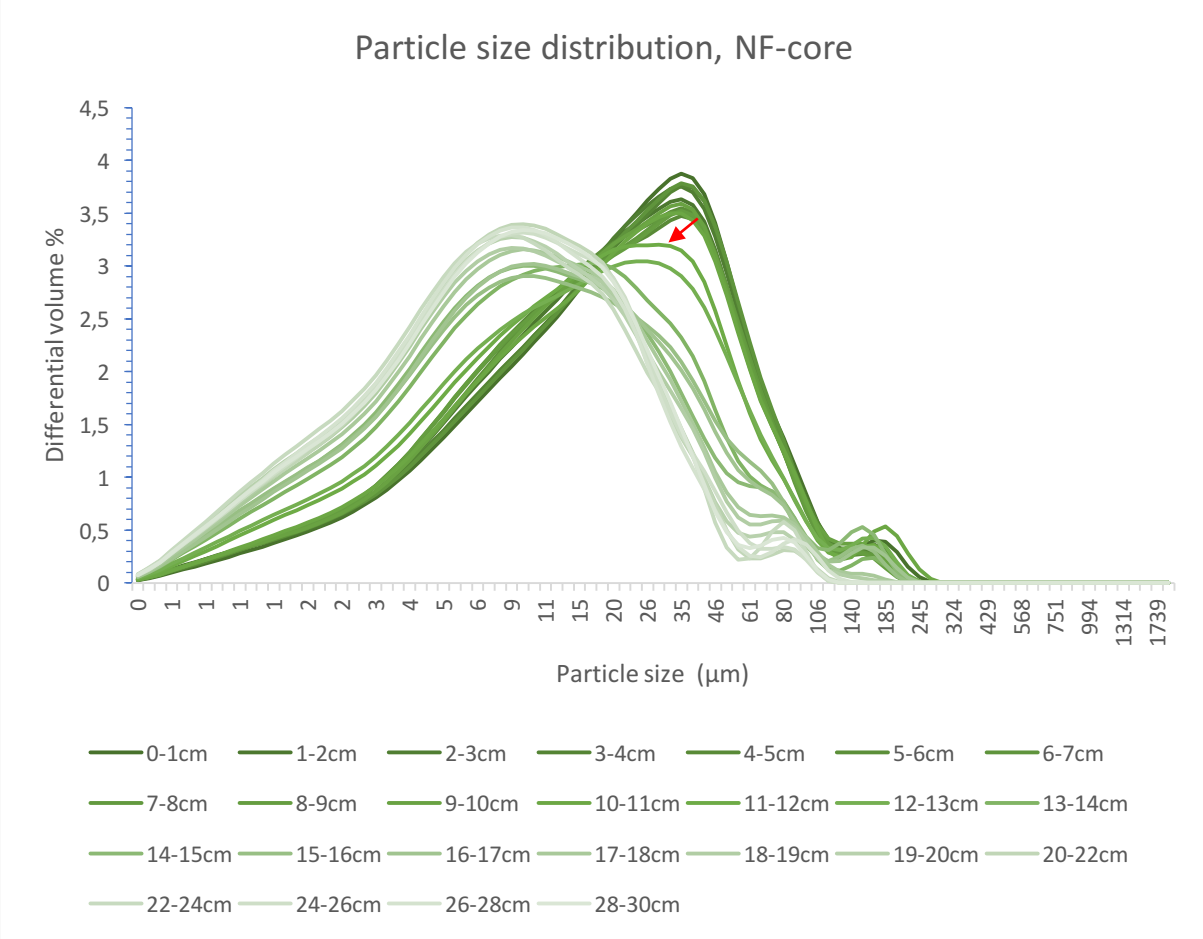

Figure 4.10: Differential volume of the complete particle size range of sediments in the NF-core. Particles > 2mm were not included in the analysis and are therefore not shown in the diagram. Red arrow marks the sample representing the dating horizon.

Between 20-30cm depth both TOC and TN concentrations are stable with a mean value of 0.74% and 0.03%, respectively (Figure 4.11A-B). An increase was observed between 20 – 10 cm and the highest concentration of both TOC and TN were found from 10 cm core depth to the surface (2.5 – 2.8% TOC; 0.12 – 0.14% TN). Stable isotope ratios for the two elements follow the same pattern: δ^{13}C-values were stable at -25.5‰ on average between 30 – 20 cm. The signal got gradually heavier in the interval 20 – 10 cm before stabilised at an average -22.2‰ between 10 – 0 cm core depth. The mean δ^{15}N was 3.4‰ in the lower 10 cm of the core, and increased up to 5.5‰ until 10 cm core depth.

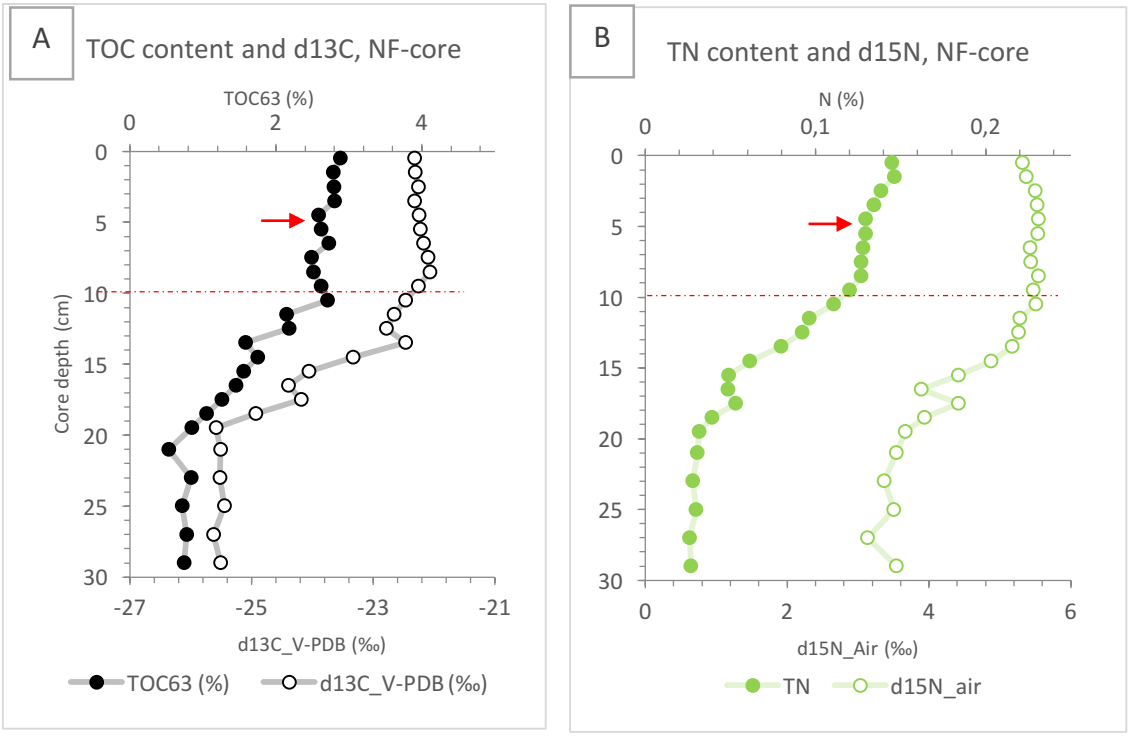

Figure 4.11A-B: A: TOC content and stable carbon isotope ratio, NF-core. B: TN content and stable nitrogen isotope ratio, NF-core. Dashed red line marks the dating horizon, red arrow marks the start of fish production.

The concentrations of heavy metals were all within 'good' or background condition, with the exception of Zn, which was predominantly at moderate levels (Figure 4.12). Concentration peaks of Zn, Cr and Cu occurred in several parts of the core but the highest values were recorded in the interval 30 – 20 cm. From this level, the general trend is stable, apart from peaks at 12, 11, 8 and 1 cm core depth.

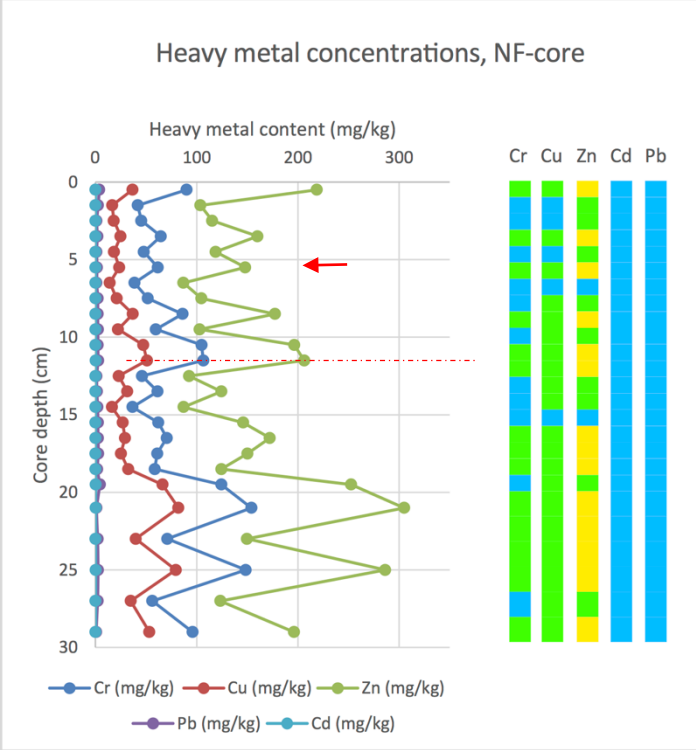

Figure 4.12: Heavy metal concentrations and their corresponding environmental classifications, NF-core. Dashed red line marks the dating horizon, red arrow marks the start of fish production.

Based on the diversity indices H'(log2) and ES(100) (Figure 4.13B), all analysed samples indicated 'good' EcoQS, except for the samples in the intervals 22 – 26 and 19 – 20 cm which were classified as 'moderate'. The concentration of foraminifera in analysed samples between 30 – 10 cm were on average 223 individuals/g dry sediment. The average concentration from 10 – 2 cm core depth was 800 individuals/g. The highest concentration was recorded in the surface sediments (2120 individuals/g dry sediment). BFAR in the upper 12cm is near constant (Figure 4.13A).

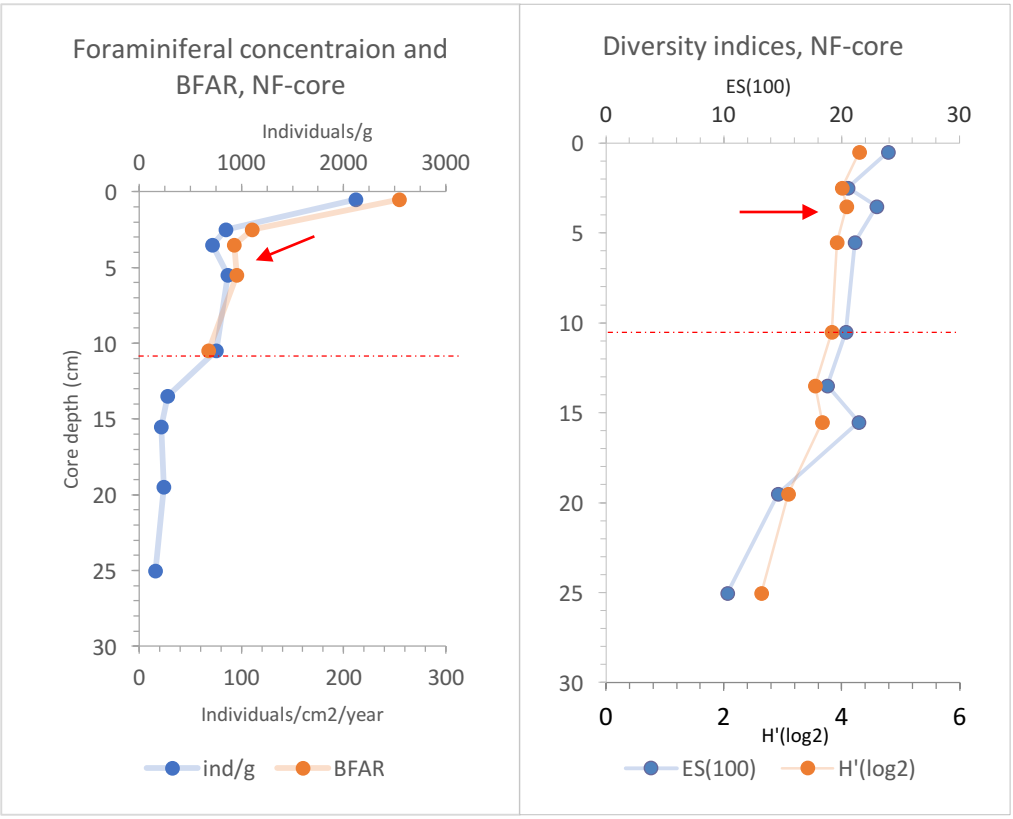

Figure 4.13: A-B: A: Foraminiferal concentration and BFAR, NF-core. Diversity indices (ES(100) and H'(log2)), NF-core. Dashed red line marks dating horizon, red arrow marks start of fish production.

The species with the highest abundance throughout the core was *Cassidulina laevigata* with an average relative abundance of 13%. *Bulimina marginata* had an average abundance of 12%, although the species was close to absent in the samples from the interval 20 – 30 cm. Among the other dominant species there was a clear differentiation between samples above and below 10cm core depth: *Eggerelloides medius* constituted 13% of the populations in the upper part and 2% in the lower, while *Stainfortia fusiformis* occurred on average at 24% in pre-1927 sediments and 4% in sediments post-1927. The MDS analysis based on relative species abundance (Figure 4.14) placed samples from the period 1983 – 2014 in one group, while the 1938 sample was grouped with FF-core samples. Pre-1927 samples clustered in two other groups, two separate groups including 13 – 14 and 15 – 16 cm, 19 – 20 and 24 – 26 cm, respectively. The species abundance illustrated in (Figure 4.16A-F, Figure 4.17A-E) reveal parts of the differences, e.g. the absence of *Brizalina skagerrakensis* and *B. marginata* and the presence of *C. reniforme* in samples from 20 – 30 cm.

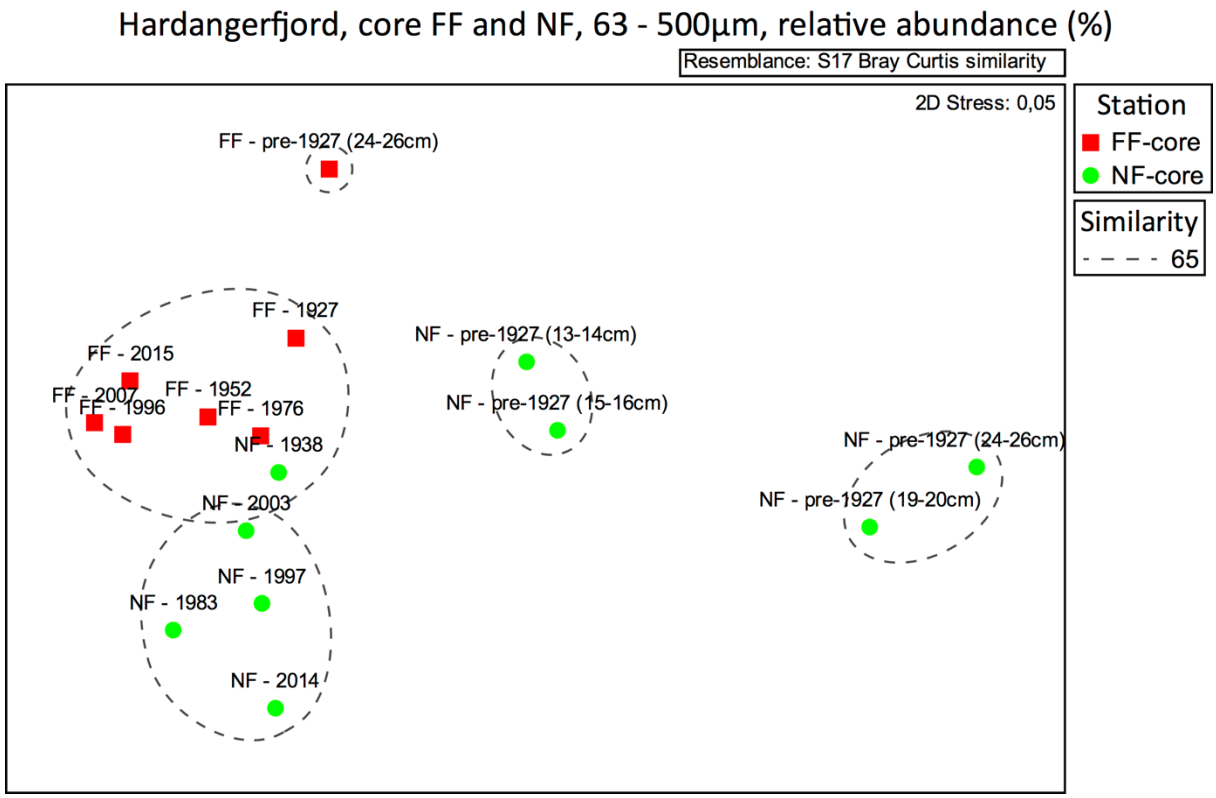

Figure 4.14: Two-dimensional MDS-ordination plot based on faunal assemblage (relative abundance) similarity between analysed samples.

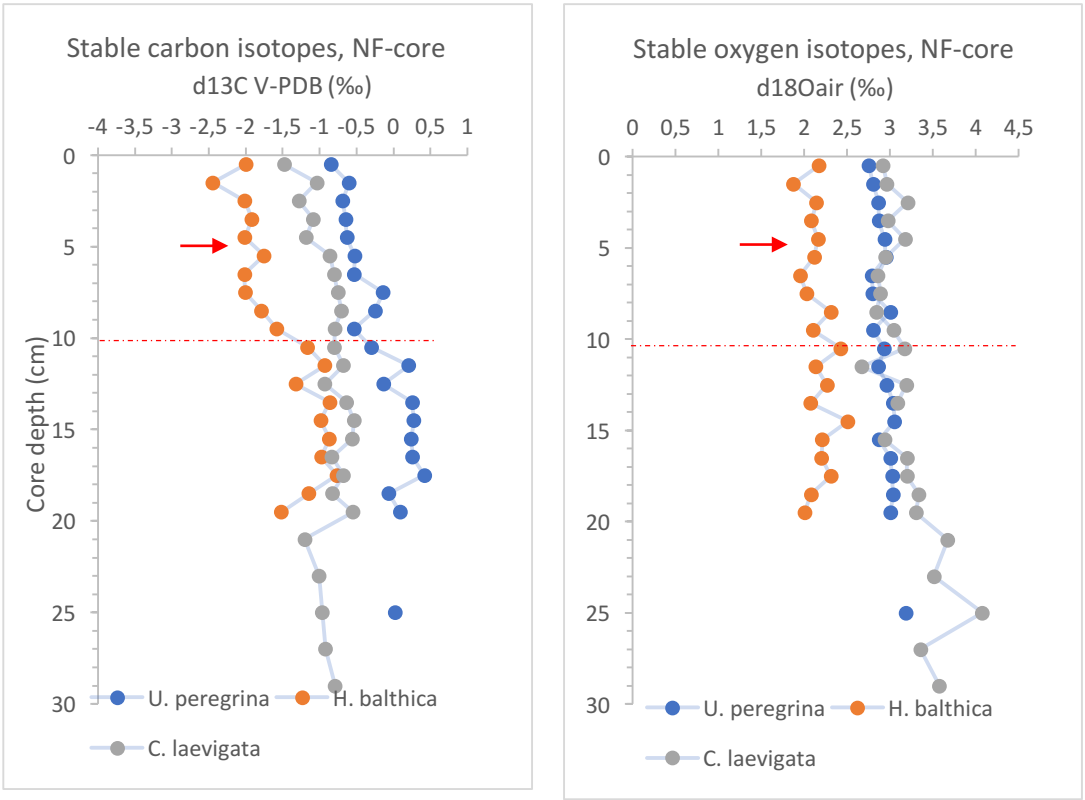

Figure 4.15A-B: A: Stable carbon isotope composition in tests of Uvigerina peregrina, Hyalinea balthica and Cassidulina laevigata. B: Stable oxygen composition of the aforementioned species. Dashed red line mark the dating horizon, red line marks the start of fish production.

Stable oxygen and carbon isotope ratios from foraminiferal tests are shown in Figure 4.15 A and B. Only *C. laevigata* had sufficient specimens for reliable measurements in the interval between 30 – 20 cm. Where all three species were represented, they reflected the same trend. The $\delta^{13}C$ signal was relatively stable in the lower 19 cm of the core. From 11 cm core depth to the surface sediment, the signal gradually became lighter. The oxygen isotope composition was relatively stable for all species throughout the core, apart from *C. laevigata* which indicated a heavier composition in samples between 30 – 20 cm. Measurements from the other species were absent in the same interval.

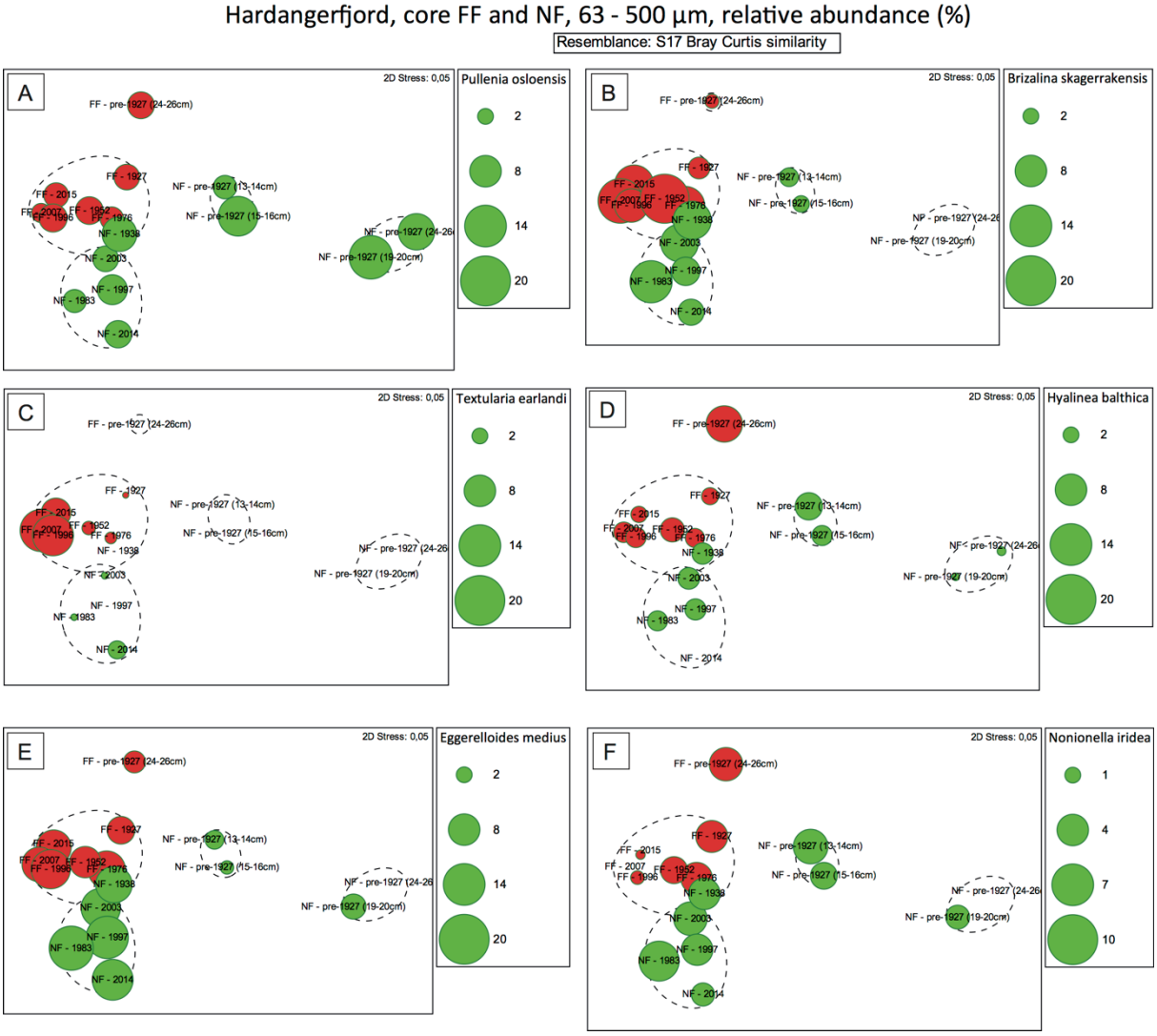

Figure 4.16 A-F: MDS- diagram showing relative occurrence of A: *P. osloensis*; B: *B. skagerrakensis*; C: *T. earlandi*; D: *H. balthica*; E: *E. medius*; F: *N. iridea* in both cores. Sphere size indicate concentration (individuals/g) of the species in each sample. Dashed line indicates 65 fauna similarity. Red spheres = FF-core, green spheres = NF-core.

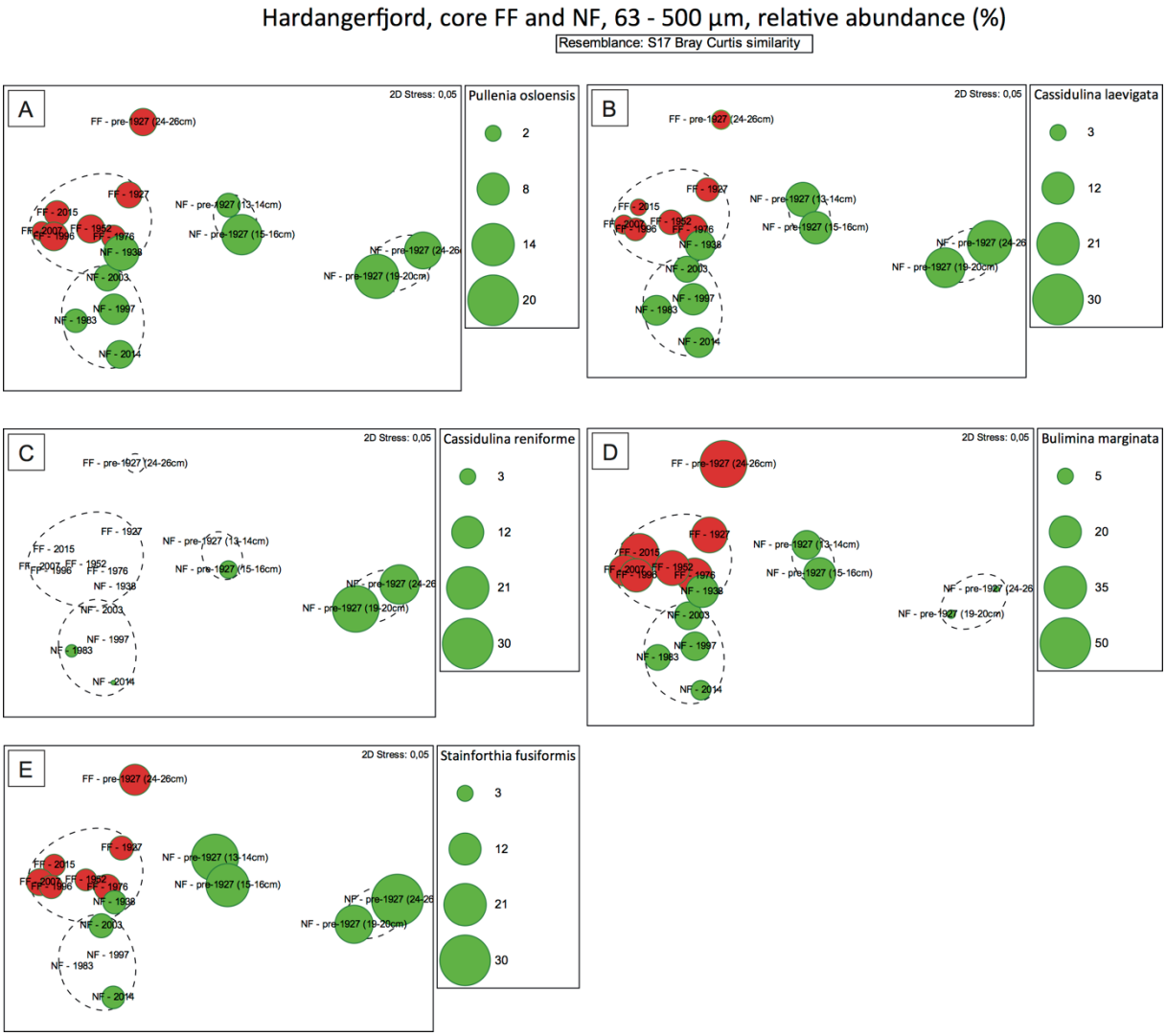

Figure 4.17 A-E: MDS- diagram showing relative occurrence of A: *P. osloensis*; B: *C. laevigata*; C: *C. reniform,* D: *B. marginata,* E: *S. fusiformis.* Sphere size indicate concentration (individuals/g) of the species in each sample. Dashed line indicates 65 fauna similarity. Red spheres = FF-core, green spheres = NF-core.

5 Discussion

5.1 Comparison of the two cores

5.1.1 Sediment chronology and accumulation rates

Both water content and sand content were relatively similar in the two cores. There were no clear visual differences between the cores – the sediment surface at both localities were undisturbed with signs of living macro fauna and absence of H_2S-smell. H_2S gas is commonly observed in anoxic sediments beneath fish farms (Braaten et al., 1983) where aerobic decomposition is replaced by sulfate reducing bacteria (Tveranger and Johnsen, 2013). The radionuclide dating results revealed different sedimentation patterns in the two cores. The dating horizon, i. e. the level at which the unsupported ^{210}Pb-activity reaches equilibrium with the supported activity, is dated to 1927 in both cores, but occurs at different core depth. The FF-core analysis showed a rapid decline in ^{210}Pb-activity in the 18 – 20 cm interval. This suggests that sediments below this level are much older. These sediments may have been deposited during a slumping event, which is a common re-deposition phenomenon in fjords (Holtedahl, 1965). Although the grain size analysis in the FF-core showed a uniform grain size distribution with no obvious signs of slumping (Figure 4.1C), it is not unlikely that the re-sedimentation simply involved deposits of a similar character and grain size. The ^{210}Pb-activity in the NF-core followed a nearly exponential decreasing trend without any signs of slumping in older sediments (Figure 4.2B). However, the dating horizon was reached at a level where the grain size distribution showed a sudden shift to coarser sediments (Figure 4.10). A similar shift of TOC- and TN content, C/N ratio and foraminiferal concentration was observed at the same core depth, further indicating a change in depositional environment. Assuming the ^{210}Pb-signal in the FF-sediments indicates a slumping event, it is possible that a re-sedimentation affected both localities, as they are only 400m apart. Based on the fact that both cores could reliably be dated to 1927 along with the sudden shift in the mentioned parameters in older sediments in the NF-core indicates that the NF-locality might also have been influenced by a re-sedimentation. Observations of pebbles (2 – 10 mm size) in pre-1927 NF-sediments could be interpreted as slump deposits. The probability of the stratigraphic succession being disrupted made it unreasonable to extrapolate age curves beyond the dating horizon. Results from older, undated samples will not be discussed in detail, but included where relevant in a wider context.

Ideally, ^{137}Cs-activity can serve as a calibration of the ^{210}Pb dating with peaks occurring at specific dates (Appleby, 2001). However, of the identified ^{137}Cs-peaks in the analysed sediment cores only one was in relatively good agreement with the ^{210}Pb-dating (the 1963 peak in the FF-core). The ambiguous ^{137}Cs-peaks may be a result of sediment dilution due to increased sedimentation rates but as described below, the calculated sedimentation rates in the particular intervals were relatively uniform. Mixing of sediments by bioturbation is the most probable cause of the offset. Macro fauna was observed burrowing 3cm into the FF-core and it is likely that similar organisms have mixed the surface sediments at both localities (remains of tubeworms were observed in both cores). Kutti et al. (2008) observed increased richness of macro fauna in the footprint of a fish farm in Uggdalsfjorden, south of Hardangerfjorden. If these findings are applicable in Onarheimsfjorden there is reason to expect severe mixing of the sediments which may disrupt the ^{137}Cs-signal. If so, there is a general uncertainty in the calculated sediment ages. In order to establish a more reliable age model additional chronostratigraphic evidence would be needed. In lack of such analyses the radio nuclide dating is, at the moment, the only basis for estimation of sediment age in the two cores. While the NF-core had a stable sedimentation rate throughout the period from 1927 until present-day, the FF-core had more than one period of increased sedimentation, most notably since the start of the 1990s (Figure 4.9). The timing of the increased sedimentation rate and the fact that it is limited to the FF-station indicates that fish farm waste contributes to the sediment accumulation.

5.1.2 Heavy metal concentrations

Heavy metal analyses of the two cores showed different patterns in concentration (Figure 4.4, Figure 4.12). Both cores had concentrations levels classified as ‘good’ or ‘background’, apart from sink concentrations which in certain intervals was classified as ‘moderate’ (Veileder M-608:2016). Certain systematic differences are worth noting. The concentration peaks of Cr, Cu, Pb and Zn in the FF-core followed one another. This might suggest that either the heavy metals were derived from the same source or that these results were artifacts from analytical errors (e. g. differences in sample weight). A similar trend is observed in the NF-core, but these sediments had substantially lower Pb-concentrations throughout the core. Fish farm net pens are commonly impregnated by copper to avoid algae growth (Skarbøvik et al., 2012) of which an estimated 85% are released in the surrounding water. Cu concentrations were slightly increasing in the upper part of the FF-core which might be related to this practice, but the historic concentration of Cu in sediments at both localities do not indicate such influence.

Heavy metal analysis of fish farm waste sludge did not show high concentrations (Vangdal et al., 2014) so it would not be expected that fish farm waste contributes to heavy metal concentrations in the sediments. The most peculiar feature of the heavy metal concentrations however, is how the highest values are measured in the lower half of both cores. Assuming the deeper parts of the cores are deposited before any anthropogenic activity (e.g. industrial discharge) it may seem that the recorded values of heavy metal concentration are natural.

5.1.3 Carbon accumulation rates, source of organic matter and stable isotopes

Total organic carbon content in the FF-sediments were higher throughout the core, compared to the NF-core (Figure 4.3, Figure 4.11). In sediments deposited between 1927 - 1990, the TOC accumulation rate was twice as high in the FF-core (Figure 5.1). Since the start of the 1990s the carbon accumulation rate at the FF-station increased and the present-day carbon accumulation rate is more than three times as large as the control station (41.8 *vs.* 12.5 g C $m^{-2}y^{-1}$). The same trend is seen in the nitrogen flux.

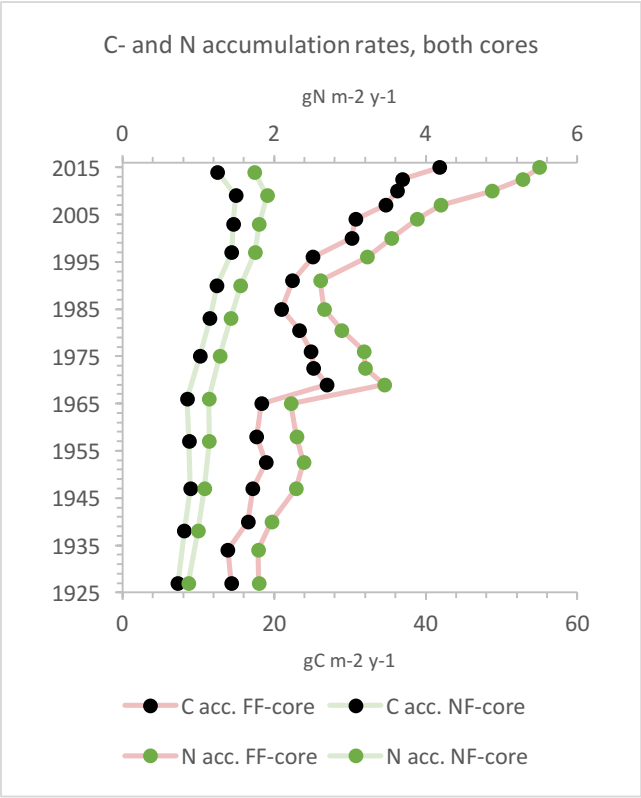

Figure 5.1: TOC- and TN accumulation rates of both cores since 1927.

The stable C-isotope values of sedimentary organic carbon were relatively stable in the NF-core deposited after 1927 (Figure 4.11). In the FF-core sediments $\delta^{13}C$-values gradually decreased after 1970, a trend that continues until present-day. Average $\delta^{13}C$ in sediments deposited since 1990 were -22.8 and -22.3‰ for the FF- and NF-core, respectively, which are

essentially the same. Similar $\delta^{13}C$ values were measured in particulate organic matter below a fish farm in the neighboring fjord Uggdalsfjorden (Kutti, Ervik, et al., 2007). Sediment traps installed 6 m above the sea floor directly below and 556m away from the fish farm had POM with -22.3 and -22.9‰, while a control station 3000m away had POM with measured $\delta^{13}C$ values of -27‰ (Kutti, unpublished data). The isotopic signal of fish feces was measured in the same project, $\delta^{13}C$ values ranging between -24.8 and -27‰. Large fluxes of fish feces to the sea floor beneath a fish farm might be thought to contribute to sedimentary $\delta^{13}C$ values close to this range, but considering the measurements both from Onarheimsfjorden and Uggdalsfjorden it seems this is not the case. In the lower, undated core sediments, the isotopic signals indicate a larger input of terrestrial organic matter, particularly in the NF-core (Figure 4.11). During photosynthesis, land plants preferentially take up ^{12}C resulting in a light (-32 - -21‰) isotope signal (Lamb et al., 2006). Below the dating horizon, the NF-core showed a clear shift to lighter C-isotope composition, indicating a stronger influence of terrestrial organic carbon. This can be seen in context with a potential slumping event which could have deposited sediments from a shallower site closer to land with lighter $\delta^{13}C$ values than what would be expected at the NF-core locality (Figure 5.2).

The C/N ratio in the post-1927 sediments are stable throughout the period (average 7.9 (± 0.9)) in both cores. Marine derived organic matter has C/N values ranging between 4 – 10. Terrestrial material is typically more nitrogen rich compared to marine organic matter and has C/N values > 10 (Meyers, 1994). Valdemarsen et al. (2012) measured C/N-ratios in the range of 12 - 28 in material collected from sediment traps below a fish farm. They argued that fecal matter was the main contributor to this value rather than fish food pellets, as the latter typically has C/N-values ranging between 7.5 – 10 (Nordi et al., 2011). The C/N signature of fish feed is fairly similar to the measured values both at the FF- and the NF-locality, but it is rather considered the natural C/N composition as it has been mostly stable at this level since 1927. Pre-1927 sediments in the FF-core had nearly constant C/N values while they were significantly higher in the lower part of the NF-core (ranging between 10 – 15). Figure 5.2 plot all analysed FF-core samples and post-1927 samples of the NF-core within C/N-$\delta^{13}C$ range characteristic of marine algae and marine particulate organic carbon (POC). Pre-1927 NF-sediments have values characteristic of C3 terrestrial plants which suggests that the organic matter in these sediments are derived from a different source than those found in the FF-core.

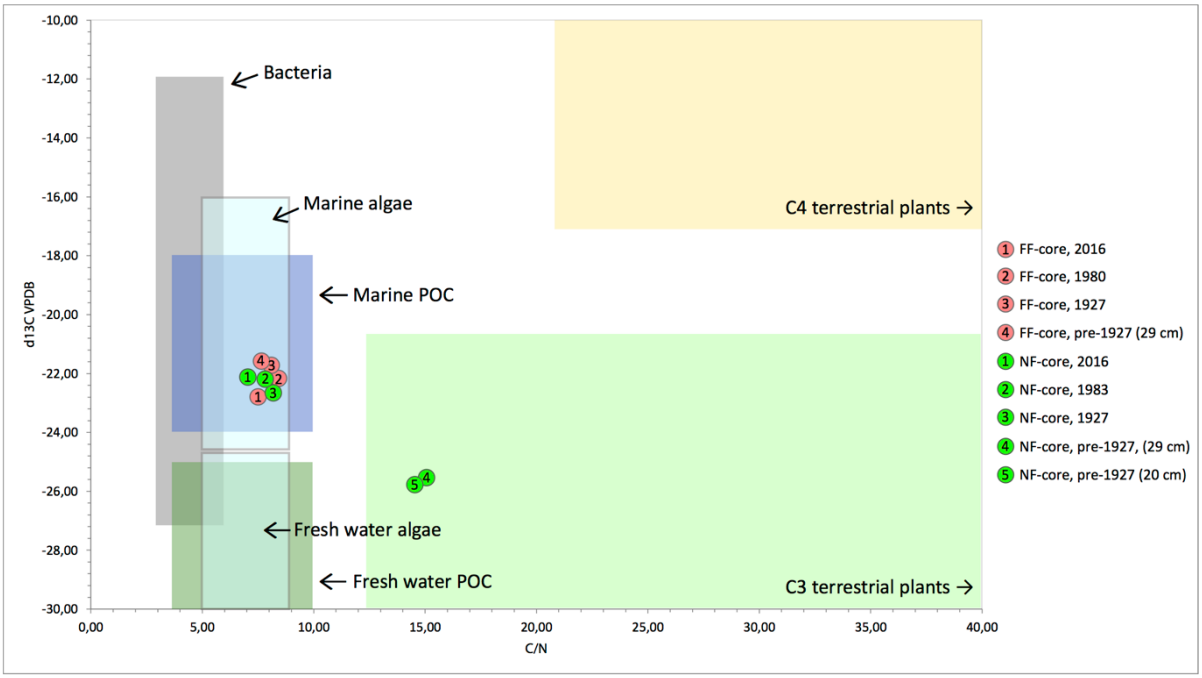

Figure 5.2: Diagram showing characteristic ranges of C/N- and δ^{13}C-values of organic matter from different sources. C3 and C4 relates to modes of carbon fixation through different photosynthetic pathways. 90% of all terrestrial plants utilize the C3 pathway (Lamb et al. 2006 and references therein). Figure modified from Lamb et al. (2006).

5.1.4 Stable isotope ratios of foraminiferal tests

Calcareous benthic foraminifera construct their tests in equilibrium with the pore water. Because of this, the stable isotope ratio measured in the tests does not only reflect the dissolved carbon in the ambient sea water, but also the specific species' microhabitat (Fontanier et al., 2006). The isotope composition of the test is in part determined by how deep within the sediments the organism lives. Compared with the water-sediment interface, dissolved carbon in the pore water of sediments is richer in ^{12}C due to progressive degradation of organic material and bacterial respiration (Brückner and Mackensen, 2008; Fontanier et al., 2006). Therefore, shallow infaunal species of foraminifera commonly have different isotopic composition compared to species with deeper microhabitats, an offset due to vital effects (Fontanier et al., 2006). This study has only focused on general trends and correcting for vital effects have not been performed. δ^{13}C-signals of *U. peregrina* and *C. laevigata* showed similar patterns in post-1927 sediments in both cores (Figure 4.6, Figure 4.15). In contrast, *H. balthica* had a lighter isotope composition in the FF-core (av. -2.4‰) compared to the NF-core (av. -1.8‰). The measured δ^{13}C in sediment TOC of the two cores did not differ substantially (Figure 4.3, Figure 4.11), so it is more probable that the observed difference of *H. balthica* is related to the higher accumulation rate of TOC at the fish farm locality.

Duffield et al. (2017) present similar results with lower $\delta^{13}C$ values in *H. balthica* at a locality with higher sedimentation rates, compared to other sites in Lysefjorden, SW Norway. Regardless, the $\delta^{13}C$-signals of foraminiferal tests in Onarheimsfjorden were rather stable within in sediments deposited after 1927 and there were no indications for changes in organic supply. The analysed foraminiferal tests in pre-1927 sediments of both cores were heavier compared to the younger samples. This would suggest a stronger influence of marine derived organic material in this period, although this does not agree with the higher C/N-values in the same interval discussed above.

Stable oxygen isotope ratios in the tests of the selected species were relatively similar between the cores except for *H. balthica* and *C. laevigata* which had slightly heavier O-isotope compositions in the NF-core. While the $\delta^{18}O$ signal is stable for all three species in pre-1927 samples (not considering the 30 – 20 cm interval of the NF-core due to lacking data) the post-1927 signals of all species indicate a gradually heavier signal. Stable oxygen isotope ratio of foraminiferal tests reflects the temperature and salinity of the ambient sea water. Although the lower part of the cores are of unknown date, it is considered unlikely that water salinity in Norwegian water masses has changed substantially over the period represented by the two cores (Kjennbakken et al., 2011). Therefore, it is assumed that changes in isotopic composition of foraminiferal tests are controlled by water temperature alone. Isolating the temperature effect means a 0.25‰ decrease of $\delta^{18}O$ represent a temperature increase of 1°C, using *U. peregrina* as a reference (Shackleton, 1974). Based on this assumption the analysed foraminifera indicate a water temperature increase of 2°C between 1927 and present. Kjennbakken et al. (2011) measured $\delta^{18}O$ in isotope tests from Voldafjorden, NW Norway which indicated temperature changes of about 1°C over a 1000 year period in the Holocene. Compared with these findings, the temperature change reflected in foraminifera from Onarheimsfjorden seems unrealistic for such a short time period. On the other hand, recorded water temperatures at the Norwegian coast south of Hardangerfjorden have increased since the first measurements in the early 1940s (Figure 5.3). Since the age of the sediment interval with the highest recorded values is unknown, it cannot be ruled out that they are in fact representative of a time when sea water temperature was significantly lower.

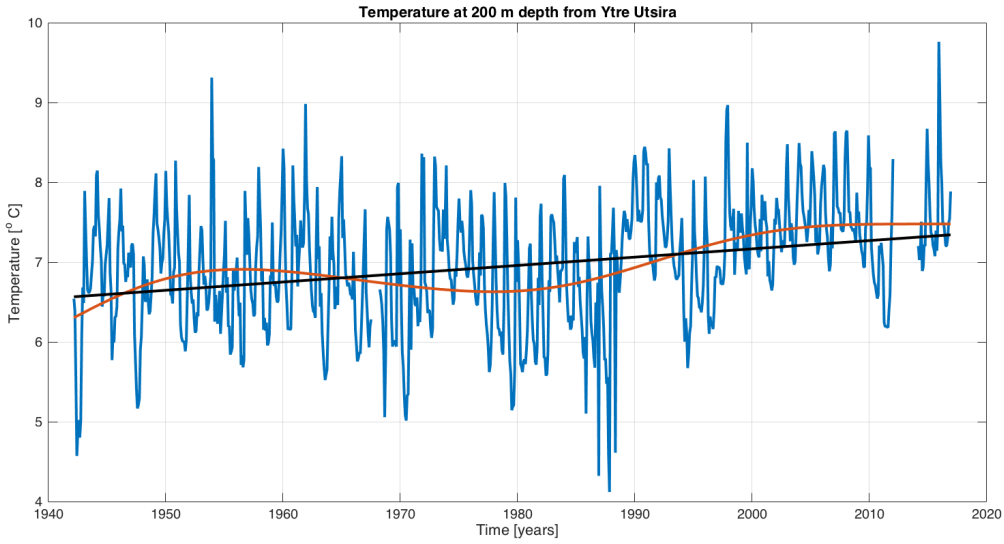

Figure 5.3: Temperature curve from measuring station at Ytre Utsira, measuring coastal water temperatures at 200m depth (data from IMR, Lars Asplin, pers comm Apr. 2017)

5.1.5 Foraminiferal assemblages

The foraminiferal fauna compositions in the two cores shared common characteristics, both in terms of diversity and relative occurrence of different species. The biggest differences in faunal assemblages were observed in undated samples, while more recent sediments shared common features (Figure 4.14). The concentration of foraminifera (individuals/g dry sediment) on the other hand differed substantially between the cores, with higher density of foraminiferal tests in the NF-core. The surface sediment of the NF-core had almost 10 times as high density of foraminiferal tests, compared to the surface sample of the FF-core. Although the surface sample was abnormally rich in foraminifera, the NF-core had more than twice as high concentration in all analysed samples younger than 1927. The difference was also reflected in the BFAR values, which were twice as high in the NF-core (Figure 5.4).

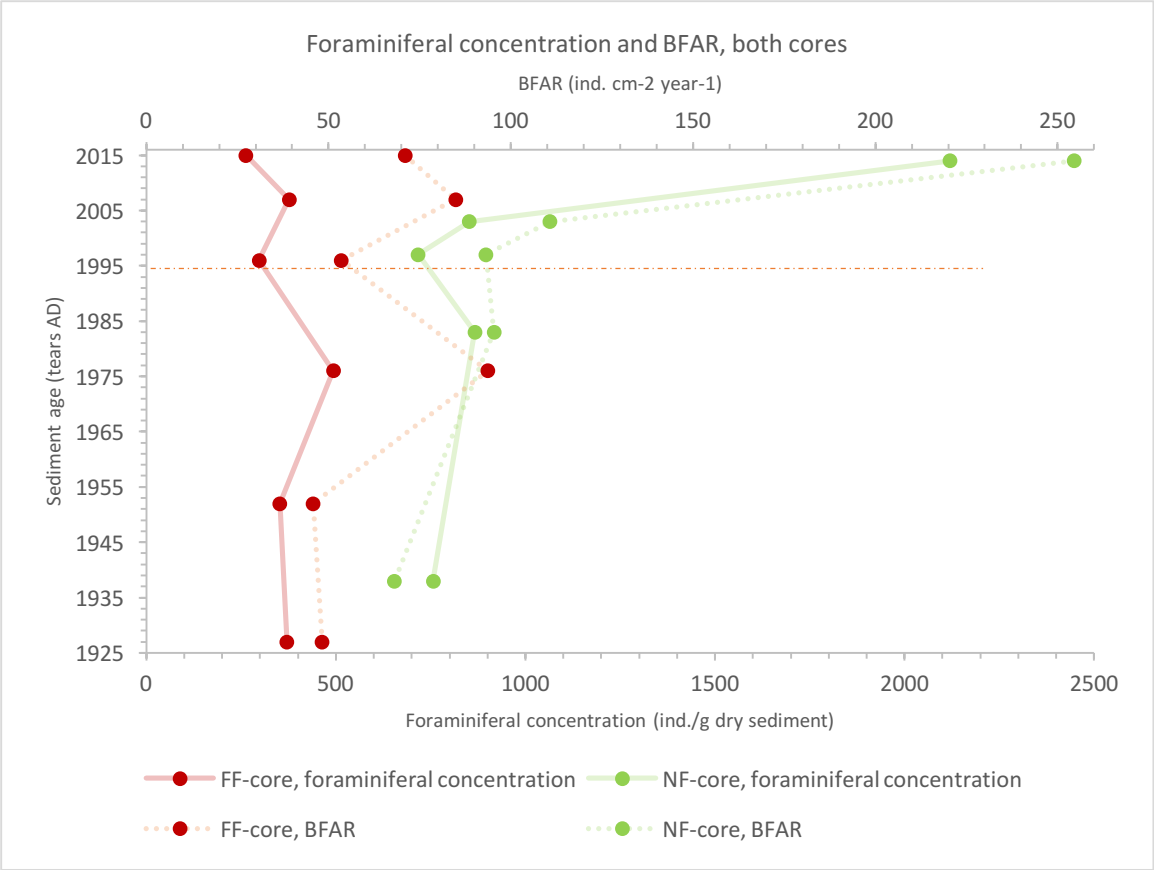

Figure 5.4: Foraminiferal concentration and BFAR in sediments younger than 1927, both cores. Dashed red line marks the start of fish production.

Foram-AMBI values were higher in the FF-core compared to the NF-core, which indicates a more stressed environment in terms of nutrient input. However, all samples from both cores had AMBI-values within the range of 'slightly polluted environment' with unbalanced benthic community health (Borja et al., 2000). The ecological quality status (EcoQS) (based on the H'(log2) and ES(100) diversity values of the benthic foraminifera community) is nonetheless classified as 'good' in both cores. The differences observed in AMBI values were consistent throughout all analysed samples and do not serve as an argument for influence from the fish farm, but rather reflect natural differences of benthic environments at the two localities.

Both cores had an average proportion of agglutinated tests of 25%, but with a gradual decrease to 6% and 0% in the 24-26cm interval in the FF-core and NF-core, respectively. This may be related to taphonomic processes, as there have been shown (Alve, 1996) that some agglutinated foraminifera species are easily disintegrated and are not preserved in the fossil record. Some agglutinated species observed in this study, particularly *Eggerelloides medius* and *Textularia earlandi*, were indeed very fragile and would frequently break apart during the

picking treatment. However, the relative abundance of these species in samples younger than 1927 (Figure 4.17A, Figure 4.16F) suggests that variations in their occurrence reflect ecological differences rather than taphonomic effects, as there would have been a more pronounced decrease of their occurrence relative to the surface layers otherwise.

Certain species showed an apparent stratigraphic development in both cores (Figure 4.16A-F, Figure 4.17A-E). *Brizalina skagerrakensis* was not very abundant in samples from 1927 and older (average relative abundance 2.7% in the FF-core, 1.2% in the NF-core), but had abundance > 10% in all analysed samples younger than 1927. *B. skagerrakensis* has been shown to respond positively to phytodetritus input to the sea floor (Alve et al., 2011), which can be thought to dominate the sedimentary organic matter judged by the C/N ratio post-1927. *B. skagerrakensis* is also shown to be intolerant of low oxygen conditions (Christopher James Duffield et al., 2015) which implies that bottom waters have been well oxygenated in the period since 1927 until present. Another species associated with oxygen rich environments is *Cassidulina laevigata* (Asteman et al. 2013 and references therein) which had high relative abundance throughout the NF-core. The low occurrence of *C. laevigata* in the FF-core could indicate that this environment was less favorable to the species, possibly due to higher organic input and increased oxygen consumption. *Bulimina marginata* is the most abundant species in both cores, with relative abundance ranging between 15 – 40% throughout both cores, except for samples from 20 – 26 cm core depth in the NF-core where it is close to absent. *B. marginata* belongs to the ecological group III (Alve et al., 2016) characteristic of being tolerant to excessive organic enrichment, but also as occurring at low TOC.

Textularia earlandi is close to absent in the NF-core except from the surface layer, where it represents 2.4% of the faunal assemblage. In the FF-core, the species had an average 1% abundance in the period between 1927 and 1996 before its abundance increased to 11% on average in sediments deposited after the onset of fish production. *T. earlandi* is described as an opportunistic species which responds to a wide range of food resources (e. g. Alve 2010 and references therein). The increased occurrence of *T. earlandi* could be interpreted as a response to organic matter from the fish farm, although the species' wide range of preferred nutrient sources make it difficult to determine the exact reason for its increased abundance.

5.2 Impact of fish farming on the benthic environment and the natural condition

Although the uncertainties of the radio nuclide dating hampered an interpretation of natural background conditions from pre-industrial times, the results allowed for the comparison of present-day conditions with conditions before the fish farm was established. The most important and perhaps clearest indicator of fish farm activity is an increased sedimentation rate at the FF-core station in 100 m distance from the installation, which becomes evident at the time the fish production was initiated Figure 4.9. No sedimentation rate increase was observed at the NF-core sampling site 500 m away. Another period of increased sedimentation rates at the FF-locality in the late 1960s implies that natural fluctuations do occur. Whereas the sedimentation increase observed in this period was only brief and decreased again after a short time, the recent increase observed since fish production started in 1994 has gradually increased and continues until present day, giving reason to believe that the increase is indeed related to the fish farm activity. Organic carbon (OC) accumulation rates (Figure 5.1) followed the total sedimentation rates. However, the measured TOC content in the sediments are not particularly high, compared to other fjords (see 5.3). If particulate organic matter was the main contributor to increased sedimentation rates in Onarheimsfjorden, one would expect to observe a substantial increase of TOC content in the sediments, which is not the case. Bulk sediment TOC content represents the organic carbon left after degradation by the benthic community. As organic carbon fluxes in Onarheimsfjorden are unknown (no sediment trap data are available) it cannot be said how much organic carbon sinks to the sea floor before eventual degradation. However, as there was not observed any substantial increase of TOC content that could be related to the increased sedimentation rate, it cannot be said that particulate organic carbon from the fish farm contributes to the sediment flux beneath the fish farm. The reason for the increased sedimentation rate is therefore difficult to interpret. One hypothesis is that the net pens of the fish farm disrupt the current flow, causing suspended particles to sink out of the transporting current as the current velocity drops.

The sedimentation rate and carbon fluxes to the sea floor at the FF-locality is in fact within normal conditions observed in fjords at localities without any influence of fish farms (see 5.3). The other parameters (TOC, TN, C/N, $\delta^{13}C$, $\delta^{15}N$, heavy metal concentrations) do not indicate considerable differences between the two localities in recent times. The $\delta^{13}C$ signal in

sediments deposited during fish production in Onarheimsfjorden are similar to the results found by Kutti et al. (2007) in Uggdalsfjorden. If the $\delta^{13}C$ values in the two cores are influenced by fish farm effluents, the influence is similar at both sites. In Uggdalsfjorden, a similar signal was observed both at 227 m and 556 m distance from the fish farm in Uggdalsfjorden (Kutti, Ervik, et al., 2007). C/N values in both cores have been stable since 1927 until present day with no apparent effect from fish farm waste.

The foraminiferal fauna assemblages do not reflect any significant changes since the establishment of the fish farm in Onarheimsfjorden. Diversity indices indicate 'good' ecological status throughout the period of fish production. The strongest change in terms of foraminiferal ecology is the high foraminiferal assemblage density found in the surface sediment of the NF-core (Figure 5.4). This observation is confirmed by living (rose Bengal stained) benthic foraminifera analyses of surface sediments from the same location – the foraminiferal concentrations were higher in NF than FF surface sediments, 830 *vs.* 452 individuals/10cm^2 (S. Hess, unpublished data). Along a 3000 m transect from the mooring point of a fish farm in Uggdalsfjorden south of Hardangerfjorden, Kutti, Hansen, et al. (2007) observed the richest macrofauna species abundance at stations 550 – 900 m away from the fish farm. The benthic community in the area within 250 m radius from the fish farm was characterized by high biomass and lower diversity dominated by opportunistic species (Kutti, Hansen, et al., 2007). Bannister et al. (2014) reported a similar spatial pattern in the macrofaunal structure beneath a fish farm located south of the Huglo sill. Species diversity will typically be low close to a point source of organic matter due the stress level imposed by the nutrient supply. Only a few opportunistic species will tolerate such stress and without competition their populations will become abundant (Pearson and Rosenberg, 1978). With increasing distance from the point source, diversity increases while species abundance become more balanced (Pearson and Rosenberg, 1978). A similar spatial pattern can be seen in the foraminifera assemblages of Onarheimsfjorden, although there are no indications for ecological degradation in terms of diversity at neither site. The foraminiferal assemblages bear no clear signs of oxygen depletion and MOM-surveys conducted at the locality have all reported well oxygenated bottom water (7.6 – 8.3 O_2 Ml/l (Haveland, 2005; Ingebrigtsen et al., 2014)). This should also be seen in relation with the topography of Onarheimsfjorden, as prolonged stagnation of bottom waters is unlikely in the absence of any sills.

Considering the accumulated amount of fish food consumed at the fish farm (see 2.4) and observations from other studies on fish farming localities (Brown et al., 1987; Findlay et al., 1995; Kutti, Ervik, et al., 2007) the impact from organic loading in the area surrounding the fish farm in Onarheimsfjorden is small. The small impact is likely a result of the fish farm design in combination with the hydrography of Onarheimsfjorden. Since the net pens are able to rotate freely around its mooring point, waste from the fish farm is distributed over a much larger area than if it was stationary. Although increased sedimentation rates and carbon/nitrogen accumulation rates are observed, the increase does not seem to be related to POM-discharge from the fish farm. Since no time series on current velocity observations exist, it is not possible to estimate the dispersal of POM in the area or the potential of redistribution of sediments by bottom currents. The only available current measurements (at 5- and 15 m depth) indicate moderately good conditions with respect to particle dispersion (Y. K. Johansen, 2016). Results from the geochemical and foraminiferal analyses suggest they are sufficient to avoid disturbances on the benthic environment caused by organic loading from the fish farm. The results may have been different if the FF-core had been collected closer than 100 m from the fish farm facility, as observations from previous studies show that the effects from organic loading is limited to ~100 m distance from the net pens (Brown et al., 1987). MOM-surveys (Ingebrigtsen et al., 2014; P. O. Johansen and Botnen, 2008) conducted at the farm site reported low macrofaunal diversity indices in samples collected below the farm sites (Table 5-1).

Table 5-1: Macrofauna diversity indices at various distances from the fish farm in Onarheimsfjorden. Data from MOM-C surveys in 2008 and 2014 (Ingebrigtsen et al., 2014; P. O. Johansen and Botnen, 2008).

Distance from fish farm	H’		ES(100)	
	2008	2014	2008	2014
0 m	0.92	1.48	2.0	4.0
300 m	2.76	2.51	13.49	10.87
1000 m	2.67	2.86	15.0	17.5

No clear differences are observed in sediment characteristics (sedimentary C- and N stable isotopes, TOC and TN contents and C/N-ratio) in the two cores after the fish production started in Onarheimsfjorden in 1994. Concentration of benthic foraminifera increased in the

NF-core around 1994, but the differences between cores observed in fauna composition has been consistent throughout the period since 1927 (figure 4-X MDS). This suggests that the two cores represent naturally different benthic environments, which raises the question of how useful the NF-core is as a reference sample. Based on C/N-values, TOC and TN content and foraminiferal fauna composition, sediments deposited before 1927 show clear differences in sediment characteristics and source of organic matter. If the hypothesis of slump re-deposition is correct, the pre-1927 differences are likely related to the extent of such an event. If it is not correct, the mentioned parameters indicate fundamentally different depositional environments. The strength of geologic analyses such as the one described in this text is how just a small sample can yield information from many parameters over a long time. On the other hand – its perhaps biggest weakness is that given the small surface area it covers there is a risk that two sediment cores by chance represent entirely different environments in spite of their relative proximity. This risk may be especially relevant in a complex fjord environment. Supplementary hydrographic time series (e. g. current measurements) would give additional insight regarding potential differences in depositional environments between the two localities. In order to construct a more complete picture of the depositional environment in the area, additional samples would be required which was beyond the scope of the present work. Regardless, the material deposited after 1927 have been compared with confidence.

5.3 Comparison with other fjords

There are no environmental stratigraphic studies similar to this analysis available from Hardangerfjorden. Two recent studies from two other Western Norwegian fjords applied similar methods to investigate the historic development of benthic environmental conditions in their respective study areas. Although these localities are from fjord basins that differ from Onarheimsfjorden both in depth and degree of isolation, a comparison is useful with respect to a consistent pool of data on both foraminiferal assemblages and the carbon burial rates in Norwegian fjords.

Table 5-2: Overview of various parameters in three Western Norwegian fjords (Onarheimsfjorden (this study), Lurefjorden (Torper, 2017), Lysefjorden (C. J. Duffield et al., 2017)): Average sedimentation rate, average TOC content, range of C/N ratio, carbon accumulation rates, average sand content, and diversity indices ES(100) and H'(log2). Colour refers to ecological quality status (EcoQS) according to table 4-1.

	Onarheimsfjorden (FF-core) 127m depth	Lurefjorden (L1D-M) (Torper, 2017) 444 m depth	Lysefjorden (St. 3) (C. J. Duffield et al., 2017) 446 m depth
Average sedimentation rate (g cm^{-2} y^{-1})	0.18	0.03	0.1
Average TOC content (%)	1.3	13.9	3.3
Range of C/N ratio	7 - 8.6	9.4 - 11.4	10.8 - 14.4
Carbon accumulation rate (g C m-2 y-1)	13.8 - 41.8	25.2 - 72.5	22.5 - 60.8
Average sand content	6	6	26
ES(100)	20 ('good' EcoQS)	23 ('good' EcoQS)	25 ('good' EcoQS)
H'(log2)	3,6 ('good' EcoQS)	4,1 ('good' EcoQS)	4,2 ('good' EcoQS)

Lurefjorden, situated NW of Bergen, is a 26 km long, 1.5 – 2.5 km narrow fjord with basin depth of around 445 m (Torper, 2017). It covers a significantly smaller area than Hardangerfjorden and compared to Onarheimsfjorden it is an isolated basin with shallow sills (all shallower than 30m). It is a distinctive fjord with dark murky waters, low abundance of fish and large, reoccurring blooms of jellyfish (Fosså, 1992). There are no large rivers running into Lurefjorden. Basin water renewal happens occasionally in spite of the narrow and shallow fjord inlet, which is reflected by well oxygenated bottom waters (Torper, 2017). One sediment core was collected at 444 m depth. The oldest sample was dated to 1642 (Torper, 2017).

Lysefjorden stretches approximately 40 km in a E/W direction, E of Stavanger. It covers a surface area of 44 km^2 and has a maximum water depth of 460 m. It is connected to Høgsfjorden in the western end of the fjord, separated by a sill at 14 m water depth (C. J. Duffield et al., 2017). Two other sills (at depths > 100 m) separate the fjord into three basins. St. 3 was collected in the deepest basin, at 446 m water depth.

Of the three cores, the FF-core is the only one sampled close to a fish farm. The sedimentation rate in Onarheimsfjorden is the highest among the three fjords. This might be

related to the greater depths of the sampling stations in Lurefjorden and Lysefjorden, where a greater fraction of suspended particles may be settled before reaching the stations. In spite of this, the carbon accumulation rates are considerably larger in Lurefjorden and Lysefjorden, compared to Onarheimsfjorden. Average TOC contents are also higher in Lurefjorden and Lysefjorden, particularly in Lurefjorden which has abnormally high TOC values. C/N-values in St. 3 core from Lysefjorden indicate a larger input of terrestrially sourced organic matter, compared to the other two fjords. The Lurefjorden sediments has a C/N signal more characteristic of marine POC, but still more nitrogen rich compared to Onarheimsfjorden.

The OC accumulation rates in the three Western Norwegian fjords are comparable with other fjords in other regions. In fjords along the Skagerrak coast recorded OC accumulation rates range between 8 – 185 g C cm^{-2} y^{-1} (Husum and Alve, 2006). Data from Dolven et al. (2013) show OC accumulation rates in Inner Oslofjord between 14 – 60 g C cm^{-2} y^{-1}, while Sepulveda et al. (2011) calculated OC accumulation rates in Patagonian fjords ranging between 1 – 83 g C cm^{-2} y^{-1}.

The stable carbon isotope signal of *C. laevigata* in Lysefjorden was stable at an average -0.58‰. This value is higher than in Onarheimsfjorden (average -0.82‰) the opposite of what could be expected at a site with higher terrestrial input. In Lurefjorden, the $\delta^{13}C$ signal of *C. laevigata* gradually decreased since 1786, from < -0,5‰ to present values at around -1‰. It was argued that this trend was related to the Suess effect, that increased CO_2 emissions since the 18th century caused an enrichment of atmospheric ^{12}C which is reflected in foraminiferal tests (Torper, 2017). No such trend was observed in foraminifera in Onarheimsfjorden or Lysefjorden.

The tests of *C. laevigata* had similar $\delta^{18}O$ values in all three fjords (2.62‰ in Lurefjorden, 2.63‰ in Lysefjorden and 2.85‰ in the FF-core from Onarheimsfjorden), which indicate similar water temperatures at all stations. *H. balthica* had lighter O-isotope composition in Onarheimsfjorden compared to St. 3 in Lysefjorden.

The most abundant species foraminiferal assemblages at the three stations are listed in Table 5-3. *Brizalina skagerrakensis* was virtually absent (maximum occurrence < 2%) in Lysefjorden (C. J. Duffield et al., 2017) but was occurring with similar abundances in Onarheimsfjorden and Lurefjorden (Torper, 2017). The species' low occurrence in Lysefjorden might be related to the amount of terrestrial organic matter input in the fjord, as

B. skagerrakensis are thought to feed on fresh organic matter (Alve et al., 2011) and might not be able to process the terrestrial organic matter in Lysefjorden (C. J. Duffield et al., 2017). Sediments in Lurefjorden and Onarheimsfjorden have a similar C/N-ratio and are seemingly more suitable environments for *B. skagerrakensis*. The opportunistic species *Stainforthia fusiformis* have been observed to reach great abundances in rapidly changing environments, e. g. basins which experience periods of dysoxia/anoxia (Alve, 2003). *S. fusiformis* were present throughout all three cores but did not reach relative abundance > 15%. In general, the benthic foraminiferal species assemblage in all three cores represented 'good' ecological status Table 5-3. Both the FF-core in Onarheimsfjorden and St. 3 Lysefjorden represented stable benthic environments with little changes in fauna assemblage throughout the core (C. J. Duffield et al., 2017). The Lurefjorden core on the other hand showed a decreasing foraminiferal concentration up-core and a clear faunal distinction between sediments before and after around 1980 (Torper, 2017).

Table 5-3: Species of foraminifera with occurrence > 10% in at least one sample in Onarheimsfjorden, Lurefjorden (Torper, 2017), and Lysefjorden (C. J. Duffield et al., 2017).

Onarheimsfjorden (FF-core), 127m depth (>10% in one or more samples)	Lurefjorden (L1D-M), 444m depth (>10% in one or more samples)	Lysefjorden (St. 3), 446 m depth (>10% in one or more samples)
Brizalina skagerrakensis	*Alabaminella weddellensis*	*Alabaminella weddellensis*
Bulimina marginata	*Brizalina skagerrakensis*	*Bulimina marginata*
Cassidulina laevigata	*Cassidulina laevigata*	*Cassidulina laevigata*
Eggerelloides medius	*Cibicidoides bradyi*	*Cibicides lobatulus*
Pullenia osloensis	*Globobulimina auriculata*	*Nonionella iridea*
Stainforthia fusiformis	*Nonionella iridea*	*Pullenia osloensis* (≤ 9.5%)
Textularia earlandi	*Pullenia osloensis*	*Stainforthia fusiformis*

Conclusions

- The dating horizon, where $^{210}Pb/^{226}Ra$ equilibrium was reached, was dated to 1927 both in the core 100 m from to the fish farm (FF-core), and in the control core 500 m away from the fish farm (NF-core). Rapid decrease in ^{210}Pb activity in the FF-core and a sudden shift in multiple parameters (grain size distribution, TOC- and TN content, C/N-ratio, stable C- and N isotope ratio and foraminiferal species assemblage) in the NF-core indicated that sediments older than 1927 in both cores were re-deposited, making it unreasonable to extrapolate the age curves. The time interval represented by the dated samples allowed for comparison of environmental conditions before and after fish production was performed.

- Sedimentation rate in the NF-core was more or less stable throughout the period from 1927 until present-day (0.9 - 0.13 g cm-2 y-1). The FF-core locality had higher sedimentation rates compared to the NF-core, particularly after the onset of fish production, when the sedimentation rate increased from 0.15 g cm-2 y-1 to the present rate at 0.27 g cm-2 y-1.

- No substantial changes in total organic carbon (TOC) content, total nitrogen (TN) content, C/N-ratio, or stable C- and N-isotope ratios were observed in the period since 1927 until present-day. C/N-ratios in both cores were 7.9 (± 0.9) on average, characteristic of marine particulate organic carbon. TOC content ranged between 1.8 – 3.4% in the FF-core and 0.7 – 2.8% in the NF-core. The increased sedimentation rate in the FF-core was not reflected by a proportional increase in TOC content.

- Stable carbon isotope ratios in the tests of *Cassidulina laevigata, Hyalinea balthica* and *Uvigerina peregrina* were stable and did not indicate changes in input or source of organic carbon in the period since 1927 until present-day. The $\delta^{18}O$-signal in the same period gradually became heavier up-core, which may indicate a water temperature increase.

- Based on the relative abundance of different benthic foraminiferal species, samples were grouped according to their similarity in a MDS-ordination plot. Undated samples clustered in three separate groups. Post-1927 samples from the FF-core clustered in

one group which also included one NF-core sample (the latter dated to 1938). NF-core samples deposited since 1983 until present-day clustered in another group. Differences in benthic foraminiferal species composition assemblage between the cores are therefore considered to be related to natural differences in benthic environments at the two sampling stations.

- In the NF-core, a substantial increase of benthic foraminiferal accumulation rate (BFAR) was observed during the period of fish production, starting in 1994 (from 93 to 254 individuals cm-2 y-1 in 1997 and 2014, respectively). No similar trend was observed in the FF-core. The BFAR increase in the NF-core may reflect altered benthic conditions in terms of food supply. The ecological quality status (EcoQS), based on diversity indices, were 'good' in all samples deposited after 1927 and indicate no deteriorating effects from fish farming.

- The dated samples of both cores shared similar sediment characteristics. At the same time, there were consistent differences in foraminiferal species assemblage between them which indicated somewhat different depositional environments at the two localities. The differences made the cores sub-optimal for comparison. Pre-1927 samples showed great differences between the cores in nearly all parameters (grain size distribution, TOC- and TN content, C/N-ratio, stable C- and N isotope ratio and foraminiferal species assemblage). Because the ages of pre-1927 samples are unknown, the results cannot be correlated between the two cores in this period.

- Total organic carbon content and –accumulation rates in Onarheimsfjorden were comparable with observations from other fjords, both in Norway and other parts of the world. Organic carbon accumulation rates in Onarheimsfjorden ranged between 7 – 41 g m^{-2} y^{-1}, substantially less than in two other Western Norwegian fjords Lysefjorden (22 – 60 g m^{-2} y^{-1}) and Lurefjorden (25 – 72 g m^{-2} y^{-1}).

References:

Ackefors, H., & Enell, M. (1994). The release of nutrients and organic matter from aquaculture systems in Nordic countries. *Journal of Applied Ichthyology,* 10(4): 225-241.

Lov om akvakultur (akvakulturloven) m. v. av 01. 01. 2006, (2005).

Alve, E. (1996). Benthic foraminiferal evidence of environmental change in the Skagerrak over the past six decades. *Nor. Geol. Unders., Bull.,* 430: 85-93.

Alve, E. (2003). A common opportunistic foraminiferal species as an indicator of rapidly changing conditions in a range of environments. *Estuarine, Coastal and Shelf Science,* 57(3): 501-514.

Alve, E. (2010). Benthic foraminiferal responses to absence of fresh phytodetritus: A two-year experiment. *Marine Micropaleontology,* 76(3): 67-75.

Alve, E., Korsun, S., Schönfeld, J., Dijkstra, N., Golikova, E., Hess, S., Husum, K., & Panieri, G. (2016). Foram-AMBI: A sensitivity index based on benthic foraminiferal faunas from North-East Atlantic and Arctic fjords, continental shelves and slopes. *Marine Micropaleontology,* 122: 1-12.

Alve, E., Murray, J. W., & Skei, J. (2011). Deep-sea benthic foraminifera, carbonate dissolution and species diversity in Hardangerfjord, Norway: An initial assessment. *Estuarine, Coastal and Shelf Science,* 92(1): 90-102.

Anon. (2012). *Strømmålinger Juli-August 2012*.

Appleby, P. G. (2001). Chronostratigraphic Techniques in Recent Sediments. In W. M. Last & J. P. Smol (Eds.), *Tracking Environmental Change Using Lake Sediments: Basin Analysis, Coring, and Chronological Techniques* (pp. 171-203). Dordrecht: Springer Netherlands.

Appleby, P. G., Nolan, P. J., Gifford, D. W., Godfrey, M. J., Oldfield, F., Anderson, N. J., & Battarbee, R. W. (1986). 210Pb dating by low background gamma counting. *Hydrobiologia,* 143(1): 21-27.

Asplin, L. (2017). [Pers. comm].

Asplin, L., Johnsen, I. A., Sandvik, A. D., Albretsen, J., Sundfjord, V., Aure, J., & Boxaspen, K. K. (2014). Dispersion of salmon lice in the Hardangerfjord. *Marine Biology Research,* 10(3): 216-225.

Asteman, I., & Nordberg, K. (2013). Foraminiferal fauna from a deep basin in Gullmar Fjord: The influence of seasonal hypoxia and North Atlantic Oscillation. *Journal of Sea Research,* 79: 40-49.

Aure, J. (2015). Omsetning av tilført partikulært organisk materiale i fjordbasseng med dype terskler. *Fisken og Havet,* 1: 18.

Aure, J., & Østensen, Ø. (1993). Hydrografiske normaler og langtidsvariasjoner i norske kystfarvann. *Fisken og Havet,* 6: 75.

Aure, J., & Stigebrandt, A. (1989). On the influence of topographic factors upon the oxygen consumption rate in sill basins of fjords. *Estuarine, Coastal and Shelf Science,* 28(1): 59-69.

Bakke, T., Breedveld, G., Källqvist, T., Oen, A., Eek, E., Ruus, A., Kibsgaard, A., Hellan, A., & Hylland, K. (2007). *Veileder for klassifisering av miljøkvalitet i fjorder og kystfarvann - Revisjon av klassifisering av metaller og organiske miljøgifter i vann og sedimenter*. (TA 2229/2007). SFT

Bannister, R. J., Valdemarsen, T., Hansen, P. K., Holmer, M., & Ervik, A. (2014). Changes in benthic sediment conditions under an atlantic salmon farm at a deep, well-flushed coastal site. *Aquaculture Environment Interactions,* 5(1): 29-47.

Borja, A., Franco, J., & Pérez, V. (2000). A Marine Biotic Index to Establish the Ecological Quality of Soft-Bottom Benthos Within European Estuarine and Coastal Environments. *Marine Pollution Bulletin,* 40(12): 1100-1114.

Børsheim, K. (2007). *Miljøundersøkelse (MOMB) ved lokaliteten Onarøy i Tysnes kommune. 11 juli 2007*. FOMAS, Fiskehelse og Miljø

Bouchet, V. M. P., Alve, E., Rygg, B., & Telford, R. J. (2012). Benthic foraminifera provide a promising tool for ecological quality assessment of marine waters. *Ecological Indicators,* 23: 66-75.

Braaten, B., Aure, J., Ervik, A., & Boge, E. (1983). *Pollution problems in Norwegian fish farming*: ICES.

Bray, J. R., & Curtis, J. T. (1957). An Ordination of the Upland Forest Communities of Southern Wisconsin. *Ecological Monographs,* 27(4): 325-349.

Brooks, K. M., & Mahnken, C. V. W. (2003). Interactions of Atlantic salmon in the Pacific northwest environment: II. Organic wastes. *Fisheries Research,* 62(3): 255-293.

Brown, J. R., Gowen, R. J., & McLusky, D. S. (1987). The effect of salmon farming on the benthos of a Scottish sea loch. *Journal of Experimental Marine Biology and Ecology,* 109(1): 39-51.

Brückner, S., & Mackensen, A. (2008). Organic matter rain rates, oxygen availability, and vital effects from benthic foraminiferal δ 13C in the historic Skagerrak, North Sea. *Marine Micropaleontology,* 66(3): 192-207.

Clark, R. B., Frid, C., & Attrill, M. (2001). *Marine pollution* (5th ed. ed.). Oxford: Oxford University Press.

Clarke, K. R., & Gorley, R. N. (2006). *PRIMER V6: user manual-tutorial*: Plymouth Marine Laboratory.

Direktoratsgruppen. (2013). *Klassifisering av miljøtilstand i vann - Økologisk og kjemisk klassifiseringssystem for kystvann, grunnvann, innsjøer og elver*. (02:2013).

Dolven, J. K., Alve, E., Rygg, B., & Magnusson, J. (2013). Defining past ecological status and in situ reference conditions using benthic foraminifera: A case study from the Oslofjord, Norway. *Ecological Indicators,* 29: 219-233.

Duffield, C. J., Alve, E., Andersen, N., Andersen, T., Hess, S., & Strohmeier, T. (2017). Spatial and temporal organic carbon burial along a fjord to coast transect: A case study from Western Norway. *The Holocene*.

Duffield, C. J., Hess, S., Norling, K., & Alve, E. (2015). The response of Nonionella iridea and other benthic foraminifera to "fresh" organic matter enrichment and physical disturbance. *Marine Micropaleontology,* 120: 20-30.

Ervik, A., Agnalt, A.-L., Asplin, L., Aure, J., Bekkvik, T. C., Døskeland, I., Hageberg, A. A., Hansen, T., Karlsen, Ø., Oppedal, F., & Strand, Ø. (2008). *AkvaVis – dynamisk GIS-verktøy for lokalisering av oppdrettsanlegg for nye oppdrettsarter. Miljøkrav for nye oppdrettsarter og laks*. Havforskningsinstituttet

Findlay, R., Watling, L., & Mayer, L. (1995). Environmental impact of salmon net-pen culture on marine benthic communities in Maine: A case study. *Estuaries,* 18(1): 145-179.

Fontanier, C., Mackensen, A., Jorissen, F. J., Anschutz, P., Licari, L., & Griveaud, C. (2006). Stable oxygen and carbon isotopes of live benthic foraminifera from the Bay of Biscay: Microhabitat impact and seasonal variability. *Marine Micropaleontology,* 58(3): 159-183.

Fosså, J. H. (1992). Mass occurrence of Periphylla periphylla (Scyphozoa, Coronatae) in a Norwegian fjord. *Sarsia,* 77(3-4): 237-251.

Gilbert, R., Niels, N., Moller, H., Desloges, J. R., & Rasch, M. (2002). Glacimarine sedimentation in Kangerdluk (Disko Fjord), West Greenland, in response to a surging glacier. *Marine Geology*(191): 1-18.

Hansen, P. K., Ervik, A., & Pittman, K. (1990). Effects of organic waste from marine fish farms on the seabottom beneath the cages. *ICES,* 34.

Haveland, F. (2005). *Resipientgranskning, C-undersøkelse*. Resipientanalyse AS

Haveland, F. (2009). *Resipientgransking, MOM-B, Lokalitet Onarøy, Tysnes kommune*. Resipientanalyse AS

Haveland, F. (2011). *Resipientgransking, MOM-B, Lokalitet Onarøy, Tysnes kommune*. Resipientanalyse AS

Hellen, B. A., Kambestad, M., & Johnsen, G. H. (2013). *Habitatkartlegging og forslag til tiltak for sjøaure i utvalgte vassdrag ved Hardangerfjorden*. Rådgivende Biologer

Herguera, J. C., & Berger, W. H. (1991). Paleoproductivity from benthic foraminifera abundance: glacial to postglacial change in the west-equatorial Pacific. *Geology,* 19(12): 1173-1176.

Hilton, R. G., Galy, A., Hovius, N., Horng, M.-J., & Chen, H. (2011). Efficient transport of fossil organic carbon to the ocean by steep mountain rivers: an orogenic carbon sequestration mechanism. *Geology,* 39(1): 71.

Holtedahl, H. (1965). Recent turbidities in the Hardangerfjord, Norway. *Submarine geology and geophysics,* 13: 107–140.

Hurlbert, S. H. (1971). The Nonconcept of Species Diversity: A Critique and Alternative Parameters. *Ecology,* 52(4): 577-586.

Husa, V., Kutti, T., Ervik, A., Sjøtun, K., Hansen, P. K., & Aure, J. (2014). Regional impact from fin-fish farming in an intensive production area (Hardangerfjord, Norway). *Marine Biology Research,* 10(3): 241-252.

Husum, K., & Alve, E. (2006). Retrospektiv foraminiferfauna. I Effekter av oksygensvikt på fjordfauna. Bunnfauna og miljø i fjorder på Skagerakkysten. *Fisken og Havet,* 3: 83 - 97.

Ingebrigtsen, E.-B., Isaksen, T. E., & Alme, Ø. (2014). *MOM-C undersøkelse fra lokalitet Onarøy i Tysnes kommune, mars 2014*. Uni Research

Johansen, P. O., & Botnen, H. (2008). *MOM-C undersøkelse fra lokaliteten Onarøy i Tysnes kommune i 2008*. UNIFOB - Seksjon for anvendt miljøforskning

Johansen, Y. K. (2016). *Resipientgransking, B-gransking, Lokalitet Onarøy, Tysnes kommune*. Resipientanalyse AS

Kartverket Sjødivisjonen. (2016). *Den Norske Los bind 3.* (6. ed.): Kartverket.

Keil, R. (2015). Carbon cycle: Hoard of fjord carbon. *Nature Geosci,* 8(6): 426-427.

Kjennbakken, H., Sejrup, H. P., & Haflidason, H. (2011). Mid- to late-Holocene oxygen isotopes from Voldafjorden, western Norway. *The Holocene,* 21(6): 897-909.

Kutti, T., Ervik, A., & Hansen, P. K. (2007). Effects of organic effluents from a salmon farm on a fjord system. I. Vertical export and dispersal processes. *Aquaculture,* 262(2): 367-381.

Kutti, T., Ervik, A., & Høisæter, T. (2008). Effects of organic effluents from a salmon farm on a fjord system. III. Linking deposition rates of organic matter and benthic productivity. *Aquaculture,* 282(1): 47-53.

Kutti, T., Hansen, P. K., Ervik, A., Høisæter, T., & Johannessen, P. (2007). Effects of organic effluents from a salmon farm on a fjord system. II. Temporal and spatial patterns in infauna community composition. *Aquaculture,* 262(2): 355-366.

Lamb, A. L., Wilson, G. P., & Leng, M. J. (2006). A review of coastal palaeoclimate and relative sea-level reconstructions using δ13C and C/N ratios in organic material. *Earth-Science Reviews,* 75(1–4): 29-57.

Meyers, P. A. (1994). Preservation of elemental and isotopic source identification of sedimentary organic matter. *Chemical Geology,* 114(3): 289-302.

Miljødirektoratet. (2016). *Grenseverdier for klassifisering av vann, sediment og biota*. (M-608).

Molvær, J. (1997). *Klassifisering av miljøkvalitet i fjorder og kystfarvann*. (97:03). SFT

Murray, J. W. (2006). *Ecology and applications of Benthic foraminifera*. Cambridge: Cambridge University Press.

Nordi, G., Glud, R. N., Gaard, E., & Simonsen, K. (2011). Environmental impacts of coastal fish farming: carbon and nitrogen budgets for trout farming in Kaldbaksfjorour (Faroe Islands). *Mar. Ecol.-Prog. Ser.,* 431: 223-241.

Norsk Standard. (2007). *Miljøovervåkning av marine matfiskanlegg*. (NS 9410:2007). Norges Standardiseringsforbund

Pearson, T. H., & Rosenberg, R. (1978). Macrobenthic succession in relation to organic enrichment and pollution of the marine environment. *Oceanography Marine Biological Annual Reviewi,* 16: 229-311.

Petterson, L. E. (2008). *Beregning av totalavløp til Hardangerfjorden* (Oppdragsrapport A:9). The Norwegian Water Resources and Energy Directorate

Rohling, E. J., & Cooke, S. (1999). Stable oxygen and carbon isotopes in foraminiferal carbonate shells. In B. K. Sen Gupta (Ed.), *Modern foraminifera*. Dordrecht: Kluwer.

Rygg, B. (1995). *Vanlige konsentrasjoner av organisk karbon (TOC) i sedimenter i norske fjorder og kystfarvann* (1894-7948). NIVA

Sætre, R. (2007). *The Norwegian Coastal Current: Oceanography and Climate*: Tapir Academic Press.

Schmiedl, G., Pfeilsticker, M., Hemleben, C., & Mackensen, A. (2004). Environmental and biological effects on the stable isotope composition of recent deep-sea benthic foraminifera from the western Mediterranean Sea. *Marine Micropaleontology,* 51(1): 129-152.

Sepúlveda, J., Pantoja, S., & Hughen, K. A. (2011). Sources and distribution of organic matter in northern Patagonia fjords, Chile (~44–47°S): A multi-tracer approach for carbon cycling assessment. *Continental Shelf Research,* 31(3): 315-329.

Shackleton, N. J. (1974). Attainment of isotopic equilibrium between ocean water and the benthonic foraminifera genus *Uvigerina*: Isotopic changes in the ocean during the last glacial. *Centre National de la Recherche Scientifique Colleagues Internationeaux*(219): 203-209.

Shannon, C. E., & Weaver, W. (1949). *The mathematical theory of communication*. Urbana: University of Illinois Press.

Skarbøvik, E., Stålnacke, P., Selvik, J. R., Aakerøy, P. A., Høgåsen, T., & Kaste, Ø. (2012). *Elvetilførselsprogrammet (RID) - 20 års overvåking av tilførsler til norske kystområder (1990-2009)*. Norwegian Institute of Water Research

Skei, J. (1983). Geochemical and sedimentological considerations of a permanently anoxic fjord — Framvaren, south Norway. *Sedimentary Geology,* 36(2): 131-145.

Skei, J., Price, N., Calvert, S., & Holtedahl, H. (1972). The distribution of heavy metals in sediments of Sörfjord, West Norway. *An International Journal of Environmental Pollution,* 1(4): 452-461.

Skogen, M. D., Eknes, M., Asplin, L. C., & Sandvik, A. D. (2009). Modelling the environmental effects of fish farming in a Norwegian fjord. *Aquaculture,* 298(1): 70-75.

Smith, R. W., Bianchi, T. S., Allison, M., Savage, C., & Galy, V. (2015). High rates of organic carbon burial in fjord sediments globally. *Nature Geosci,* 8(6): 450-453.

Statistics Norway. (2016). Akvakultur, 2015, endelige tall. Retrieved from https://www.ssb.no/jord-skog-jakt-og-fiskeri/statistikker/fiskeoppdrett/aar/2016-10-28 - content [Accessed:

Strohmeier, T., Strand, H. K., & Strand, Ø. (2014). *Karbonfangst og matproduksjon i fjorder* (7). Institute of Marine Research

Sundfjord, V. N. (2010). *Volume transport due to coastal wind-driven internal pulses in the Hardangerfjord.* (Master thesis), University of Oslo.

Svåsand, T., Karlsen, Ø., Kvamme, B. O., Stien, L. H., Taranger, G. L., & Boxaspen, K. K. (2016). *Risikovurdering norsk fiskeoppdrett 2016*. Havforskningsinstituttet

Sweetman, A. K., Norling, K., Gunderstad, C., Haugland, B. T., & Dale, T. (2014). Benthic ecosystem functioning beneath fish farms in different hydrodynamic environments. *Limnology and Oceanography,* 59(4): 1139-1151.

Syvitski, J. P. M., Burrell, D. C., & Skei, J. (1987). *Fjords : processes and products*. New York: Springer.

Torper, M. (2017). *Den historiske utviklingen av organisk karbon og naturtilstanden i dypbassenget til Lurefjorden, Hordaland: En mikropaleontologisk og geokjemisk studie.* (Master thesis), University of OSlo.

Tveranger, B., & Johnsen, G. H. (2013). *Resipientundersøkelse i sjøområdene utenfor Nesfosssen Smolt AS i Lindås kommune vinteren 2013*. Rådgivende Biologer AS

Valdemarsen, T., Bannister, R. J., Hansen, P. K., Holmer, M., & Ervik, A. (2012). Biogeochemical malfunctioning in sediments beneath a deep-water fish farm. *Environmental Pollution,* 170: 15.

Valdemarsen, T., Hansen, P. K., Ervik, A., & Bannister, R. J. (2015). Impact of deep-water fish farms on benthic macrofauna communities under different hydrodynamic conditions. *Marine Pollution Bulletin,* 101(2): 776-783.

Vangdal, E., Kvamm-Lichtenfeld, K., Sørheim, R., & Svalheim, Ø. (2014). *Fiskeslam frå oppdrettsanlegg - Gjødsel til planter eller råstoff for biogass?* Bioforsk

Winterhalter, B. (2001). The Ultimate Corer For Soft Sediments. Retrieved from http://www.kolumbus.fi/boris.winterhalter/GEMAX.pdf [Accessed: 18.03]

WoRM. (2017). World Register of Marine Species. Retrieved from http://www.marinespecies.org/ [Accessed: 2 May 2017]

Appendices:

Appendix A: Lab report from sediment dating

Radiometric Dating of three marine sediment cores from Hardangerfjorden, Norway

(Final Report April 2017)

P.G.Appleby and G.T.Piliposian

Environmental Radioactivity Research Centre

University of Liverpool

Methods

Dating by ^{210}Pb and ^{137}Cs was carried out on marine sediment cores AKS-201A and AKS202A collected from Hardangerfjorden and core M1-D from Masfjorden in southern Norway. Sub-samples from each core were analysed for ^{210}Pb, ^{226}Ra, and ^{137}Cs by direct gamma assay in the Liverpool University Environmental Radioactivity Laboratory, using Ortec HPGe GWL series well-type coaxial low background intrinsic germanium detectors (Appleby *et al*. 1986). ^{210}Pb was determined via its gamma emissions at 46.5 keV, and ^{226}Ra by the 295 keV and 352 keV γ-rays emitted by its daughter radionuclide ^{214}Pb following 3 weeks storage in sealed containers to allow radioactive equilibration. ^{137}Cs was measured by its emissions at 662 keV. The absolute efficiencies of the detectors were determined using calibrated sources and sediment samples of known activity. Corrections were made for the effect of self-absorption of low energy γ-rays within the sample (Appleby *et al.* 1992).

Results

The results of the radiometric analyses carried out on each core are given in Tables 1–3 and shown graphically in Figures 1.i–3.i. Supported ^{210}Pb activity was assumed to be equal to the measured ^{226}Ra activity, and unsupported ^{210}Pb activity calculated by subtracting supported ^{210}Pb from the measured total ^{210}Pb activity.

Hardangerfjorden Core AKS-201A

Lead-210 Activity

Total ^{210}Pb activity (Figure 1.i(a)) appears to reach equilibrium with the supporting ^{226}Ra at a depth of around 20 cm. Unsupported ^{210}Pb concentrations (Figure 1.i(b)) vary irregularly with depth. In particular there is a significant non-monotonic feature between 10-14 cm that may indicate an episode of rapid accumulation due e.g. to a sediment slump. Excluding this event, a fairly modest decline in unsupported ^{210}Pb concentrations down to a depth of 15 cm suggests that this entire section of the core could span no more than around two or three ^{210}Pb half-lives (45-67 years). Although an abrupt decline in concentrations below 18 cm could simply show that sediments at this depth are close to the ^{210}Pb

dating horizon (~80 years in this core) they could also indicate an earlier episode of more rapid accumulation.

Artificial Fallout Radionuclides

^{137}Cs concentrations have an initial relatively well defined peak between 12-15 cm (Figure 1.i(c)) that most probably records the peak levels of fallout in the 1960s from the atmospheric testing of nuclear weapons. A further more recent peak in the 6-7 cm sample could possibly record fallout from the Chernobyl nuclear reactor fire though other causes can't be ruled out. Since ^{137}Cs records may also be affected by sedimentological events such as that causing the 10-14 cm non-monotonic feature in the ^{210}Pb record the ^{137}Cs/^{210}Pb activity ratio is sometimes a better guide to the significance of features in the ^{137}Cs record. A plot of ^{137}Cs/^{210}Pb activity versus depth, also shown in Figure 1.i(c), emphasises the significance of the 12-15 cm ^{137}Cs feature but greatly reduces that of the 6-7 cm feature.

Core Chronology

^{210}Pb dates calculated using the CRS (Appleby and Oldfield 1978) place 1963 at a depth of between 13-14 cm, in good agreement with the 1963 depth suggested by the weapons test ^{137}Cs record. The more recent ^{137}Cs peak at 6-7 cm is dated to the mid-1990s making it unlikely that this feature is due to Chernobyl. The ^{210}Pb calculations date the episode of rapid accumulation associated with the 10-14 cm non-monotonic feature to the late 1960s or early 1970s. They further suggest that after period of slower accumulation in the 1980s and 1990s there has been another more sustained increase during the past decade. Although this latter increase could to some extent be an artefact of the ^{210}Pb calculations caused by mixing of the surficial sediments, the fact that the fallout records have preserved a number distinct features suggests that this has not been a major factor.

Dates prior to 1960 are more problematic. Whereas relatively high ^{210}Pb concentrations in the 17-18 cm sample suggest that sediments at this depth are relatively modern, very low concentrations in samples below 20 cm suggest that sediments at these depths could be relatively old though an alternative possibility is that the record here has been diluted by an earlier episode of rapid accumulation. The ^{210}Pb record between 14-18 cm suggests a mean sedimentation rate for this part of the core of 0.13 g cm^{-2} y^{-1} (0.17 cm y^{-1}). The results, shown in Figure 1.ii and given in detail in Table 4, date the base of the ^{210}Pb record at 20 cm to the early 1920s. In light of the above uncertainties the results for this section of the core should be regarded with caution unless supported by other chronostratigraphic evidence.

Hardangerfjorden Core AKS-202A

Lead-210 Activity

^{210}Pb/^{226}Ra equilibrium in this core is reached at a depth of around 13 cm, significantly shallower than in AKS-201A (Figure 2.i(a)). Apart from a small monotonic feature in the 2-3 cm sample unsupported ^{210}Pb concentrations decline more or less exponentially with depth (Figure 2.i(b)), indicating relatively uniform sedimentation during most of the period of time spanned by the core.

Artificial Fallout Radionuclides

^{137}Cs concentrations again have two relatively well defined peaks, at 6-7 cm and 1-2 cm. The earlier peak may record the 1963 fallout peak from the atmospheric testing of nuclear weapons. The more recent peak appears too close to the top of the core to record fallout from the 1986 Chernobyl nuclear reactor fire.

Core Chronology

^{210}Pb dates calculated using the CRS model place 1986 at a depth of just over 5 cm, supporting the suggestion that the 1-2 cm ^{137}Cs peak is unlikely to be a record of fallout from the Chernobyl accident. The 1963 depth is placed within the 7-8 cm sample. Although this does support the suggestion that the 6-7 cm sample dates from the period of maximum weapons test fallout, it is difficult to reconcile a 1963 date for this sample with the ^{210}Pb results. The ^{210}Pb activity versus depth record down to 10 cm closely follows that of an exponential function the gradient of which corresponds to a mean sedimentation rate significantly higher than that indicated by the ^{137}Cs record. Two possible explanation for the discrepancy are firstly the loss of around 1 cm from the top of the core shortly before or during coring, and secondly the possibility that the ^{137}Cs peak in the 6-7 cm sample is not an accurate record of atmospheric fallout. The ^{137}Cs peak in the 1-2 cm sample shows that such features can be caused by other presumably sedimentological processes. The CRS model dates provide a reasonable compromise and form the basis of the results shown in Figure 2.ii and given in detail in Table 5. The calculations have however been slightly modified to take account of the fact that the relatively high concentrations between 10-13 cm indicate that sediments at these depths are within the 90% ^{210}Pb equilibrium depth. In view of the above uncertainties these results too should be regarded with some caution unless supported by other chronostratigraphic evidemce.

References

Appleby,P.G., P.J.Nolan, D.W.Gifford, M.J.Godfrey, F.Oldfield, N.J.Anderson & R.W.Battarbee, 1986. ^{210}Pb dating by low background gamma counting. *Hydrobiologia*, **141**:21-27.

Appleby,P.G. & F.Oldfield, 1978. The calculation of ^{210}Pb dates assuming a constant rate of supply of unsupported ^{210}Pb to the sediment. *Catena*, **5**:1-8

Appleby,P.G., N.Richardson, & P.J.Nolan, 1992. Self-absorption corrections for well-type germaniun detectors. *Nucl. Inst.& Methods B*, **71**: 228-233.

Table 1. Fallout radionuclide concentrations in the Hardangerfjorden sediment core AKS-201A

Depth		^{210}Pb						^{137}Cs	
		Total		Unsupported		Supported			
cm	g cm^{-2}	Bq kg^{-1}	±	Bq kg^{-1}	±	Bq kg^{-1}	±	Bq kg^{-1}	±
0.5	0.3	104.0	6.3	69.6	6.5	34.4	1.4	3.9	0.7
2.5	1.5	117.3	6.3	80.1	6.4	37.2	1.3	3.4	0.8
4.5	3.0	95.6	6.2	62.9	6.3	32.7	1.4	3.1	0.7
6.5	4.5	106.5	5.9	72.5	6.0	34.0	1.3	5.3	0.8
7.5	5.3	97.1	5.2	65.8	5.3	31.3	1.0	3.5	0.6
8.5	6.1	90.2	5.3	57.9	5.5	32.3	1.1	3.3	0.6
10.5	7.7	63.5	5.8	29.3	5.9	34.2	1.4	2.1	0.7
12.5	9.2	56.1	4.7	21.5	4.9	34.7	1.1	3.7	0.6
13.5	10.0	59.6	5.5	32.8	5.7	26.8	1.2	4.4	0.8
14.5	10.7	74.9	5.4	41.3	5.5	33.6	1.2	3.5	0.7
16.5	12.1	67.0	5.0	32.9	5.1	34.2	1.1	2.9	0.6
17.5	12.9	55.9	5.9	23.0	6.0	32.9	1.3	2.6	0.7
18.5	13.8	42.3	4.1	7.2	4.1	35.1	0.9	1.8	0.5
19.5	14.6	44.1	3.1	10.7	3.2	33.4	0.7	1.2	0.4
21.0	16.0	38.7	4.3	3.7	4.4	35.1	0.9	0.0	0.0
24.5	19.2	37.9	4.0	1.4	4.1	36.5	1.0	0.0	0.0

Table 2. Fallout radionuclide concentrations in the Hardangerfjorden sediment core AKS-202A

Depth		^{210}Pb						^{137}Cs	
		Total		Unsupported		Supported			
cm	g cm^{-2}	Bq kg^{-1}	±	Bq kg^{-1}	±	Bq kg^{-1}	±	Bq kg^{-1}	±
0.5	0.3	140.1	9.7	105.8	9.8	34.4	1.9	3.2	0.9
1.5	0.9	132.1	8.8	101.7	9.0	30.5	1.8	5.7	1.0
2.5	1.6	97.9	8.0	63.5	8.1	34.4	1.6	4.8	1.0
3.5	2.4	99.9	9.0	67.3	9.1	32.5	1.7	4.2	1.1
4.5	3.2	88.0	5.6	54.7	5.7	33.3	1.1	4.3	0.7
5.5	4.1	79.7	8.1	46.3	8.3	33.4	1.6	4.1	0.8
6.5	4.9	78.2	5.0	43.3	5.1	34.9	1.1	5.4	0.7
7.5	5.8	69.5	5.7	35.8	5.8	33.7	1.3	3.7	0.7
8.5	6.7	62.7	5.5	27.4	5.6	35.3	1.2	3.4	0.6
9.5	7.5	61.5	5.4	26.0	5.5	35.5	1.3	3.0	0.6
10.5	8.5	55.0	5.4	16.0	5.5	39.0	1.3	2.1	0.6
11.5	9.4	52.5	4.3	10.2	5.0	42.3	1.1	3.1	0.6
12.5	10.4	56.7	5.5	9.8	5.6	46.9	1.3	1.6	0.7
13.5	11.4	47.2	5.2	-1.6	5.3	48.8	1.2	0.0	0.0
14.5	12.5	47.0	5.5	-4.5	5.7	51.5	1.3	0.3	0.7
16.5	14.7	53.5	5.5	2.9	5.7	50.6	1.3	0.0	0.0
18.5	16.9	49.6	4.7	-3.4	4.8	53.0	1.2	0.0	0.0
21.0	19.3	54.0	5.6	-5.1	5.8	59.1	1.3	0.0	0.0

Table 3 ^{210}Pb chronology of the Hardangerfjorden sediment core AKS-201A

Depth		Chronology			Sedimentation Rate		
		Date	Age				
cm	g cm^{-2}	AD	y	±	g cm^{-2} y^{-1}	cm y^{-1}	± (%)
0.0	0.0	2016	0	0			
0.5	0.3	2015	1	1	0.27	0.44	10.2
2.5	1.5	2010	6	2	0.24	0.36	9.2
4.5	3.0	2004	12	2	0.21	0.28	11.2
6.5	4.5	1996	20	2	0.18	0.23	10.2
7.5	5.3	1991	25	2	0.15	0.19	10.5
8.5	6.1	1985	31	2	0.16	0.20	13.1
10.5	7.7	1976	40	3	0.19	0.24	15.0
12.5	9.2	1969	47	3	0.20	0.27	12.8
13.5	10.0	1965	51	4	0.13	0.18	15.6
14.5	10.7	1958	58	4	0.13	0.16	13.8
16.5	12.1	1947	69	6	0.13	0.17	15.9
17.5	12.9	1940	76	9	0.13	0.15	19.4
18.5	13.8	1934	82	12	0.13	0.15	22.8
19.5	14.6	1927	89	16	0.13	0.14	27.1

Table 4. ^{210}Pb chronology of the Hardangerfjorden sediment core AKS-202A

Depth		Chronology			Sedimentation Rate		
		Date	Age				
cm	g cm^{-2}	AD	y	±	g cm^{-2} y^{-1}	cm y^{-1}	± (%)
0.0	0.0	2016	0	0			
0.5	0.3	2014	2	1	0.12	0.21	10.8
1.5	0.9	2009	7	2	0.13	0.18	10.8
2.5	1.6	2003	13	2	0.13	0.17	10.8
3.5	2.4	1997	19	2	0.13	0.16	10.8
4.5	3.2	1990	26	3	0.12	0.14	10.8
5.5	4.1	1983	33	3	0.11	0.13	10.8
6.5	4.9	1975	41	4	0.10	0.11	10.8
7.5	5.8	1966	50	5	0.09	0.11	10.8
8.5	6.7	1957	59	5	0.09	0.11	10.8
9.5	7.5	1947	69	6	0.09	0.10	10.8
10.5	8.5	1938	78	7	0.09	0.10	10.8
11.5	9.4	1927	89	8	0.09	0.10	10.8

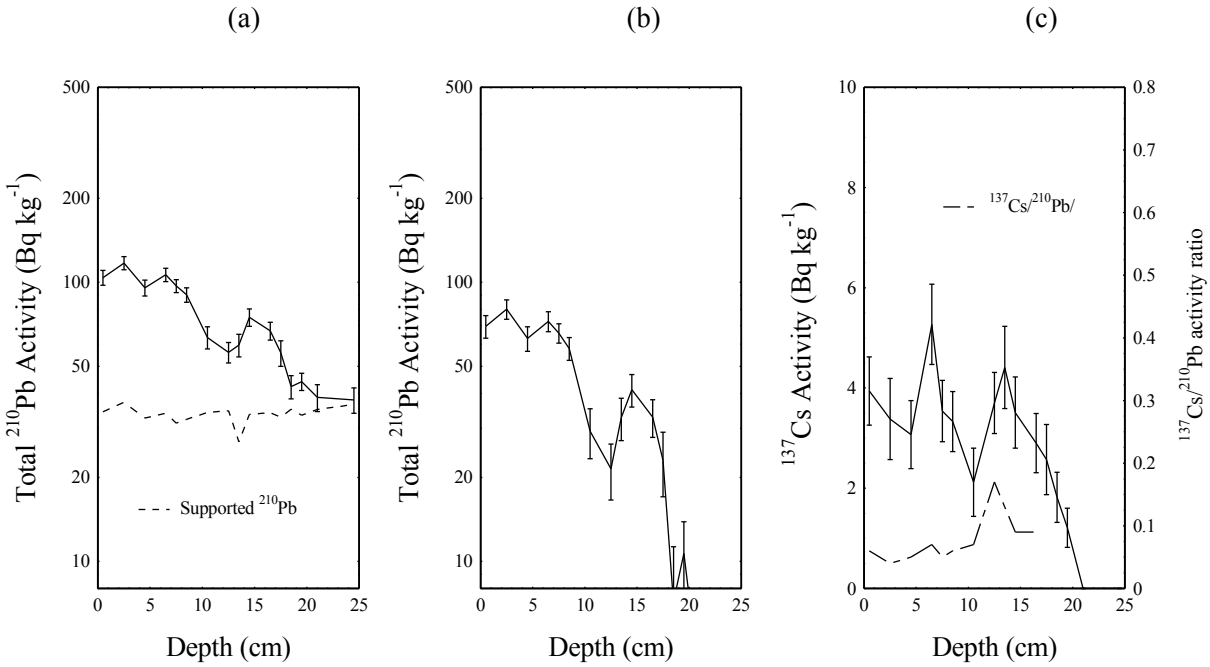

Figure 1.i. Fallout radionuclides in the Hardangerfjorden sediment core AKS-201A showing (a) total and supported ^{210}Pb, (b) unsupported ^{210}Pb, (c) ^{137}Cs concentrations versus depth. Plot (c) also shows the ^{137}Cs/^{210}Pb activity ratio.

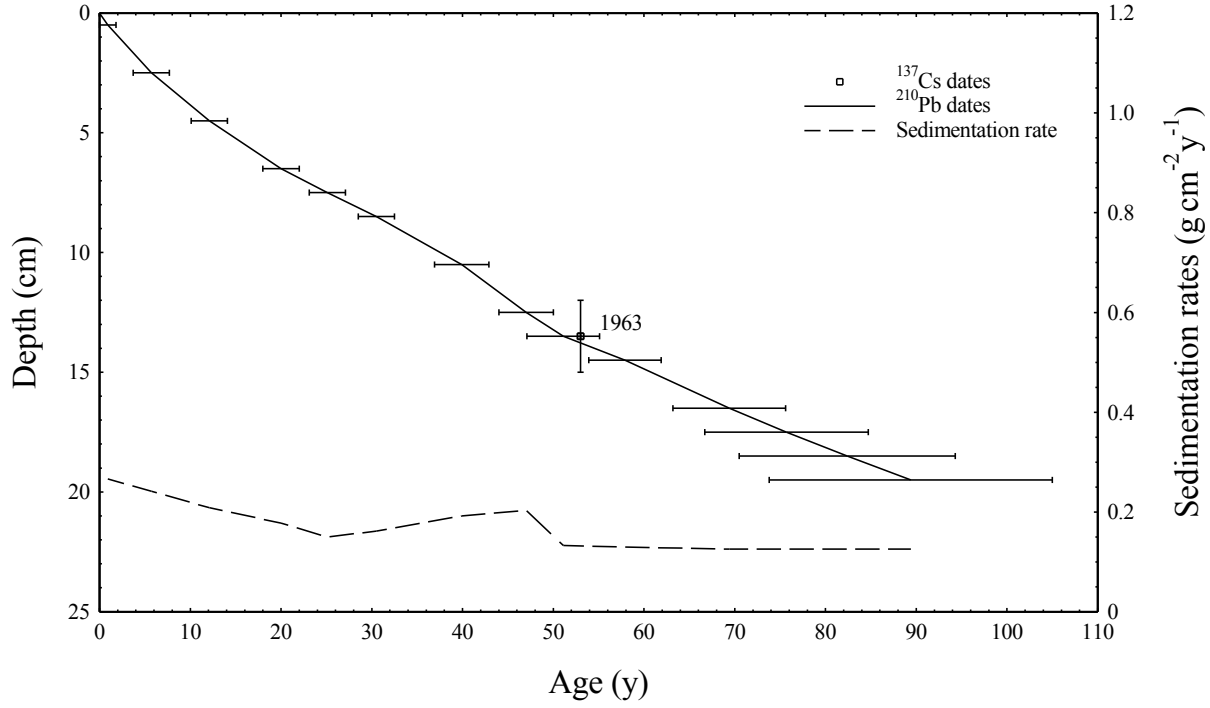

Figure 1.ii. Radiometric chronology of the Hardangerfjorden sediment core AKS-201A showing the ^{210}Pb dates and sedimentation rates and the possible 1963 depth suggested by the ^{137}Cs fallout record.

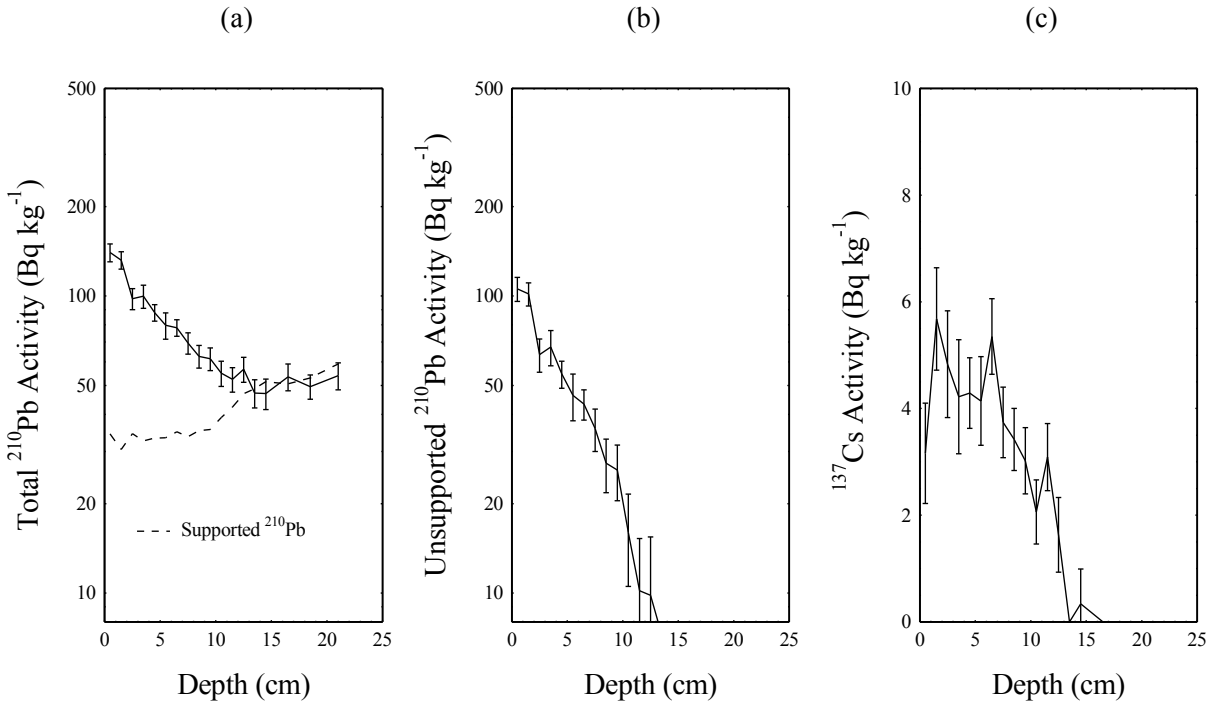

Figure 2.i. Fallout radionuclides in the Hardangerfjorden sediment core AKS-202A showing (a) total and supported ^{210}Pb, (b) unsupported ^{210}Pb, (c) ^{137}Cs concentrations versus depth.

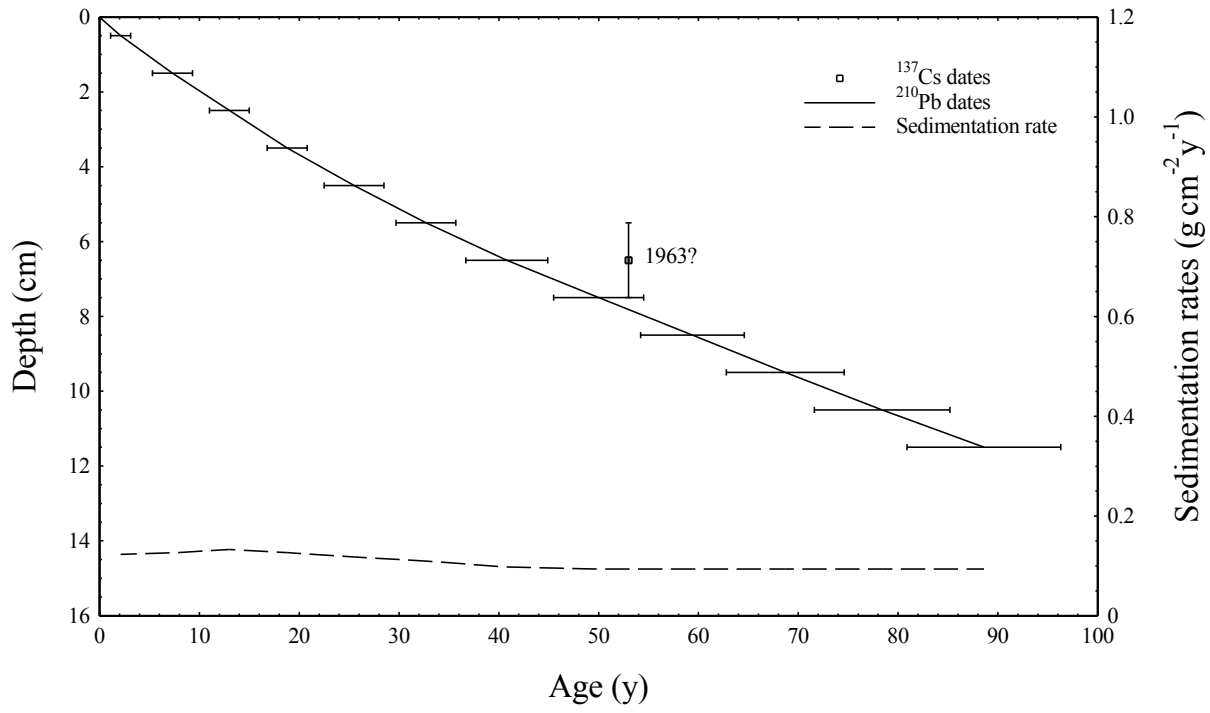

Figure 2.ii. Radiometric chronology of the Hardangerfjorden sediment core AKS-202A showing the ^{210}Pb dates and sedimentation rates and the possible 1963 depth suggested by the ^{137}Cs fallout record.

Appendix B: Laboratory report for carbon and nitrogen analysis of sediment samples

Prepared for: University of Oslo	Contact: Dr Silvia Hess
Iso-Analytical Ref. No.: 161205-3	P.O. No.: 152200, Elizabeth Alve
Material: Sediments	Analysis: $\delta^{15}N_{total}$ and $\delta^{13}C_{organic}$
Date Arrived: December 5, 2016	Report Date: February 6, 2017
Reported by: Ian Begley	Results File: 161205-3-results.xls

We have completed carbon and nitrogen isotope analysis of the 73 sediment samples received from you on December 5, 2016.

The results of analysis can be found in the attached MS Excel worksheet with the filename 161205-3-results.xls.

Sample preparation

In preparation for carbon isotope analysis 500 mg amounts of your sediment samples were acidified with 1M hydrochloric acid and left overnight to allow inorganic carbon to be liberated as CO_2. The samples were then neutralized by repetitively washing with distilled water and subsequently oven dried at 60 °C.

Nitrogen isotope analysis of sediments

Nitrogen isotope analysis of your sediment samples was undertaken by Elemental Analyser - Isotope Ratio Mass Spectrometry (EA-IRMS).

In brief, tin capsules containing sample or reference material are loaded into an auto-sampler on a Europa Scientific elemental analyser. From where they were dropped in sequence into a furnace held at 1000°C, where they are combusted in an oxygen rich environment, raising the temperature in the region of the sample to ~1700 °C. The gases produced on combustion are swept in a helium stream over combustion catalyst (Cr_2O_3), copper oxide wires to oxidize hydrocarbons and silver wool to remove sulfur and halides. The resultant gases, N_2, NO_x, H_2O, O_2 and CO_2 are swept through a

reduction stage of pure copper wires held at 600 °C. This step removes O_2 and converts NO_x species to N_2. A magnesium perchlorate chemical trap is used to remove H_2O and a carbosorb trap used to remove CO_2. Nitrogen is resolved using a packed column gas chromatograph held at an isothermal temperature of 100 °C. The resultant chromatographic peak for N_2 enters the ion source of a Europa Scientific 20-20 IRMS where it is ionized and accelerated. Gas species of different mass are separated in a magnetic field then simultaneously measured using a Faraday cup collector array to measure the isotopomers of N_2 at m/z 28, 29, and 30.

Both references and samples are converted to N_2 and analysed using this method. The analysis proceeds in a batch process by which a reference is analysed followed by a number of samples and then another reference.

The reference material used during $\delta^{15}N$ analysis of your sediment samples was IA-R001 (wheat flour, $\delta^{15}N_{Air}$ = 2.55 ‰). For quality control purposes check samples of IA-R001, IA-R045 (ammonium sulfate, $\delta^{15}N_{Air}$ = -4.71 ‰) and IA-R046 (ammonium sulfate, $\delta^{15}N_{Air}$ = 22.04 ‰) were analysed during batch analysis of your samples.

IA-R001, IA-R045 and IA-R046 are calibrated against and traceable to IAEA-N-1 (ammonium sulfate, $\delta^{15}N_{Air}$ = 0.4 ‰). IAEA-N-1 is an inter-laboratory comparison standard distributed by the International Atomic Energy Agency (IAEA), Vienna.

The measured values for the check samples are provided in the attached table.

Carbon isotope analysis of acid washed sediments

Carbon isotope analysis of your acid washed sediment samples was undertaken by Elemental Analyser - Isotope Ratio Mass Spectrometry (EA-IRMS).

In brief, tin capsules containing sample or reference material are loaded into an auto-sampler on a Europa Scientific elemental analyser. From where they were dropped in sequence into a furnace held at 1000 °C and combusted in an oxygen rich environment, raising the temperature in the region of the sample to ~1700 °C. The gases produced on combustion are swept in a helium stream over combustion catalyst (Cr_2O_3), copper oxide wires to oxidize hydrocarbons and silver wool to remove sulfur and halides. The resultant gases, N_2, NO_x, H_2O, O_2 and CO_2 are swept through a reduction stage of pure copper wires held at 600 °C. This step removes O_2 and converts NO_x species to N_2. A magnesium perchlorate chemical trap removes water. Carbon dioxide is separated from nitrogen by a packed column gas chromatograph held at an isothermal temperature of 100 °C. The resultant CO_2 chromatographic peak

enters the ion source of the Europa Scientific 20-20 IRMS where it is ionised and accelerated. Gas species of different mass are separated in a magnetic field then simultaneously measured using a Faraday cup collector array to measure the isotopomers of CO_2 at m/z 44, 45, and 46.

Both references and samples are converted and analysed in this manner. The analysis proceeds in a batch process, whereby a reference is analysed followed by a number of samples and then another reference.

The reference material used during $\delta^{13}C$ analysis of your acid washed sediment samples was IA-R001 (wheat flour, $\delta^{13}C_{V\text{-}PDB}$ = of -26.43 ‰). For quality control purposes check samples of IA-R001, IA-R005 (beet sugar, $\delta^{13}C_{V\text{-}PDB}$ = -26.03 ‰) and IA-R006 (cane sugar, $\delta^{13}C_{V\text{-}PDB}$ = -11.64 ‰) were analysed during batch analysis of your samples.

IA-R001, IA-R005 and IA-R006 are calibrated against and traceable to IAEA-CH-6 (sucrose, $\delta^{13}C_{V\text{-}PDB}$ = -10.43 ‰). IAEA-CH-6 is an inter-laboratory comparison standard distributed by the International Atomic Energy Agency (IAEA), Vienna.

Appendix C: Results from geochemical analyses

FF-core, 100 m from fish farm installation															
Core interval (cm)	Core depth (cm)	Sediment age (years AD)	Water content (%)	Sand content (% > 63 µm)	TOC (%)	TOC63 (%)	TN (%)	C/N	d13CV-PDB (‰)	d15NAIR (‰)	Cr (mg/kg)	Cu (mg/kg)	Zn (mg/kg)	Cd (mg/k)	Pb (mg/kg)
0-1	0,5	2016	59,4	10,5	1,5	3,4	0,20	7,6	-22,91	4,7	64,1	34,4	159,3	0,2	63,9
1-2	1,5	2015	54,9	10,7	1,4	3,4	0,21	7,0	-22,87	4,8	41,5	22,6	103,2	0,1	41,8
2-3	2,5	2013	52,2	8,7	1,5	3,1	0,20	7,4	-22,87	4,7	56,7	29,9	137,7	0,1	55,3
3-4	3,5	2010	48,8	8,5	1,5	3,1	0,19	8,3	-22,80	4,8	39,4	20,9	97,3	0,1	38,6
4-5	4,5	2007	48,2	6,2	1,5	2,6	0,18	7,9	-22,72	4,8	43,3	22,8	110,1	0,1	43,2
5-6	5,5	2004	48,0	6,5	1,5	2,7	0,18	8,5	-22,96	5,0	54,0	28,5	128,9	0,1	52,5
6-7	6,5	2000	47,3	6,6	1,4	2,6	0,18	7,8	-22,61	4,9	42,5	25,1	102,5	0,1	40,6
7-8	7,5	1996	47,3	8,3	1,5	3,0	0,17	8,6	-22,68	5,1	46,4	21,1	108,7	0,1	44,4
8-9	8,5	1991	46,2	9,0	1,3	2,9	0,17	7,9	-22,30	5,2	43,2	18,3	96,1	0,1	36,8
9-10	9,5	1985	46,0	6,2	1,3	2,5	0,17	8,1	-22,32	5,3	51,7	20,1	125,8	0,1	50,2
10-11	10,5	1981	46,7	6,3	1,3	2,4	0,17	7,8	-22,15	5,4	36,3	14,4	79,7	0,1	31,9
11-12	11,5	1976	47,3	4,3	1,3	2,1	0,16	7,9	-22,06	5,5	51,7	20,0	116,1	0,1	51,1
12-13	12,5	1973	48,7	4,2	1,3	2,1	0,17	7,8	-22,04	5,5	63,9	24,5	142,9	0,1	67,0
13-14	13,5	1969	50,4	5,5	1,4	2,4	0,17	8,2	-22,09	5,4	43,3	17,7	97,8	0,1	42,9
14-15	14,5	1965	50,1	4,8	1,4	2,2	0,18	7,7	-22,23	5,3	43,5	17,4	98,6	0,1	43,1
15-16	15,5	1958	50,2	5,3	1,5	2,4	0,18	7,9	-22,26	5,3	103,7	41,8	227,0	0,2	99,9
16-17	16,5	1953	49,1	5,7	1,3	2,3	0,18	7,5	-22,17	5,3	50,6	21,0	111,0	0,1	45,3
17-18	17,5	1947	45,1	5,2	1,3	2,2	0,15	8,4	-22,39	5,3	61,4	21,6	116,8	0,1	38,3
18-19	18,5	1940	43,7	7,4	1,1	2,4	0,14	7,7	-22,01	5,3	43,9	14,3	77,8	0,1	20,8
19-20	19,5	1934	42,6	5,9	1,1	2,2	0,14	8,0	-21,90	5,3	56,4	17,6	96,2	0,1	25,5
20-22	21,0	1927	42,2	4,6	1,1	1,9	0,14	7,8	-21,77	5,4	49,8	14,9	79,3	0,1	16,7
22-24	23,0	n/a	41,6	6,7	1,0	2,2	0,13	7,8	-21,79	5,3	91,6	26,1	138,4	0,1	26,9
24-26	25,0	n/a	41,1	4,7	1,0	1,9	0,13	8,0	-21,85	5,3	56,7	17,1	89,3	0,1	17,7
26-28	27,0	n/a	40,0	5,0	1,1	2,0	0,13	8,4	-21,82	5,3	81,9	23,1	123,3	0,1	22,5
28-29	28,5	n/a	40,2	5,6	1,0	2,0	0,13	7,9	-21,87	5,2	49,3	14,5	78,9	0,1	14,3
			Background		*Good*		*Moderate*		Poor		Bad				

NF-core, 500m from fish farm installation															
Core interval (cm)	Core depth (cm)	Sediment age (years AD)	Water content (%)	Sand content (% > 63 µm)	TOC (%)	TOC63 (%)	TN (%)	C/N	d13CV-PDB (‰)	d15NAIR (‰)	Cr (mg/kg)	Cu (mg/kg)	Zn (mg/kg)	Cd (mg/k)	Pb (mg/kg)
0-1	0,5	2016	59,1	*10,2*	1,0	2,9	0,15	7,2	-22,32	5,3	90,0	36,5	218,8	0,1	3,7
1-2	1,5	2014	51,0	*9,1*	1,1	2,8	0,15	7,8	-22,31	5,4	41,7	16,6	103,7	0,1	2,5
2-3	2,5	2009	46,9	*9,3*	1,1	2,8	0,14	8,1	-22,26	5,5	45,3	18,1	115,3	0,1	1,0
3-4	3,5	2003	47,0	*9,4*	1,1	2,8	0,13	8,2	-22,32	5,5	64,6	24,8	160,1	0,1	1,9
4-5	4,5	1997	45,2	*8,6*	1,0	2,6	0,13	8,0	-22,25	5,5	47,9	18,4	118,7	0,1	1,0
5-6	5,5	1990	44,6	*9,7*	1,0	2,6	0,13	8,1	-22,23	5,5	61,5	23,4	148,0	0,1	1,5
6-7	6,5	1983	44,1	*10,0*	1,0	2,7	0,13	8,0	-22,17	5,4	38,5	14,2	86,9	0,1	1,1
7-8	7,5	1975	42,9	*8,7*	0,9	2,5	0,13	7,5	-22,10	5,4	51,8	20,9	104,7	0,1	2,2
8-9	8,5	1966	43,3	*10,0*	1,0	2,5	0,13	7,7	-22,07	5,5	86,0	36,9	177,3	0,1	2,2
9-10	9,5	1957	42,4	*12,0*	1,0	2,6	0,12	8,3	-22,25	5,5	59,7	22,3	102,9	0,1	2,4
10-11	10,5	1947	40,5	*13,7*	0,9	2,7	0,11	8,2	-22,47	5,5	104,9	47,2	196,4	0,1	2,3
11-12	11,5	1938	39,2	*9,3*	0,8	2,1	0,10	8,4	-22,66	5,3	106,6	50,9	206,2	0,1	2,7
12-13	12,5	1927	39,1	*10,3*	0,7	2,2	0,09	8,1	-22,78	5,3	45,9	23,0	92,5	0,1	1,1
13-14	13,5	n/a	35,0	*5,0*	0,7	1,6	0,08	8,5	-22,47	5,2	61,5	31,5	124,4	0,1	1,5
14-15	14,5	n/a	35,3	*6,6*	0,6	1,8	0,06	9,3	-23,33	4,9	36,5	16,3	87,0	0,0	2,0
15-16	15,5	n/a	33,8	*9,7*	0,5	1,6	0,05	10,9	-24,06	4,4	62,1	26,9	145,9	0,1	2,4
16-17	16,5	n/a	34,1	*6,4*	0,5	1,5	0,05	11,2	-24,39	3,9	70,4	29,2	172,3	0,1	2,5
17-18	17,5	n/a	35,5	*4,1*	0,6	1,3	0,05	10,9	-24,18	4,4	61,0	25,2	150,3	0,1	2,8
18-19	18,5	n/a	36,0	*9,6*	0,5	1,0	0,04	11,8	-24,93	3,9	58,6	32,3	124,4	0,1	1,7
19-20	19,5	n/a	38,8	*4,0*	0,4	0,8	0,03	14,0	-25,58	3,7	124,4	66,3	252,7	0,2	4,4
20-22	21,0	n/a	40,3	*0,9*	0,4	0,5	0,03	13,7	-25,51	3,5	154,1	81,9	305,0	0,2	0,9
22-24	23,0	n/a	39,8	*2,5*	0,4	0,8	0,03	14,7	-25,52	3,4	70,9	39,7	149,7	0,1	2,2
24-26	25,0	n/a	38,4	*2,1*	0,4	0,7	0,03	13,8	-25,45	3,5	148,6	79,3	286,3	0,2	2,5
26-28	27,0	n/a	36,9	*3,8*	0,4	0,8	0,03	15,1	-25,62	3,1	56,2	34,8	123,4	0,1	2,2
28-30	29,0	n/a	37,4	*3,6*	0,4	0,7	0,03	14,0	-25,51	3,5	96,1	53,3	196,2	0,1	0,6

Appendix D: Results from stable isotope analyses of foraminiferal tests.

Core	Core depth	Species	No. of tests	Size (µm)	delta 13C (permil	±	delta 18O (permil	±	44 (mV) Pr 1.Cycle
FF-core	0,5	*Uvigerina peregrina*	10	150 - 500	-0,383	0,01	2,727	0,03	4817
FF-core	1,5	*Uvigerina peregrina*	9	150 - 500	-0,574	0,01	2,868	0,02	7915
FF-core	2,5	*Uvigerina peregrina*	13	150 - 500	-0,771	0,01	2,678	0,03	8849
FF-core	3,5	*Uvigerina peregrina*	7	150 - 500	-0,239	0,01	3,033	0,01	5353
FF-core	4,5	*Uvigerina peregrina*	10	150 - 500	-0,54	0,03	2,766	0,05	3529
FF-core	5,5	*Uvigerina peregrina*	12	150 - 500	-0,126	0,01	2,89	0,03	8719
FF-core	6,5	*Uvigerina peregrina*	11	150 - 500	-0,469	0,02	2,787	0,03	6729
FF-core	7,5	*Uvigerina peregrina*	8	150 - 500	-0,595	0,03	2,893	0,06	9860
FF-core	8,5	*Uvigerina peregrina*	12	150 - 500	-0,477	0,02	2,855	0,03	8091
FF-core	9,5	*Uvigerina peregrina*	12	150 - 500	-0,571	0,01	2,826	0,03	8625
FF-core	10,5	*Uvigerina peregrina*	10	150 - 500	-0,776	0,02	2,76	0,04	6302
FF-core	11,5	*Uvigerina peregrina*	5	150 - 500	-0,197	0,01	3,096	0,02	8765
FF-core	12,5	*Uvigerina peregrina*	4	150 - 500	-0,761	0,01	2,765	0,02	5976
FF-core	13,5	*Uvigerina peregrina*	4	150 - 500	-0,52	0,03	2,776	0,04	4786
FF-core	14,5	*Uvigerina peregrina*	10	150 - 500	-0,396	0,01	2,662	0,01	4241
FF-core	15,5	*Uvigerina peregrina*	10	150 - 500	-0,52	0,02	2,789	0,02	6096
FF-core	16,5	*Uvigerina peregrina*	7	150 - 500	-0,469	0,03	2,921	0,05	10074
FF-core	17,5	*Uvigerina peregrina*	8	150 - 500	-0,573	0,02	2,838	0,03	9110
FF-core	18,5	*Uvigerina peregrina*	9	150 - 500	-0,124	0,02	2,821	0,03	8701
FF-core	19,5	*Uvigerina peregrina*	4	150 - 500	0,149	0,01	3,213	0,02	5308
FF-core	21	*Uvigerina peregrina*	12	150 - 500	0,038	0,02	2,811	0,04	8796
FF-core	23	*Uvigerina peregrina*	3	150 - 500	0,118	0,02	3,239	0,05	9764
FF-core	25	*Uvigerina peregrina*	5	150 - 500	0,192	0,02	3,072	0,03	5563
FF-core	27	*Uvigerina peregrina*	3	150 - 500	0,123	0,01	3,172	0,03	8165
FF-core	28,5	*Uvigerina peregrina*	2	150 - 500	0,034	0,01	2,882	0,01	6860

Core	Core depth	Species	No. of tests	Size (µm)	delta 13C (permil	±	delta 18O (permil	±	44 (mV) Pr 1.Cycle
NF-core	0,5	*Uvigerina peregrina*	12	150 - 500	-0,85	0,01	2,76	0,03	5565,87
NF-core	1,5	*Uvigerina peregrina*	15	150 - 500	-0,61	0,01	2,80	0,02	5196,97
NF-core	2,5	*Uvigerina peregrina*	15	150 - 500	-0,69	0,02	2,87	0,04	9943,07
NF-core	3,5	*Uvigerina peregrina*	14	150 - 500	-0,65	0,01	2,87	0,03	7661,10
NF-core	4,5	*Uvigerina peregrina*	16	150 - 500	-0,63	0,02	2,94	0,05	7976,33
NF-core	5,5	*Uvigerina peregrina*	13	150 - 500	-0,53	0,01	2,95	0,01	5438,44
NF-core	6,5	*Uvigerina peregrina*	12	150 - 500	-0,53	0,01	2,79	0,02	5265,31
NF-core	7,5	*Uvigerina peregrina*	8	150 - 500	-0,14	0,02	2,80	0,04	5764,48
NF-core	8,5	*Uvigerina peregrina*	5	150 - 500	-0,25	0,01	3,00	0,03	9388,92
NF-core	9,5	*Uvigerina peregrina*	9	150 - 500	-0,54	0,02	2,81	0,04	10508,46
NF-core	10,5	*Uvigerina peregrina*	9	150 - 500	-0,30	0,02	2,93	0,03	11138,43
NF-core	11,5	*Uvigerina peregrina*	7	150 - 500	0,20	0,02	2,86	0,04	9359,64
NF-core	12,5	*Uvigerina peregrina*	3	150 - 500	-0,14	0,01	2,96	0,03	4645,46
NF-core	13,5	*Uvigerina peregrina*	7	150 - 500	0,25	0,01	3,04	0,02	10907,72
NF-core	14,5	*Uvigerina peregrina*	4	150 - 500	0,28	0,00	3,05	0,01	3985,94
NF-core	15,5	*Uvigerina peregrina*	9	150 - 500	0,24	0,01	2,87	0,02	4546,28
NF-core	16,5	*Uvigerina peregrina*	14	150 - 500	0,26	0,01	3,01	0,02	9686,45
NF-core	17,5	*Uvigerina peregrina*	3	150 - 500	0,42	0,01	3,03	0,03	6047,23
NF-core	18,5	*Uvigerina peregrina*	3	150 - 500	-0,06	0,03	3,03	0,04	8135,74
NF-core	19,5	*Uvigerina peregrina*	4	150 - 500	0,09	0,01	3,01	0,03	5741,65
NF-core	21	*Uvigerina peregrina*	0	150 - 500	nd	nd	nd	nd	nd
NF-core	23	*Uvigerina peregrina*	0	150 - 500	nd	nd	nd	nd	nd
NF-core	25	*Uvigerina peregrina*	2	150 - 500	0,02	0,02	3,19	0,04	2805,12
NF-core	27	*Uvigerina peregrina*	0	150 - 500	nd	nd	nd	nd	nd
NF-core	29,0	*Uvigerina peregrina*	0	150 - 500	nd	nd	nd	nd	nd

FF-core	0,5	*Hyalinea balthica*	13	150 - 500	-2,999	0,02	1,586	0,05	4443	NF-core	0,5	*Hyalinea balthica*	11	150 - 500	-2,00	0,01	2,17	0,03	5515,24
FF-core	1,5	*Hyalinea balthica*	12	150 - 500	-2,495	0,01	1,821	0,01	4237	NF-core	1,5	*Hyalinea balthica*	11	150 - 500	-2,45	0,01	1,87	0,03	7745,22
FF-core	2,5	*Hyalinea balthica*	13	150 - 500	-2,22	0,02	1,888	0,03	4745	NF-core	2,5	*Hyalinea balthica*	12	150 - 500	-2,02	0,02	2,14	0,05	9557,04
FF-core	3,5	*Hyalinea balthica*	7	150 - 500	-2,976	0,01	1,884	0,02	5140	NF-core	3,5	*Hyalinea balthica*	14	150 - 500	-1,92	0,02	2,08	0,04	7699,27
FF-core	4,5	*Hyalinea balthica*	13	150 - 500	-2,427	0,01	1,797	0,02	5567	NF-core	4,5	*Hyalinea balthica*	14	150 - 500	-2,01	0,01	2,16	0,02	8557,95
FF-core	5,5	*Hyalinea balthica*	5	150 - 500	-3,059	0,03	1,715	0,05	3735	NF-core	5,5	*Hyalinea balthica*	14	150 - 500	-1,75	0,01	2,12	0,03	4393,09
FF-core	6,5	*Hyalinea balthica*	11	150 - 500	-2,245	0,01	1,898	0,03	6857	NF-core	6,5	*Hyalinea balthica*	12	150 - 500	-2,02	0,02	1,95	0,04	8990,62
FF-core	7,5	*Hyalinea balthica*	14	150 - 500	-2,308	0,02	1,827	0,05	3076	NF-core	7,5	*Hyalinea balthica*	10	150 - 500	-2,01	0,01	2,03	0,03	9677,96
FF-core	8,5	*Hyalinea balthica*	17	150 - 500	-2,131	0,02	2,009	0,05	4722	NF-core	8,5	*Hyalinea balthica*	9	150 - 500	-1,79	0,01	2,31	0,02	9279,45
FF-core	9,5	*Hyalinea balthica*	14	150 - 500	-1,992	0,02	2,154	0,03	8186	NF-core	9,5	*Hyalinea balthica*	10	150 - 500	-1,58	0,01	2,10	0,02	4579,33
FF-core	10,5	*Hyalinea balthica*	9	150 - 500	-2,612	0,02	2,022	0,03	9435	NF-core	10,5	*Hyalinea balthica*	14	150 - 500	-1,16	0,02	2,43	0,03	5604,65
FF-core	11,5	*Hyalinea balthica*	18	150 - 500	-2,274	0,01	2,046	0,01	7306	NF-core	11,5	*Hyalinea balthica*	14	150 - 500	-0,93	0,01	2,14	0,03	6557,81
FF-core	12,5	*Hyalinea balthica*	13	150 - 500	-2,039	0,02	2,11	0,03	4195	NF-core	12,5	*Hyalinea balthica*	13	150 - 500	-1,33	0,01	2,26	0,02	4608,68
FF-core	13,5	*Hyalinea balthica*	15	150 - 500	-2,333	0,01	1,943	0,03	4789	NF-core	13,5	*Hyalinea balthica*	10	150 - 500	-0,87	0,01	2,08	0,02	6229,46
FF-core	14,5	*Hyalinea balthica*	11	150 - 500	-2,169	0,01	2,03	0,02	8660	NF-core	14,5	*Hyalinea balthica*	8	150 - 500	-0,99	0,02	2,51	0,03	7768,32
FF-core	15,5	*Hyalinea balthica*	19	150 - 500	-2,707	0,02	1,86	0,04	4606	NF-core	15,5	*Hyalinea balthica*	16	150 - 500	-0,87	0,03	2,21	0,06	6236,75
FF-core	16,5	*Hyalinea balthica*	13	150 - 500	-2,846	0,03	1,983	0,05	7718	NF-core	16,5	*Hyalinea balthica*	14	150 - 500	-0,98	0,01	2,20	0,01	9637,01
FF-core	17,5	*Hyalinea balthica*	12	150 - 500	-2,944	0,02	1,904	0,03	9844	NF-core	17,5	*Hyalinea balthica*	10	150 - 500	-0,77	0,01	2,31	0,03	7632,70
FF-core	18,5	*Hyalinea balthica*	16	150 - 500	-1,779	0,01	2,196	0,02	5153	NF-core	18,5	*Hyalinea balthica*	5	150 - 500	-1,15	0,02	2,08	0,05	3956,18
FF-core	19,5	*Hyalinea balthica*	15	150 - 500	-1,151	0,02	2,296	0,04	8439	NF-core	19,5	*Hyalinea balthica*	4	150 - 500	-1,52	0,02	2,00	0,06	4354,45
FF-core	21	*Hyalinea balthica*	16	150 - 500	-0,958	0,01	2,136	0,01	6086	NF-core	21	*Hyalinea balthica*	0	150 - 500	nd	nd	nd	nd	nd
FF-core	23	*Hyalinea balthica*	15	150 - 500	-1,092	0,02	2,463	0,04	8427	NF-core	23	*Hyalinea balthica*	0	150 - 500	nd	nd	nd	nd	nd
FF-core	25	*Hyalinea balthica*	17	150 - 500	-1,002	0,02	2,169	0,02	4668	NF-core	25	*Hyalinea balthica*	0	150 - 500	nd	nd	nd	nd	nd
FF-core	27	*Hyalinea balthica*	16	150 - 500	-1,074	0,01	2,094	0,04	5222	NF-core	27	*Hyalinea balthica*	0	150 - 500	nd	nd	nd	nd	nd
FF-core	28,5	*Hyalinea balthica*	13	150 - 500	-0,936	0,02	2,284	0,03	5900	NF-core	29,0	*Hyalinea balthica*	0	150 - 500	nd	nd	nd	nd	nd

FF-core	0,5	*Cassidulina laevigata*	5	150 - 500	-0,756	0,03	2,62	0,04	1337	NF-core	0,5	*Cassidulina laevigata*	20	150 - 500	-1,48	0,01	2,92	0,02	4216,83
FF-core	1,5	*Cassidulina laevigata*	8	150 - 500	-1,105	0,02	2,77	0,02	2797	NF-core	1,5	*Cassidulina laevigata*	18	150 - 500	-1,04	0,02	2,96	0,04	6044,95
FF-core	2,5	*Cassidulina laevigata*	13	150 - 500	-0,902	0,02	2,672	0,03	3049	NF-core	2,5	*Cassidulina laevigata*	20	150 - 500	-1,28	0,01	3,21	0,02	5932,46
FF-core	3,5	*Cassidulina laevigata*	6	150 - 500	-0,615	0,04	2,857	0,08	1838	NF-core	3,5	*Cassidulina laevigata*	20	150 - 500	-1,09	0,02	2,98	0,02	4278,89
FF-core	4,5	*Cassidulina laevigata*	7	150 - 500	-0,398	0,04	2,768	0,06	1956	NF-core	4,5	*Cassidulina laevigata*	19	150 - 500	-1,18	0,01	3,18	0,02	6668,04
FF-core	5,5	*Cassidulina laevigata*	7	150 - 500	-1,063	0,02	2,546	0,03	2945	NF-core	5,5	*Cassidulina laevigata*	20	150 - 500	-0,86	0,01	2,95	0,02	10037,23
FF-core	6,5	*Cassidulina laevigata*	11	150 - 500	-1,03	0,01	2,577	0,03	3892	NF-core	6,5	*Cassidulina laevigata*	16	150 - 500	-0,80	0,01	2,86	0,03	6028,65
FF-core	7,5	*Cassidulina laevigata*	7	150 - 500	-0,951	0,03	3,015	0,05	2211	NF-core	7,5	*Cassidulina laevigata*	22	150 - 500	-0,75	0,02	2,89	0,03	6818,58
FF-core	8,5	*Cassidulina laevigata*	14	150 - 500	-0,921	0,02	2,826	0,02	5462	NF-core	8,5	*Cassidulina laevigata*	17	150 - 500	-0,71	0,02	2,84	0,02	9576,31
FF-core	9,5	*Cassidulina laevigata*	14	150 - 500	-0,542	0,02	2,961	0,04	6333	NF-core	9,5	*Cassidulina laevigata*	13	150 - 500	-0,80	0,02	3,04	0,03	3211,35
FF-core	10,5	*Cassidulina laevigata*	15	150 - 500	-0,908	0,02	2,983	0,02	6552	NF-core	10,5	*Cassidulina laevigata*	18	150 - 500	-0,80	0,02	3,17	0,04	3543,85
FF-core	11,5	*Cassidulina laevigata*	13	150 - 500	-1,201	0,01	2,714	0,01	5611	NF-core	11,5	*Cassidulina laevigata*	13	150 - 500	-0,68	0,02	2,67	0,04	3813,00
FF-core	12,5	*Cassidulina laevigata*	15	150 - 500	-0,997	0,01	2,734	0,03	6241	NF-core	12,5	*Cassidulina laevigata*	13	150 - 500	-0,93	0,02	3,19	0,02	4643,41
FF-core	13,5	*Cassidulina laevigata*	16	150 - 500	-0,613	0,02	2,989	0,04	6664	NF-core	13,5	*Cassidulina laevigata*	9	150 - 500	-0,64	0,01	3,09	0,02	2855,92
FF-core	14,5	*Cassidulina laevigata*	15	150 - 500	-0,694	0,01	2,758	0,01	7638	NF-core	14,5	*Cassidulina laevigata*	5	150 - 500	-0,53	0,02		0,06	2005,31
FF-core	15,5	*Cassidulina laevigata*	12	150 - 500	-1,077	0,01	2,904	0,02	5517	NF-core	15,5	*Cassidulina laevigata*	12	150 - 500	-0,56	0,01	2,94	0,01	3414,55
FF-core	16,5	*Cassidulina laevigata*	16	150 - 500	-1,037	0,02	2,638	0,04	2934	NF-core	16,5	*Cassidulina laevigata*	15	150 - 500	-0,84	0,01	3,20	0,01	6657,89
FF-core	17,5	*Cassidulina laevigata*	10	150 - 500	-0,413	0,02	3,118	0,04	5326	NF-core	17,5	*Cassidulina laevigata*	19	150 - 500	-0,68	0,01	3,20	0,02	4623,49
FF-core	18,5	*Cassidulina laevigata*	16	150 - 500	-0,572	0,01	3,041	0,02	5984	NF-core	18,5	*Cassidulina laevigata*	22	150 - 500	-0,83	0,01	3,34	0,02	8437,93
FF-core	19,5	*Cassidulina laevigata*	15	150 - 500	-0,544	0,01	3,415	0,03	8584	NF-core	19,5	*Cassidulina laevigata*	22	150 - 500	-0,55	0,01	3,30	0,02	8842,38
FF-core	21	*Cassidulina laevigata*	13	150 - 500	-0,341	0,02	2,83	0,05	5062	NF-core	21	*Cassidulina laevigata*	9	150 - 500	-1,21	0,02	3,67	0,07	2436,61
FF-core	23	*Cassidulina laevigata*	7	150 - 500	-0,562	0,02	3,604	0,05	2364	NF-core	23	*Cassidulina laevigata*	13	150 - 500	-1,01	0,01	3,51	0,03	3698,63
FF-core	25	*Cassidulina laevigata*	10	150 - 500	-0,23	0,01	3,221	0,02	5174	NF-core	25	*Cassidulina laevigata*	8	150 - 500	-0,97	0,04	4,07	0,07	1909,98
FF-core	27	*Cassidulina laevigata*	12	150 - 500	-0,424	0,02	3,127	0,03	5343	NF-core	27	*Cassidulina laevigata*	9	150 - 500	-0,92	0,02	3,35	0,03	3349,84
FF-core	28,5	*Cassidulina laevigata*	15	150 - 500	-0,215	0,02	3,046	0,04	7696	NF-core	29,0	*Cassidulina laevigata*	13	150 - 500	-0,79	0,01	3,58	0,01	4750,59

Appendix E: Foraminifera data, total counts and diversity indices (colour codes listed in Table 4-1)

Hardangerfjorden cores	FF-core							NF-core								
63 - 500 µm	counts							counts								
Sediment depth (cm)	0,5	3,5	6,5	10,5	15,5	19,5	25	0,5	2,5	3,5	5,5	10,5	13,5	15,5	19,5	25
Sediment age (years AD)	2015	2007	1996	1976	1952	1927	n/a	2014	2003	1997	1983	1938	n/a	n/a	n/a	n/a
Sediment interval (cm)	0-1	3-4	6-7	10 - 11	15 - 16	19-20	24 - 26	0-1	2-3	3-4	5-6	10 - 11	13 - 14	15 - 16	19-20	24 - 26
Adercotryma glomeratum/wrighti	11	4	10	2	6			14	5	5	14					
Ammodiscus gullmarensis																
Ammoscalaria tenuimargo			1			1	1									
Cribrostomoides jeffreysii		1								1				1		
Cibrostomoides nitida											1					
Eggerella europea	2	1	3													
Eggerelloides medius	28	23	33	31	27	21	12	56	33	40	44	32	7	4	11	
Haplophragmoides bradyi								6								
Lagenammina arenulata											2	1	1			
Leptohalysis gracilis		1						3								
Liebusella goesi	2		2	2	2	2				4	1	2				
Recurvoides trochamminiforme								1								
Reophax fusiformis			1				1	4								
Reophax sp.				1												
Reophax scorpiurus										1						
Saccammina sp.		1														
Sigmoilopsis schlumbergeri	1								1			1				
Spiroplectammina biformis	2															
Spiroplectammina sagittula								1		2	2					
Textularia earlandi	20	34	36	3	5	1		11	1		1					
Textularia kattegatensis	2	3	3	2	2											
Textularia skagerrakensis	1	1	1		1			11	3	5	2	3		1		
Tritaxis conica				9												
Trochammina globigeriniformis	8	9	9		9	4	5	15	14	14	13	6	1	1		
Trochammina inflata								1								
Trochammina "skrumpa"	1							1								
Trochammina sp.														1		
Trochamminopsis quadriloba			2					5								
aggl unidentified				1		2		1	3							
Alabaminella weddellensis					1											
Astrononion gallowayi		1			2					1	1	3			1	
Bolivina albatrossi					2											
Bolivina pseudoplicata	3			1	2				9	2			1		1	
Bolivina sp.										1						
Bolivinellina pseudopunctata		1						16		9	2	1	3			
Brizalina skagerrakensis	35	38	24	34	66	13	5	23	30	18	40	35	7	6		
Brizalina spathulata	7	2	2	8	6	2		35	16	14	9	4	1		1	
Buccella frigida								35								
Bulimina aculeata		1														
Bulimina marginata	82	45	58	68	81	85	133	31	40	44	36	61	40	55	3	1
Cassidulina crassa				1	2		2									
Cassidulina laevigata	9	10	16	29	24	22	13	43	21	32	29	31	34	34	40	37
Cassidulina obtusa		1	2			6		9	2	8		9	19	5		
Cassidulina reniforme								1			5			10	55	29
Cibicides lobatulus	1	1		3				1		4	4			2		
Cibicides pseudoungerianus					1											
Cibicides sp.			2									2				
Dentalina sp.									1							
Discorbinella bertheloti						1		2						1	1	
Elphidium albiumbilicatum				2			1									1
Elphidium excavatum													3	8	7	4
Elphidium sp.	2													1		2
Epistominella vitrea	1	3		8	2	1	4	6	8	9	6	3	1	5	2	
Fissurina laevigata	2				3		2							5		
Fissurina sp						1		1		1				1		
Gavelinopsis praegeri		1														
Glandulina ovula							3									
Globobulimina auriculata	4	2	5	2	5	7	3		4	4	3	14	4	2		
Globocassidulina sp.											1			2	1	
Gyroidina lamarckiana	2			1												
Gyroidina orbicularis									1	1				2		
Gyroidina sp.					1											
Hyalinea balthica	6	8	9	8	16	8	33		10	10	9	11	15	9	1	1
Lagena laevis			4													
Lagena striata	2													1		
Lagenosolena distoma					2	1	4				2	1		3		1
Lagena sp.													1			
Lenticulina sp.						1				1	2			1	1	
Melonis barleeanum	3	1	3	2	3	1	1	3	6	2	1	3	4			
Nonionella iridea	1		2	11	10	14	14	9	12	11	18	12	12	8	5	
Nonionella turgida				1						1	1	1	2	1		
Nonionellina labradorica							1						3	2	2	6
Oolina globosa					1											
Oolina spp.							3			1						
Pullenia bulloides					1							1				
Pullenia osloensis	14	7	17	12	21	18	18	25	14	20	12	29	11	35	33	17
Pullenia quinqueloba	3	5		1	6			2			3	4				
Quinqueloculina sp.								1								
Sphaeroidina bulloides												1				
Stainforthia fusiformis	16	20	17	22	19	23	35	25	18			19	64	60	37	50
Stainforthia loeblichi		2	1	3	2				2	1			4	4		
Stainforthia skagerrakensis								1							12	11
Stainforthia sp.							2									
Trifarina angulosa	3	2		1		4	2	4	2	1		1	1		1	
Uvigerina peregrina	9	9	4	4	10	2	12	14	9	9	16	7	9	6		
Uvigerina mediterranea								1								
calc unidetified						3	1					1	1		2	
Sum picked	283	238	267	273	341	244	311	418	265	277	280	299	249	277	217	160
Ind / g sediment	263	377	297	493	352	371	321	2120	852	717	867	756	277	215	241	158
BFAR (indiv/cm2/år)	71,0	84,8	53,5	93,7	45,8	48,2	n/a	254,4	110,7	93,2	95,3	68,1	n/a	n/a	n/a	n/a
# species	31	30	26	29	32	25	25	36	25	32	29	29	25	31	20	12
%-calcareous tests	72	67	62	81	85	87	94	69	77	74	71	85	96	97	95	100
%-agglutinated tests	28	33	38	19	15	13	6	31	23	26	29	15	4	3	5	0
ES(100)	22,3	21,1	20,0	20,5	21,7	18,4	17,4	24,0	20,5	23,0	21,1	20,4	18,8	21,5	14,6	10,3
H'(log2)	3,8	3,8	3,8	3,7	3,8	3,4	3,1	4,3	4,0	4,1	3,9	3,8	3,6	3,7	3,1	2,6
AMBI	2,6	2,6	2,5	2,5	2,4	2,6	2,6	2,2	2,4	1,9	2,0	2,4	2,7	2,6	1,8	2,2

Appendix F: Foraminifera data, concentration of tests (individuals/g dry sediment).

Hardangerfjorden cores	FF-core							NF-core								
63 - 500 µm	**Relative abundance (%)**															
Sediment depth (cm)	0,5	3,5	6,5	10,5	15,5	19,5	25	0,5	2,5	3,5	5,5	10,5	13,5	15,5	19,5	25
Sediment age (years AD)	2015	2007	1996	1976	1952	1927	n/a	2014	2003	1997	1983	1938	n/a	n/a	n/a	n/a
Sediment interval (cm)	0-1	3-4	6-7	10 - 11	15 - 16	19-20	24 - 26	0-1	2-3	3-4	5-6	10 - 11	13 - 14	15 - 16	19-20	24 - 26
Adercotryma glomeratum/wrighti	10,2	6,3	11,1	3,6	6,2	0,0	0,0	71,0	16,1	12,9	43,3	0,0	0,0	0,0	0,0	0,0
Ammoscalaria tenuimargo	0,0	0,0	1,1	0,0	0,0	1,5	1,0	0,0	0,0	0,0	0,0	0,0	0,0	0,0	0,0	0,0
Cribrostomoides jeffreysii	0,0	1,6	0,0	0,0	0,0	0,0	0,0	0,0	0,0	2,6	0,0	0,0	0,0	0,8	0,0	0,0
Eggerella europea	1,9	1,6	3,3	0,0	0,0	0,0	0,0	0,0	0,0	0,0	0,0	0,0	0,0	0,0	0,0	0,0
Eggerelloides medius	26,0	36,4	36,7	56,0	27,9	31,9	12,4	284,0	106,0	103,5	136,2	80,9	7,8	3,1	12,2	0,0
Haplophragmoides bradyi	0,0	0,0	0,0	0,0	0,0	0,0	0,0	30,4	0,0	0,0	0,0	0,0	0,0	0,0	0,0	0,0
Lagenammina arenulata	0,0	0,0	0,0	0,0	0,0	0,0	0,0	0,0	0,0	0,0	6,2	2,5	1,1	0,0	0,0	0,0
Leptohalysis gracilis	0,0	1,6	0,0	0,0	0,0	0,0	0,0	15,2	0,0	0,0	0,0	0,0	0,0	0,0	0,0	0,0
Liebusella goesi	1,9	0,0	2,2	3,6	2,1	3,0	0,0	0,0	0,0	10,3	3,1	5,1	0,0	0,0	0,0	0,0
Recurvoides trochamminiforme	0,0	0,0	0,0	0,0	0,0	0,0	0,0	5,1	0,0	0,0	0,0	0,0	0,0	0,0	0,0	0,0
Reophax dentaliniformis	0,0	0,0	0,0	0,0	0,0	0,0	0,0	0,0	0,0	0,0	0,0	0,0	0,0	0,0	0,0	0,0
Reophax fusiformis	0,0	0,0	1,1	0,0	0,0	0,0	1,0	20,3	0,0	0,0	0,0	0,0	0,0	0,0	0,0	0,0
Reophax scorpiurus	0,0	0,0	0,0	0,0	0,0	0,0	0,0	0,0	0,0	2,6	0,0	0,0	0,0	0,0	0,0	0,0
Saccammina sp.	0,0	1,6	0,0	0,0	0,0	0,0	0,0	0,0	0,0	0,0	0,0	0,0	0,0	0,0	0,0	0,0
Sigmoilopsis schlumbergeri	0,9	0,0	0,0	0,0	0,0	0,0	0,0	0,0	3,2	0,0	0,0	2,5	0,0	0,0	0,0	0,0
Spiroplectammina biformis	1,9	0,0	0,0	0,0	0,0	0,0	0,0	0,0	0,0	0,0	0,0	0,0	0,0	0,0	0,0	0,0
Spiroplectammina sagittula	0,0	0,0	0,0	0,0	0,0	0,0	0,0	5,1	0,0	5,2	6,2	0,0	0,0	0,0	0,0	0,0
Textularia earlandi	18,6	53,8	40,1	5,4	5,2	1,5	0,0	55,8	3,2	0,0	3,1	0,0	0,0	0,0	0,0	0,0
Textularia kattegatensis	1,9	4,8	3,3	3,6	2,1	0,0	0,0	0,0	0,0	0,0	0,0	0,0	0,0	0,0	0,0	0,0
Textularia skagerrakensis	0,9	1,6	1,1	0,0	1,0	0,0	0,0	55,8	9,6	12,9	6,2	7,6	0,0	0,8	0,0	0,0
Tritaxis conica	0,0	**0,0**	0,0	16,3	0,0	0,0	0,0	0,0	0,0	0,0	0,0	0,0	0,0	0,0	0,0	0,0
Trochammina globigeriniformis	7,4	14,3	10,0	0,0	9,3	6,1	5,2	76,1	45,0	36,2	40,2	15,2	1,1	0,8	0,0	0,0
Trochammina inflata	0,0	0,0	0,0	0,0	0,0	0,0	0,0	5,1	0,0	0,0	0,0	0,0	0,0	0,0	0,0	0,0
Trochammina "skrumpa"	0,9	0,0	0,0	0,0	0,0	0,0	0,0	5,1	0,0	0,0	0,0	0,0	0,0	0,0	0,0	0,0
Trochamminopsis quadriloba	0,0	0,0	2,2	0,0	0,0	0,0	0,0	25,4	0,0	0,0	0,0	0,0	0,0	0,0	0,0	0,0
aggl unidentified	0,0	0,0	0,0	1,8	0,0	3,0	0,0	5,1	9,6	0,0	0,0	0,0	0,0	0,0	0,0	0,0
Alabaminella weddellensis	0,0	0,0	0,0	0,0	1,0	0,0	0,0	0,0	0,0	0,0	0,0	0,0	0,0	0,0	0,0	0,0
Astrononion gallowayi	0,0	1,6	0,0	0,0	2,1	0,0	0,0	0,0	0,0	2,6	3,1	7,6	0,0	0,0	1,1	0,0
Bolivina albatrossi	0,0	0,0	0,0	0,0	2,1	0,0	0,0	0,0	0,0	0,0	0,0	0,0	0,0	0,0	0,0	0,0
Bolivina pseudoplicata	2,8	0,0	0,0	1,8	2,1	0,0	0,0	0,0	28,9	5,2	0,0	0,0	1,1	0,0	1,1	0,0
Bolivina sp.	0,0	0,0	0,0	0,0	0,0	0,0	0,0	0,0	0,0	2,6	0,0	0,0	0,0	0,0	0,0	0,0
Bolivinellina pseudopunctata	0,0	1,6	0,0	0,0	0,0	0,0	0,0	81,2	0,0	23,3	6,2	2,5	3,3	0,0	0,0	0,0
Brizalina difformis (lite juletre)	0,0	0,0	0,0	0,0	0,0	0,0	0,0	0,0	0,0	0,0	0,0	0,0	0,0	0,0	0,0	0,0
Brizalina skagerrakensis	32,5	60,2	26,7	61,4	68,1	19,8	5,2	116,7	96,4	46,6	123,8	88,5	7,8	4,7	0,0	0,0
Brizalina spathulata	6,5	3,2	2,2	14,5	6,2	3,0	0,0	177,5	51,4	36,2	27,9	10,1	1,1	0,0	1,1	0,0
Bulimina aculeata	0,0	1,6	0,0	0,0	0,0	0,0	0,0	0,0	0,0	0,0	0,0	0,0	0,0	0,0	0,0	0,0
Bulimina marginata	76,1	71,3	64,6	122,8	83,6	129,2	137,5	157,2	128,5	113,8	111,4	154,3	44,5	42,7	3,3	1,0
Cassidulina crassa	0,0	0,0	0,0	1,8	2,1	0,0	2,1	0,0	0,0	0,0	0,0	0,0	0,0	0,0	0,0	0,0
Cassidulina laevigata	8,4	15,8	17,8	52,4	24,8	33,4	13,4	218,1	67,5	82,8	89,8	78,4	37,8	26,4	44,4	36,4
Cassidulina obtusa	0,0	1,6	2,2	0,0	0,0	9,1	0,0	45,6	6,4	20,7	0,0	22,8	21,1	3,9	0,0	0,0
Cassidulina reniforme	0,0	0,0	0,0	0,0	0,0	0,0	0,0	5,1	0,0	0,0	15,5	0,0	0,0	7,8	61,0	28,6
Cibicides lobatulus	0,9	1,6	0,0	5,4	0,0	0,0	0,0	5,1	0,0	10,3	12,4	0,0	0,0	1,6	0,0	0,0
Cibicides sp.	0,0	0,0	2,2	0,0	0,0	0,0	0,0	0,0	0,0	0,0	0,0	5,1	0,0	0,0	0,0	0,0
Dentalina sp.	0,0	0,0	0,0	0,0	0,0	0,0	0,0	0,0	3,2	0,0	0,0	0,0	0,0	0,0	0,0	0,0
Discorbinella bertheloti	0,0	0,0	0,0	0,0	0,0	1,5	0,0	10,1	0,0	0,0	0,0	0,0	0,0	0,8	1,1	0,0
Elphidium albiumbilicatum	0,0	0,0	0,0	3,6	0,0	0,0	1,0	0,0	0,0	0,0	0,0	0,0	0,0	0,0	0,0	1,0
Elphidium excavatum	0,0	0,0	0,0	0,0	0,0	0,0	0,0	0,0	0,0	0,0	0,0	0,0	3,3	6,2	7,8	3,9
Elphidium sp.	1,9	0,0	0,0	0,0	0,0	0,0	0,0	0,0	0,0	0,0	0,0	0,0	0,0	0,8	0,0	2,0
Epistominella vitrea	0,9	4,8	0,0	14,5	2,1	1,5	4,1	30,4	25,7	23,3	18,6	7,6	1,1	3,9	2,2	0,0
Fissurina laevigata	1,9	0,0	0,0	0,0	3,1	0,0	2,1	0,0	0,0	0,0	0,0	0,0	0,0	3,9	0,0	0,0
Fissurina sp	0,0	0,0	0,0	0,0	0,0	1,5	0,0	5,1	0,0	2,6	0,0	0,0	0,0	0,8	0,0	0,0
Glandulina ovula	0,0	0,0	0,0	0,0	0,0	0,0	3,1	0,0	0,0	0,0	0,0	0,0	0,0	0,0	0,0	0,0
Globobulimina auriculata	3,7	3,2	5,6	3,6	5,2	10,6	3,1	0,0	12,9	10,3	9,3	35,4	4,5	1,6	0,0	0,0
Globocassidulina sp.	0,0	0,0	0,0	0,0	0,0	0,0	0,0	0,0	0,0	0,0	3,1	0,0	0,0	1,6	1,1	0,0
Guttulina sp.	0,0	0,0	0,0	0,0	0,0	0,0	0,0	0,0	0,0	0,0	0,0	0,0	0,0	0,0	0,0	0,0
Gyroidina lamarckiana	1,9	0,0	0,0	1,8	0,0	0,0	0,0	0,0	0,0	0,0	0,0	0,0	0,0	0,0	0,0	0,0
Gyroidina orbicularis	0,0	0,0	0,0	0,0	0,0	0,0	0,0	0,0	3,2	2,6	0,0	0,0	0,0	1,6	0,0	0,0
Hyalinea balthica	5,6	12,7	10,0	14,5	16,5	12,2	34,1	0,0	32,1	25,9	27,9	27,8	16,7	7,0	1,1	1,0
Lagena laevis	0,0	0,0	4,5	0,0	0,0	0,0	0,0	0,0	0,0	0,0	0,0	0,0	0,0	0,0	0,0	0,0
Lagena striata	1,9	0,0	0,0	0,0	0,0	0,0	0,0	0,0	0,0	0,0	0,0	0,0	0,0	0,8	0,0	0,0
Lagenosolena distoma	0,0	0,0	0,0	0,0	2,1	1,5	4,1	0,0	0,0	0,0	6,2	2,5	0,0	2,3	0,0	1,0
Lenticulina sp.	0,0	0,0	0,0	0,0	0,0	1,5	0,0	0,0	0,0	2,6	6,2	0,0	0,0	0,8	1,1	0,0
Melonis barleeanum	2,8	1,6	3,3	3,6	3,1	1,5	1,0	15,2	19,3	5,2	3,1	7,6	4,5	0,0	0,0	0,0
Nonionella iridea	0,9	0,0	2,2	19,9	10,3	21,3	14,5	45,6	38,6	28,5	55,7	30,3	13,4	6,2	5,5	0,0
Nonionella turgida	0,0	0,0	0,0	1,8	0,0	0,0	0,0	0,0	0,0	2,6	3,1	2,5	2,2	0,8	0,0	0,0
Nonionellina labradorica	0,0	0,0	0,0	0,0	0,0	0,0	1,0	0,0	0,0	0,0	0,0	0,0	3,3	1,6	2,2	5,9
Oolina globosa	0,0	0,0	0,0	0,0	1,0	0,0	0,0	0,0	0,0	0,0	0,0	0,0	0,0	0,0	0,0	0,0
Oolina spp.	0,0	0,0	0,0	0,0	0,0	0,0	3,1	0,0	0,0	2,6	0,0	0,0	0,0	0,0	0,0	0,0
Planulina sp.	0,0	0,0	0,0	0,0	0,0	0,0	0,0	0,0	0,0	0,0	0,0	0,0	0,0	0,0	0,0	0,0
Pullenia bulloides	0,0	0,0	0,0	0,0	1,0	0,0	0,0	0,0	0,0	0,0	0,0	2,5	0,0	0,0	0,0	0,0
Pullenia osloensis	13,0	11,1	18,9	21,7	21,7	27,4	18,6	126,8	45,0	51,7	37,1	73,3	12,2	27,2	36,6	16,7
Pullenia quinqueloba	2,8	7,9	0,0	1,8	6,2	0,0	0,0	10,1	0,0	0,0	9,3	10,1	0,0	0,0	0,0	0,0
Quinqueloculina sp.	0,0	0,0	0,0	0,0	0,0	0,0	0,0	5,1	0,0	0,0	0,0	0,0	0,0	0,0	0,0	0,0
Sphaeroidina bulloides	0,0	0,0	0,0	0,0	0,0	0,0	0,0	0,0	0,0	0,0	0,0	2,5	0,0	0,0	0,0	0,0
Stainforthia fusiformis	14,9	31,7	18,9	39,7	19,6	35,0	36,2	126,8	57,8	59,5	40,2	48,1	71,2	46,6	41,1	49,2
Stainforthia loeblichi	0,0	3,2	1,1	5,4	2,1	0,0	0,0	0,0	6,4	2,6	0,0	0,0	4,5	3,1	0,0	0,0
Stainforthia skagerrakensis	0,0	0,0	0,0	0,0	0,0	0,0	0,0	5,1	0,0	0,0	0,0	0,0	0,0	0,0	13,3	10,8
Trifarina angulosa	2,8	3,2	0,0	1,8	0,0	6,1	2,1	20,3	6,4	2,6	0,0	2,5	1,1	0,0	1,1	0,0
Uvigerina peregrina	8,4	14,3	4,5	7,2	10,3	3,0	12,4	71,0	28,9	23,3	49,5	17,7	10,0	4,7	0,0	0,0
Uvigerina mediterranea	0,0	0,0	0,0	0,0	0,0	0,0	0,0	5,1	0,0	0,0	0,0	0,0	0,0	0,0	0,0	0,0
calc unidetified	0,0	0,0	0,0	0,0	0,0	4,6	1,0	0,0	0,0	0,0	0,0	2,5	1,1	0,0	2,2	0,0

Appendix G: Foraminifera data, relative species abundance (%)

Hardangerfjorden cores	Relative abundance (%)																
63 - 500 µm	FF-core							NF-core									
Sediment depth (cm)	0,5	3,5	6,5	10,5	15,5	19,5	25	0,5	2,5	3,5	5,5	10,5	13,5	15,5	19,5	25
Sediment age (years AD)	2015	2007	1996	1976	1952	1927	n/a	2014	2003	1997	1983	1938	n/a	n/a	n/a	n/a
Sediment interval (cm)	0-1	3-4	6-7	10 - 11	15 - 16	19-20	24 - 26	0-1	2-3	3-4	5-6	10 - 11	13 - 14	15 - 16	19-20	24 - 26
Adercotryma glomeratum/wrighti	4	2	4	1	2	0	0	3	2	2	5	0	0	0	0	0
Eggerella europea	1	0	1	0	0	0	0	0	0	0	0	0	0	0	0	0
Eggerella sp.	0	0	0	0	0	0	0	0	0	0	0	0	0	0	0	0
Eggerelloides medius	10	10	12	11	8	6	4	13	12	14	16	11	3	1	5	0
Eggerelloides scaber	0	0	0	0	0	0	0	0	0	0	0	0	0	0	0	0
Haplophragmoides bradyi	0	0	0	0	0	0	0	1	0	0	0	0	0	0	0	0
Liebusella goesi	1	0	1	1	1	1	0	0	0	1	0	1	0	0	0	0
Reophax fusiformis	0	0	0	0	0	0	0	1	0	0	0	0	0	0	0	0
Textularia earlandi	7	14	13	1	1	0	0	3	0	0	0	0	0	0	0	0
Textularia kattegatensis	1	1	1	1	1	0	0	0	0	0	0	0	0	0	0	0
Textularia skagerrakensis	0	0	0	0	0	0	0	3	1	2	1	1	0	0	0	0
Trochammina globigeriniformis	3	4	3	0	3	1	2	4	5	5	5	2	0	0	0	0
Trochamminopsis quadriloba	0	0	1	0	0	0	0	1	0	0	0	0	0	0	0	0
Astrononion gallowayi	0	0	0	0	1	0	0	0	0	0	0	1	0	0	0	0
Bolivina pseudoplicata	1	0	0	0	1	0	0	0	3	1	0	0	0	0	0	0
Bolivinellina pseudopunctata	0	0	0	0	0	0	0	4	0	3	1	0	1	0	0	0
Brizalina skagerrakensis	12	16	9	12	19	4	2	6	11	6	14	12	3	2	0	0
Brizalina spathulata	2	1	1	3	2	1	0	8	6	5	3	1	0	0	0	0
Bulimina marginata	29	19	22	25	24	25	43	7	15	16	13	20	16	20	1	1
Cassidulina laevigata	3	4	6	11	7	6	4	10	8	12	10	10	14	12	18	23
Cassidulina obtusa	0	0	1	0	0	2	0	2	1	3	0	3	8	2	0	0
Cassidulina reniforme	0	0	0	0	0	0	0	0	0	0	2	0	0	4	25	18
Cibicides lobatulus	0	0	0	1	0	0	0	0	0	1	1	0	0	1	0	0
Elphidium excavatum	0	0	0	0	0	0	0	0	0	0	0	0	1	3	3	3
Elphidium sp.	1	0	0	0	0	0	0	0	0	0	0	0	0	0	0	1
Epistominella vitrea	0	1	0	3	1	0	1	1	3	3	2	1	0	2	1	0
Fissurina laevigata	1	0	0	0	1	0	1	0	0	0	0	0	0	2	0	0
Fissurina sp	0	0	0	0	0	0	0	0	0	0	0	0	0	0	0	0
Gavelinopsis praegeri	0	0	0	0	0	0	0	0	0	0	0	0	0	0	0	0
Glandulina ovula	0	0	0	0	0	0	1	0	0	0	0	0	0	0	0	0
Globobulimina auriculata	1	1	2	1	1	2	1	0	2	1	1	5	2	1	0	0
Gyroidina lamarckiana	1	0	0	0	0	0	0	0	0	0	0	0	0	0	0	0
Gyroidina orbicularis	0	0	0	0	0	0	0	0	0	0	0	0	0	1	0	0
Hyalinea balthica	2	3	3	3	5	2	11	0	4	4	3	4	6	3	0	1
Lagena laevis	0	0	1	0	0	0	0	0	0	0	0	0	0	0	0	0
Lagenosolena distoma	0	0	0	0	1	0	1	0	0	0	1	0	0	1	0	1
Lenticulina sp.	0	0	0	0	0	0	0	0	0	0	1	0	0	0	0	0
Melonis barleeanum	1	0	1	1	1	0	0	1	2	1	0	1	2	0	0	0
Nonionella iridea	0	0	1	4	3	4	5	2	5	4	6	4	5	3	2	0
Nonionella turgida	0	0	0	0	0	0	0	0	0	0	0	0	1	0	0	0
Nonionellina labradorica	0	0	0	0	0	0	0	0	0	0	0	0	1	1	1	4
Oolina spp.	0	0	0	0	0	0	1	0	0	0	0	0	0	0	0	0
Pullenia bulloides	0	0	0	0	0	0	0	0	0	0	0	0	0	0	0	0
Pullenia osloensis	5	3	6	4	6	5	6	6	5	7	4	10	4	13	15	11
Pullenia quinqueloba	1	2	0	0	2	0	0	0	0	0	1	1	0	0	0	0
Quinqueloculina sp.	0	0	0	0	0	0	0	0	0	0	0	0	0	0	0	0
Stainforthia fusiformis	6	8	6	8	6	7	11	6	7	0	0	6	26	22	17	31
Stainforthia loeblichi	0	1	0	1	1	0	0	0	1	0	0	0	2	1	0	0
Trifarina angulosa	1	1	0	0	0	1	1	1	1	0	0	0	0	0	0	0
Uvigerina peregrina	3	4	1	1	3	1	4	3	3	3	6	2	4	2	0	0
calc unidetified	0	0	0	0	0	1	0	0	0	0	0	0	0	0	1	0

Appendix H: Foraminifera reference list, based on The World Register of Marine Species (WoRMS, 2017)

Adercotryma glomeratum (Brady) = Lituola glomerata Brady, 1878.
Alabaminella weddellensis (Earland) = Eponides weddellensis Earland, 1936.
Ammodiscus gullmarensis Höglund, 1948
Astrononion gallowayi Loeblich & Tappan, 1953.
Ammoscalaria tenuimargo (Brady) = Haplophragmium tenuimargo Brady, 1882.
Bolivina albatrossi Cushman 1922.
Bolivina pseudoplicata Heron-Allen & Earland, 1930.
Bolivinellina pseudopunctata (Höglund) = Bolivina pseudopunctata Höglund, 1947.
Brizalina skagerrakensis (Qvale & Nigam) = Bolivina skagerrakensis Qvale & Nigam, 1985.
Brizalina spathulata (Williamson) = Bolivina spathulata Williamson, 1858.
Bulimina marginata d'Orbigny, 1826.
Cassidulina laevigata d'Orbigny, 1826.
Cassidulina obtusa Williamson, 1858.
Cassidulina reniforme Nørvang, 1945.
Cibicidoides lobatulus (Walker & Jacob) = Nautilus lobatulus Walker & Jacob, 1798.
Cribrostomoides jeffreysii (Williamson) = Veleroninoides jeffreysii Williamson, 1856.
Cribrostomoides nitida (Goës) = Haplophragmium nitidum Goës, 1896.
Discorbinella bertheloti (d'Orbigny) = Rosalina bertheloti d'Orbigny, 1839.
Eggerella europea (Christiansen) = Verneuilina europeum Christiansen, 1958.
Eggerelloides medius (Höglund) = Verneuilina media Höglund, 1947.
Elphidium albiumbilicatum (Weiss) = Nonion pauciloculum Cushman subsp. albiumbilicatum Weiss, 1954.
Elphidium excavatum (Terquem) = Polystomella excavata Terquem, 1875.
Epistominella vitrea (Parker) = Epistominella vitrea Parker, 1953.
Globobulimina auriculata Bailey = Bulimina auriculata Bailey, 1894.
Gyroidina lamarckiana (d'Orbigny) = Rotalina lamarckiana d'Orbigny, 1839.
Gyroidina orbicularis d'Orbigny 1826.Haplophragmoides bradyi (Robertson) = Trochammina bradyi Robertson, 1891.
Hyalinea balthica (Schröter in Gmelin) = Nautilus balthicus Schröter in Gmelin, 1791.
Lagenammina arenulata (Skinner) = Reophax difflugiformis var. arenulata Skinner, 1961.
Leptohalysis gracilis (Kiaer) = Nodulina gracilis Kiaer, 1900.
Liebusella goesi Höglund, 1947.
Melonis barleeanum (Williamson) = Nonionina barleeana Williamson, 1858.
Nonionella iridea Heron-Allen & Earland, 1932.
Nonionella turgida (Williamson) = Rotalina turgida Williamson,1858.
Nonionellina labradorica (Dawson) = Nonionina scapha var. labradorica Dawson, 1860.
Pullenia bulloides (d'Orbigny) = Nonionina bulloides d'Orbigny, 1846.
Pullenia osloensis Feyling-Hanssen, 1954.
Pullenia quinqueloba (Reuss) = Nonionina quinqueloba Reuss, 1851.
Recurvoides trochamminiforme Höglund, 1947.
Reophax fusiformis (Williamson) = Proteonina fusiformis Williamson, 1858.
Reophax scorpiurus Montfort, 1808.
Sigmoilopsis schlumbergeri (Silvestri) = Sigmoilina schlumbergeri Silvestri, 1904.Spiroplectammina biformis (Parker & Jones) = Textularia agglutinans var. biformis Parker & Jones, 1865.

Spiroplectammina sagittula (Defrance) = Textularia sagittula Defrance, 1824.
Stainforthia fusiformis Williamson, 1858.= Bulimina pupoides d'Orbigny var. fusiformis Williamson
Stainforthia loeblichi (Feyling-Hanssen) = Virgulina loeblichi Feyling-Hanssen, 1954
Stainforthia skagerakensis (Höglund) = Virgulina skagerakensis Höglund, 1947.
Textularia earlandi Parker, 1952.
Textularia kattegatensis Höglund, 1948.
Textularia skagerakensis Höglund, 1947.
Tritaxis conica (Parker & Jones) = Valvulina conica Parker & Jones, 1865.
Trochammina globigeriniformis (Parker & Jones) = Ammoglobigerina globigeriniformis Parker & Jones, 1865.
Trochammina inflate (Montagu) = Nautilus inflatus Montagu, 1808.
Trochamminopsis quadriloba (Höglund) = Trochammina quadriloba Höglund, 1948.
Uvigerina mediterranea Hofker, 1932.
Uvigerina peregrina Cushman, 1923.